Fermilab

ELEMENTARY STOCHASTIC COOLING[*]

A. V. Tollestrup and G. Dugan

December 1983

ELEMENTARY STOCHASTIC COOLING

A. V. Tollestrup and G. Dugan
Fermi National Accelerator Laboratory, Batavia, Illinois 60510

TABLE OF CONTENTS

FIGURE CAPTIONS

Fig. 1.5.1. Electron cooling arrangement (schematic).

Fig. 3.1.1. Antiproton production rates into 0-30 mrad per GeV/c per interacting proton on tungsten vs. antiproton momentum, for various proton energies (Ref. 15).

Fig. 3.2.1. Calculated antiproton yield ($\bar{p}$/incident proton) vs. transverse acceptance, within a longitudinal $\Delta p/p$ = .04 (Ref. 15). Lens gradient 1000 T/m.

Fig. 4.2.1. Debuncher RF voltage vs. turn number (Ref. 2).

Fig. 4.2.2. Debuncher longitudinal phase space at injection (Ref. 2).

Fig. 4.2.3. Debuncher longitudinal phase space after 23 turns (Ref. 2).

Fig. 4.2.4. Debuncher longitudinal phase space after 53 turns (Ref. 2).

Fig. 5.2.1. Cooling of σ^2 vs. turn number, from computer model, for g = 1 and various mixing parameter valves.

Fig. 5.4.1. Cooling of debuncher transverse phase space (Ref. 2).

Fig. 8.4.1. Loop coupler frequency response, measured by the wire method (Ref. 19).

Fig. 8.4.2. Transient time response of loop coupler, measured using Linac beam (Ref. 20).

Fig. 8.4.3. Frequency and phase response of loop coupler, from Linac beam measurements (Ref. 20).

Fig. 8.4.4. Spacial sensitivity of loop coupler at 1.5 GHz (Ref. 20).

Fig. 10.7.1. Block diagram of Fermilab Accumulator stochastic cooling system (Ref. 2).

Fig. 10.7.2. F vs. E for Fermilab system (Ref. 2).

Fig. 10.7.3. $D_0 + D_1$ vs. E for Fermilab system (Ref. 2).

Fig. 10.7.4. D_2 vs. E for Fermilab system (Ref. 2).

Fig. 11.3.1. Nyquist plot for Fermilab Accumulator at 1.5 GHz (Ref. 2).

ELEMENTARY STOCHASTIC COOLING

A. V. Tollestrup and G. Dugan
Fermi National Accelerator Laboratory, Batavia, Illinois 60510

1. INTRODUCTION

When the $\bar{S}ppS$ collider at CERN commenced operating in 1981, a new technology was opened up for high energy physics to exploit. Such colliders use only one magnet system for acceleration, and colliding orbits are guaranteed through CPT invariance. The values of the $\sqrt{s}$ achieved by these techniques are truly outside of the range of possible fixed target experiments. For instance, the collider at CERN with the magnet system working at 270 GeV is equivalent to a fixed target experiment of 155 TeV, and the Fermilab collider at a $\sqrt{s} = 1800$ GeV would require a fixed target experiment at 1727 TeV to give equivalent center of mass energies.

$\bar{p}p$ colliders at present are preferred over pp colliders for several reasons: First, only one magnet system is required, and we can use the present generation of accelerators to give us access to the enormous energies mentioned above. Second, quark, anti-quark collisions are dominant for many of the interesting new processes (W/Z^0 production), and the valence quarks in this $\bar{p}p$ reaction give a much larger cross section than is possible using the sea as a source of antiquarks in pp collisions. This effect is even important for the 2 TeV × 2 TeV "Dedicated Collider" being proposed for Fermilab. Finally, adequate sources of antiprotons have become technically possible so that the $\bar{p}p$ solution can be realized.

At very high energies where the interesting cross sections decrease to very small values, it may well be that pp colliders with their higher luminosity will become the preferable solution. The recent study of 20 TeV colliders carried out in a workshop at Ithaca during March 1983 indicated some of the considerations that will be important in the future. A pp collider requires an expensive source as well as a somewhat larger aperture in order to separate the two circulating beams and thus to eliminate undesirable effects on the beam dynamics from interactions between the coherent electromagnetic fields of the passing bunches. These costs partially offset the increased cost of a double magnet system for the pp option. In addition, a proton source is a much simpler and a more reliable piece of equipment than an antiproton source.

1.1. Present $\bar{p}p$ rings

We take this opportunity to review the present status of $\bar{p}p$ colliders. We give the design characteristics of three of these in Table 1.1.

Table 1.1. $p\bar{p}$ Rings

	CERN AA[1]	Fermilab TeV I[2]	Fermilab Dedicated Collider[3]
C.M. Collision Energy (TeV)	0.54	2	4-5
Luminosity ($cm^{-2}sec^{-1}$)	10^{30}	10^{30}	4×10^{31}
Number of p's	6×10^{11}	1.8×10^{11}	4.4×10^{12}
Number of $\bar{p}$'s	6×10^{11}	1.8×10^{11}	4.4×10^{12}
Number of bunches	6	3	44
β^* (m)	4.7×1	1	1
$\bar{p}$ collection energy (GeV)	3.5	8.9	8.9
Protons targeted/pulse	10^{13}	2×10^{12}	2×10^{12}
$\bar{p}$ collected/pulse	2.5×10^{7}	7×10^{7}	7×10^{7}
$\Delta p/p$ (%)	1.5	3	3
ϵ_H, ϵ_V (mm-mrad)	100π	20π	20π
Stack core $\Delta E/E$ (%)	.15	.04	.04
Core ϵ_H (mm-mrad)	1.4π	2π	2π
ϵ_V (mm-mrad)	π	2π	2π
$\bar{p}$ source supply rate ($\bar{p}$/hour)	2.5×10^{10}	10^{11}	10^{11}

CERN, using the SPS and constructing an antiproton source, was the first to develop this new technique. At the time of this writing, they are working the SPS at an energy of 270 GeV, and the luminosity achieved has been 2×10^{29}/cm^{2}sec. In early 1983, in a period of two weeks, the integrated luminosity achieved was about 25 inverse nanobarns.

CERN's design luminosity is 10^{30}. During the runs in 1982 and '83, the luminosity climbed steadily from a level of 10^{27} up to 2×10^{29}. It can be expected that this improvement in performance will continue; however, modifications to the source will be necessary to bring the luminosity up to the design value of 10^{30}.

The source being designed and constructed at Fermilab also has a projected luminosity of 10^{30}. The initial stack should take four hours to generate, and it will replenish itself in two hours. The maximum energy of this collider will be determined by the maximum energy at which the superconducting magnets can operate and should exceed 900 GeV per beam. This source design will be used as a model for many of the discussions later in this paper.

A second collider at Fermilab called the Dedicated Collider, or DC, has been proposed in April 1983. The characteristics of this machine are also shown in the table. The maximum energy is 2-1/2 TeV per beam. It will be filled from the present accelerator complex in TeV I. The design luminosity for this machine is $>10^{31}$, and it illustrates what could be expected of $\bar{p}p$ colliders in the future.

Finally, there is an additional machine parasitic to the source at CERN called LEAR. This is not a high energy collider but rather studies $\bar{p}$'s at low energy. It is discussed here because it provides examples of both stochastic cooling and electron beam cooling and how these techniques can be used to enhance the properties of particle beams for use in either colliding beams or fixed target physics.

1.2. Simple estimate of luminosity

The luminosity in a collider must be high enough to measure currently interesting cross sections. The W production cross section, for instance, is of the order of 10^{-33} cm^2 at CERN energies. For reasons that will become apparent later, all colliders use bunched beams. Since the total cross section for $\bar{p}p$ collisions at the $\sqrt{s}$ = 1000 GeV is of the order of 100 mb, the luminosity in a single bunch crossing should not be greater than 10^{25}; otherwise, there will be more than one interaction per beam crossing. For two bunches colliding head on once per second, the luminosity per bunch crossing is given by:

$$\mathscr{L} = \frac{N_1 N_2}{A}$$

where N_1 and N_2 are the numbers of protons and antiprotons, and A is the cross sectional area of the colliding bunches. It is possible in a modern accelerator to have 10^{11} protons in an accelerator bucket. If we could collect an equal number of antiprotons into a bunch, then

an area of 10^{-3} cm^2 would give the required single crossing
luminosity. The rotation period in the SPS or Tevatron is about 50
Khz and, hence, the luminosity per second would be 5 $\times$ 10^4 $\times$ 10^{25} = 5
$\times$ 10^{29}. A run of 20 days would give a total integrated luminosity of
10^{36}, which is sufficient to study W/Z production, jets to p_t of
greater than 100 GeV, and many other significant experiments.

We shall see below that the emittance of a proton beam is small
enough so that it is easy to achieve an area of the order of 10^{-4} cm^2
(compare with 10^{-3} cm^2 in our example above). However, antiprotons
must be formed by bombarding a target with high energy protons. Not
only is the yield low, but the phase space is large. To give an
order of magnitude, we must collect $\bar{p}$'s from about 3,000 pulses and
increase their phase space density by many orders of magnitude before
we can collect 10^{11} in a single RF bucket. It is for these two
reasons that cooling is required.

1.3. Cooling

By cooling, we mean the reduction of the random motion of
particles in a beam. For instance, protons are created in a plasma
source and as a result have a longitudinal as well as a transverse
spread of momentum. The longitudinal spread is contained by the RF
system. The transverse spread is constrained by the focussing
properties of the lattice. The cooling system is able to reduce
these two random components of motion.

There are two such techniques available. They both operate by
removing random momentum components each time a particle passes a
given point in a circular orbit, i.e., both require a small storage
ring for their operation.

The first system is electron cooling. In this scheme, the
antiprotons are brought into contact with an electron beam of the
same average velocity. In the reference system of the antiprotons,
we have a plasma that is not in thermal equilibrium. The antiprotons
are "hot", and the electrons are very "cool". They exchange energy
through coulomb collisions, the protons losing energy, and the
electrons gaining it. The beams separate and on the next pass, the
$\bar{p}$'s again encounter fresh electrons that are cool, and the process
repeats.

The second technique is called stochastic cooling and utilizes
electrodes to measure the random components of a $\bar{p}$'s transverse or
longitudinal momentum. This signal is amplified by a very wide band,
high gain amplifier. It is then sent across the diameter of the ring
to circumvent the time delays accumulated in the amplifier and is
applied to a kicker in a phase that damps the random motion. Thus,
each antiproton corrects its own errors. However, as we shall see
later, due to the finite band width of the amplifier, of the pickups
and of the kickers, the neighboring antiprotons are also disturbed by
this signal. The process, which would work very rapidly for a single
particle, works more slowly for densely packed particles due to these
cross interference terms.

Both of these methods will be discussed in what follows. Their
properties tend to be rather complimentary. We will see in the next

section on LEAR how both schemes may be used in a modern accelerator storage ring.

1.4. LEAR

The LEAR (Low Energy Antiproton Ring)[4-7] project at CERN is a 12.5 m mean radius storage ring facility for physics at low energies (5 MeV – 1.3 GeV) with intense cold antiproton beams. The antiprotons in LEAR are obtained from cooled $\bar{p}$'s in the AA via the CERN PS. In LEAR, the $\bar{p}$'s will be able to be decelerated or accelerated to cover the energy range indicated above, and stochastically cooled both transversely and longitudinally. In the standard LEAR operating mode, they are then slowly extracted from the storage ring for use in fixed-target experiments.

This standard operating mode ("stretcher mode") will consist of the following steps:

1. ~10^9 cooled $\bar{p}$'s will be extracted from the AA into the PS at 3.5 GeV/c every 10^3 sec (this is ≤10 percent of the $\bar{p}$'s in the AA).

2. These $\bar{p}$'s are decelerated in the PS to 0.6 GeV/c and injected into LEAR.

3. The $\bar{p}$'s in LEAR are stochastically cooled at 0.6 GeV/c, both transversely and longitudinally.

4. The $\bar{p}$'s are then decelerated or accelerated to the required extraction energy, and extracted slowly over a period of ~10^3 sec.

The stochastic cooling in step 3 is especially important for low extraction energies because of the adiabatic antidamping which occurs during deceleration. With this cooling, the extracted beams will have a high quality ($\Delta p/p \leq 0.2$ percent), as well as high intensity (~10^6 $\bar{p}$/sec) over the entire operating range in energy. This constitutes an improvement factor of ~10^3 over presently existing low-energy (<500 MeV) $\bar{p}$ beams in terms of beam intensity alone; of course, the duty cycle, beam quality (transverse and longitudinal), and beam purity are also all substantially improved over existing beams.

The standard operating mode outlined above will also be supplemented by the following options:

1. Electron cooling is planned to be installed in one of the straight sections; it will be applied to low energy (<200 MeV/c) beams prior to extraction to further improve the extracted beam quality.

2. An atomic jet target will be available in one of the straight sections for interaction studies with the internal $\bar{p}$ beam, and for production of antineutrons. The cooling equipment can compensate for beam heating produced by coulomb scattering in the jet. (Note all $\bar{p}$'s interact.)
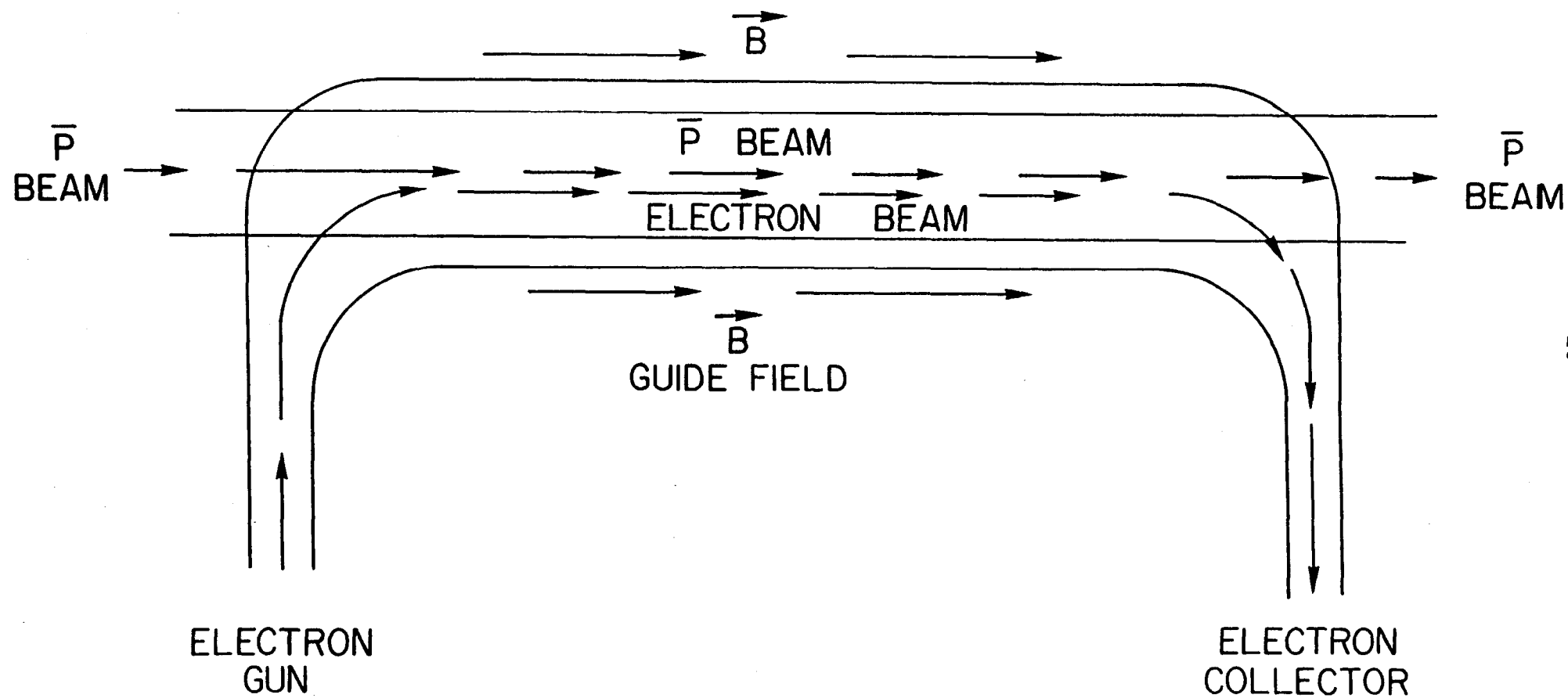
3. H⁻ ions injected into LEAR and corotating with the stored $\bar{p}$'s
    will result in the formation of neutral protonium ($\bar{p}p$) atoms, via
    Auger capture. A neutral beam of $\bar{p}p$ atoms, having the common
    $(H^-,\bar{p})$ beam energy and an intensity of ~10⁴/sec, will emerge from
    one of the straight sections: this will allow high precision
    studies of this exotic atomic system.

4. Protons injected into LEAR will collide with counterrotating $\bar{p}$'s
    to provide $p\bar{p}$ collision events with CM energies up to 4.4 GeV
    (the "mini collider" option). If LEAR is loaded with a day's
    worth of AA $\bar{p}$'s (~6 × 10¹¹) and the same number of protons is
    injected, a luminosity of ~10²⁹/cm² sec, with a 5 m long bunch
    crossing, is attainable. The spectroscopy of charmonium can be
    studied intensively with this option.

1.5. Electron cooling

Electron cooling of ion beams was first proposed[8] (1966) and
demonstrated[9] (1974-75) by G. I. Budker and co-workers at the INP at
Novosibirsk. This first demonstration of the feasibility of the
technique involved the cooling of 35-65 MeV proton beams; transverse
cooling rates of ~0.2/sec were observed. Subsequently, experiments
at CERN in the ICE ring[10] with 46 MeV protons and at Fermilab[11] with
200 MeV protons, confirmed the betatron cooling effects and also
demonstrated longitudinal cooling, achieving a reduction in the beam
momentum spread of a factor of ~50 with an initial cooling rate of
~3/sec.

The arrangement required for electron cooling[12] of a $\bar{p}$ beam is
shown schematically in Fig. 1.5.1. An electron beam (current ~1A) is
produced by thermionic emission in an electron gun and accelerated to
a momentum p_e. This electron beam is guided by magnetic fields into a
straight section of a storage ring containing $\bar{p}$'s of momentum $p_{\bar{p}}$. A
solenoidal guide field is present in the straight section: the
electron and $\bar{p}$ beams overlap here. After passing through the
straight section, the electron beam is guided into a collector where
most of the beam energy (which can be quite large, e.g., a few
hundred kW) is recovered by deceleration. The fields required to
deflect the electron beam into and out of the straight section have
little effect on the $\bar{p}$ beam because $p_{\bar{p}} >> p_e$ (see below).

Electron cooling in the straight section takes place via the
electromagnetic interactions of the overlapping electron and $\bar{p}$ beams.
The physical process is fundamentally the same as that responsible
for ionization energy loss (dE/dx) of ion beams in matter. Just as
the ionization energy loss increases as the ion velocity decreases,
until the velocity of the atomic electrons is reached, so electron
cooling is most effective when the $\bar{p}$ beam mean velocity and the
electron beam mean velocity are equal (the $\bar{p}$'s are at rest relative
to the electrons, on average). Hence, for optimum electron cooling,
the quantities p_e and $p_{\bar{p}}$ should be related by:

$\vec{B}$

$\bar{P}$ BEAM

$\bar{P}$ BEAM

$\bar{P}$
BEAM

ELECTRON BEAM

$\bar{P}$
BEAM

$\vec{B}$
GUIDE FIELD

ELECTRON
GUN

ELECTRON
COLLECTOR

$$p_e/m_e = (\beta c \gamma)_e = (\beta c \gamma)_{\bar{p}} = p_{\bar{p}}/m_{\bar{p}}$$

(For example, in the Fermilab cooling experiment, $p_{\bar{p}}$ ~645 MeV/c and p_e ~351 keV/c, T_e ~110 keV). In the common beam rest frame, the system appears as a plasma of electrons and $\bar{p}$'s. The transverse electron temperature $T^*_{e\perp}$ in this plasma is determined (in principle) by the temperature of the thermionic emission cathode T_c: typically $T^*_{e\perp} = T_c$ ~0.5 eV. The longitudinal electron temperature is usually much smaller (it is compressed from T_c by a factor (T_c/T_e) ~10^{-5}). The transverse and longitudinal temperatures of the $\bar{p}$'s, in a storage ring filled by a transfer line from a $\bar{p}$ production target, are much greater than $T^*_{e\perp}$. Thus, as the system approaches thermal equilibrium by energy exchange through the coulomb interaction, the $\bar{p}$'s cool off and the electrons heat up. The hot electrons are removed to the collector, and the net result is a cooling of the $\bar{p}$ beam. Eventually, diffusion heating of the $\bar{p}$'s in the plasma balances the coulomb-interaction cooling, and the $\bar{p}$ beam reaches its equilibrium phase-space density.

The cooling may be regarded as being driven by a velocity-dependent drag force $F(V^*)$ on the $\bar{p}$'s which (like dE/dx) varies as $(V^*)^{-2}$, where V^* is the random $\bar{p}$ velocity in the beam rest frame. As V^* approaches from above the transverse electrons velocity $V^*_{e\perp} = \sqrt{2 T^*_{e\perp}/m_e}$, the force peaks and then falls off slowly for $V^* < V^*_{e\perp}$. The corresponding $\beta^*_{e\perp}$ is

$$\beta^*_{e\perp} = \sqrt{\frac{2T^*_{e\perp}}{m_e c^2}} = \sqrt{\frac{2 \times 0.5}{511 \times 10^3}} \approx 1.4 \times 10^{-3}$$

The longitudinal lab momentum $p_{\parallel}$ of a $\bar{p}$ is related to its longitudinal momentum $p_{\parallel}^*$ in the beam rest frame by

$$p_{\parallel} = \gamma\left(p_{\parallel}^* + \frac{\beta E_{\parallel}^*}{c}\right) \simeq \gamma(p_{\parallel}^* + \beta m_{\bar{p}} c)$$

So a spread $\delta p_{\parallel}$ in lab momentum results in a longitudinal momentum relative to the electron beam $p_{\parallel}^* = \delta p_{\parallel}/\gamma$ and a longitudinal velocity

$$\beta_{\parallel}^* = \frac{p_{\parallel}^*}{m_{\bar{p}} c} = \frac{\delta p_{\parallel}}{\gamma m_{\bar{p}} c} = \frac{p_{\parallel}}{\gamma m_{\bar{p}} c}\left(\frac{\delta p_{\parallel}}{p_{\parallel}}\right) = \beta\,(\delta p_{\parallel}/p_{\parallel})$$

For optimum cooling, we need

$$\beta_{\parallel}^* = \beta(\delta p_{\parallel}/p_{\parallel}) \approx \beta_{e\perp}^* \approx 1.4 \times 10^{-3}$$

or

$$\delta p_{\parallel}/p_{\parallel} = 1/\beta \ (1.4 \times 10^{-3})$$

For low energies, a large $\delta p_{\parallel}/p_{\parallel}$ can be optimally cooled, but for $\beta \sim 1$, we need $\delta p_{\parallel}/p_{\parallel} \sim 10^{-3}$. This is typically much smaller than the momentum spread obtainable from a production target through a conventional transfer line. Nevertheless, one may obtain such values without sacrifice of $\bar{p}$ intensity by schemes which manipulate longitudinal phase space in debunching rings, and so achieve optimum longitudinal cooling even for $\beta \sim 1$. However, the situation is even worse at high energies for transverse cooling. To see this, consider a $\bar{p}$ in the beam in the storage ring, travelling at an angle θ relative to the beam axis in the cooling region:
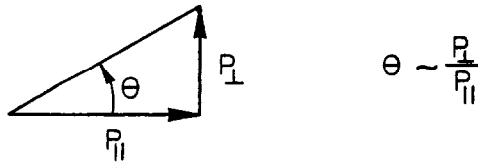
The transverse momentum in the beam rest frame is $p_{\perp}{}^* = p_{\perp} = \theta p_{\parallel}$. Then

$$\beta^*_{\perp} = \frac{V_{\perp}{}^*}{c} = \frac{p_{\perp}{}^*}{m_{\bar{p}}c} = \frac{p_{\parallel}\theta}{m_{\bar{p}}c} = \frac{m_{\bar{p}}\beta\gamma c\theta}{m_{\bar{p}}c} = \beta\gamma\theta$$

The angle θ is related to the beam emittance:

$$\epsilon_x \sim 6\pi(x^2/\lambda + \theta^2\lambda)$$

where λ = betatron wave number. For

$x \sim 0$, $\theta \sim \sqrt{\epsilon_x/6\pi\lambda}$: e.g. $\epsilon_x = 40\pi$ μm-rad, $\lambda = 5$m gives

$$\theta \sim \sqrt{\frac{40\pi \cdot 10^{-6}}{6\pi \times 5}} \approx 10^{-3}$$

Then for high-energy $\bar{p}$'s (e.g., $\beta \sim 1$, $\gamma \sim 10$), $\beta^*_{\perp} \sim 10^{-2} \gg \beta^*_{e\perp}$, so transverse cooling is not very effective. But for $\beta\gamma \sim 1$, we can easily achieve $\beta^*_{\perp} \sim \beta^*_{e\perp}$. This improvement in performance (for a given $\bar{p}$ emittance) as the energy is reduced is especially marked when one considers the transverse cooling rate. It is

$$\lambda^* = \frac{d|v_{\perp}{}^*|}{dt} \frac{1}{|v_{\perp}{}^*|}$$

The drag force is

$$F(V_\perp{}^*) = m_{\bar{p}} \frac{dV_\perp{}^*}{dt} \propto n_e{}^* \frac{1}{(V_\perp{}^*)^2}$$

where $n_e{}^*$ = electron density in the beam system. Using the lab quantities:

$$\lambda = \lambda^*/\gamma \qquad n_e = \gamma n_e{}^*$$

gives two factors of γ, and we have

$$\lambda = \lambda^*/\gamma \propto \frac{1}{\gamma} n_e{}^* \frac{1}{(V_\perp{}^*)^3} = \frac{n_e}{\gamma^2} \left(\frac{1}{\beta\gamma\theta}\right)^3 ; \quad \lambda \propto \frac{n_e}{\gamma^5 \beta^3 \theta^3}$$

The lab cooling rate varies inversely as $\gamma^5\beta^3$, a very strong energy dependence. (The dependence for the longitudinal cooling rate is weaker, only inversely as $\gamma^2\beta^3$). The complete expression for the transverse cooling[13] time is:

$$\tau = \frac{1}{\lambda} = \frac{0.5}{r_p r_e c \Lambda} \frac{\gamma^2}{n_e \eta} \begin{cases} \theta^3 \gamma^3 \beta^3 & \text{for } \beta_\perp{}^* > \beta_{e\perp}^* \\ (T_{e\perp}/m_{\bar{p}}c^2)^{3/2} & \text{for } \beta_\perp{}^* < \beta_{e\perp}^* \end{cases}$$

Here $r_{e,p} = e^2/m_{e,p}c^2$, Λ = coulomb log ($\sim$20), and η = fraction of the storage ring circumference for which electron cooling is effective.

Because of the strong energy dependence of the cooling rate, and also because of the technical difficulty in producing high energy, high current electron beams, electron cooling is best done at low energies. For a feasible $\bar{p}$ cooling scheme, one must produce the $\bar{p}$'s at high energies (where the production cross section is large), then decelerate them. The $\bar{p}$ cooling and accumulation takes place at low energies (e.g., 200-400 MeV); after cooling, the $\bar{p}$ beam must be reaccelerated for injection into the $p\bar{p}$ collider.

One final comment on electron cooling may be made. The critical velocity for which cooling is most effective is $\beta_{e\perp}^*$, the transverse electron velocity: the longitudinal velocity $\beta_{e\parallel}^*$ is usually much smaller. However, if the solenoidal field in the cooling region is strong enough ($\sim$1 kg), transverse motion of the electrons becomes primarily rotation in a plane perpendicular to the beam axis at the cyclotron frequency. Effectively transverse motion is "frozen out": no transverse momenta can be exchanged between $\bar{p}$'s and electrons, and the critical velocity for optimum cooling is reduced to $\beta_{e\parallel}^*$. Hence, for cooling of $\bar{p}$ beams with $V_\perp \ll \beta_{e\perp}^*$, the cooling rate can be substantially increased ($F(V^*)$ now peaks at $\beta_{e\parallel}^* \ll \beta_{e\perp}^*$), and the equilibrium phase space density of the $\bar{p}$ beam is much smaller. This "fast magnetized cooling" has been observed at INP[14] with very low energy (1 $\rightarrow$ 1.5 MeV) proton beams.

2. PROTON SOURCES

2.1. Proton sources and emittances

We start by first discussing proton sources. This technology is quite well developed. The protons from a plasma are accelerated by a Cockroft-Walton to perhaps 1/2 MeV and injected into a Linac. The Linac typically accelerates them to 200 MeV whereupon they are injected into a circular machine such as the booster at Fermilab. This synchrotron then accelerates them to 8 GeV at which point they can be transferred to the Main Ring. In the past, the Main Ring at Fermilab would then accelerate them to 400 GeV. However, now they will be either transferred into the Tevatron at 150 GeV for acceleration to 1 TeV or extracted at 120 GeV and used to make antiprotons at 8 GeV/c for the Source.

We will use the concept of emittance to describe the phase space of the beam. The transverse phase space has variables x, p_x, y, and p_y. More frequently, the transverse variables x, θ_x, y, and θ_y are used. The beam is assumed to be described in each dimension by an ellipse in phase space. We will use the 95 percent emittance in (x,θ_x) or (y,θ_y) space, defined by:

$$\epsilon = 6\pi \, \sigma \left(\frac{\sigma}{\beta}\right)$$

This ellipse contains 95 percent of the beam. σ is rms size, and β is the lattice function. The term in parenthesis is the rms angular spread of the particles in the beam. A useful concept is the normalized emittance ϵ_0. The emittance at any momentum p is given by:

$$\epsilon = \epsilon_0 (m_0 c/p)$$

Analogously, we can also define a longitudinal phase space given by σ_E and σ_t. The area

$$s = 6\pi \, \sigma_E \sigma_t$$

is conserved during acceleration. However, σ_E and σ_t change with energy and RF cavity voltage and for adiabatic changes, $\sigma_E \sim (EV_{RF})^{1/4}$ (see Example 2.2 below).

It is worth noting that in a practical accelerator, the emittances are not always governed by the momentum dependence as given above. For instance, the invariant transverse emittance of 24π mm-mr measured in the Fermilab Main Ring is considerably larger than the normalized phase space measured in the Linac. This blowup of phase space is thought to occur at injection into the booster where the beam spends a fair amount of time at low energy and the space charge forces between the particles are large. The equations given for emittance are only valid when these forces are not important. To give an idea of how strong this effect is, it has been calculated that the normalized transverse phase space in the Fermilab Linac is only 1π mm-mr.

2.2. Examples

Example 2.1: The invariant transverse phase space area of the
Fermilab Main Ring (R = 1km) is 24π mm-mrad. The Main Ring tune is
Q ~20. Find the rms beam size at injection (8 GeV) and at extraction
for $\bar{p}$ production (120 GeV). Assuming the same invariant area for the
Tevatron, find the rms beam size at 1 TeV in the $p\bar{p}$ intersection
region, for which β = 1m.

Solution: The transverse invariant phase space area is the area
in (p_x, x) space, where $p_x = m_0 c \gamma \beta_x$ is the transverse momentum. The
variables (p_x, x) are canonical coordinates, and hence by Liouville's
theorem the area in this phase space is an invariant. This area (ϵ_0)
is related to the area ϵ in (x' = dx/ds, x) space by

$$\epsilon_0 = \frac{p_x x}{m_0} = c\gamma\beta_x x = \gamma \, (dx/ds) \, (ds/dt) \, x$$

$$= \gamma\beta x'x = (p/m_0 c)\epsilon$$

Hence the quantity $p\epsilon/m_0 c$ is an invariant during acceleration. The
area ϵ, corresponding to 95% of a beam whose angular and position rms
widths are σ_x', σ_x respectively, is

$$\epsilon = 6\pi\sigma_x\sigma_x'$$

The betatron oscillation of x can be described by the equation

$$x = x_0 \cos(2\pi s/\lambda)$$

where λ = betatron oscillation wavelength (assumed constant over the
ring in this simplified analysis). The betatron function $\beta = \lambda/2\pi$.
Then

$$x' = dx/ds = x_0/\beta \, \sin(s/\beta) = x_0' \sin(s/\beta)$$
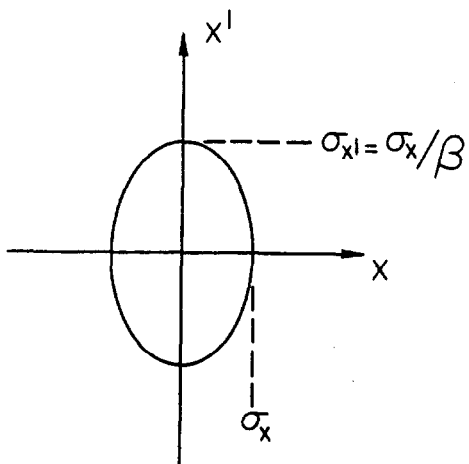
so

$$x_0' = x_0/\beta$$

The rms widths of x and x' will be proportional to x_0 and x_0' so

$$\sigma_x' = \sigma_x/\beta$$

and

$$\epsilon = 6\pi \, \sigma_x^2/\beta$$

expresses the phase-space area in terms of rms beam size.

The invariant is

$$\varepsilon_0 = \left(\frac{p}{m_0 c}\right) (6\pi\sigma_x^2/\beta), \quad \text{so } \sigma_x^2 = \frac{\beta}{(p/m_0 c)} \frac{\varepsilon_0}{6\pi}$$

In one turn, a particle travels a distance of $2\pi R$, and also completes Q betatron oscillations (Q = tune), so

$$Q\lambda = 2\pi R, \qquad \lambda/2\pi = R/Q = \bar{\beta} \qquad \bar{\beta} = \text{average } \beta$$

For the Fermilab Main Ring, $\bar{\beta} = 1\text{km}/20 \sim 50\text{m}$. At injection, $p = 8.9$ GeV/c so we have

$$\sigma_x^2 = \frac{50}{(8.9/.94)} \left(\frac{24\times10^{-6}}{6}\right) = 2.11 \times 10^{-5} \text{m}^2$$

$$\sigma_x = 4.4 \text{ mm}$$

At extraction

$$\sigma_x^2 = \frac{50}{(120/.94)} (4\times10^{-6}) = 1.57\times10^{-6}\text{m}^2$$

$$\sigma_x = 1.25 \text{ mm}$$

In the Tevatron

$$\sigma_x^2 = \frac{1}{(1000/.94)} (4\times10^{-6}) = 3.79\times10^{-9}\text{m}^2$$

$$\sigma_x = .061 \text{ mm}$$

Example 2.2: (i) The invariant longitudinal phase space area in the Fermilab Main Ring is 0.3 eV-sec. The harmonic number h = 1113 and the transition energy is $\gamma_t \simeq 20$. Find the rms energy spread, time spread and bunch length at E = 120 GeV, when the RF voltage is 4 Mv and the synchronous phase angle $\phi_s \sim 0$.

(ii) In the Tevatron, for $p\bar{p}$ collisions, the invariant bunch area will be $\sim$3 eV-sec. Find the rms energy spread, time spread and bunch length at 1000 GeV, when $V_{RF} \sim$1.4 Mv and $\phi_s \sim 0$.

(iii) Show that if the bunch area is an invariant, then $\sigma_t \propto (EV_{RF})^{-1/4}$.

Solution: The longitudinal invariant phase space area is the area in $(\Delta E, \Delta t)$ space, where ΔE is the energy spread and Δt the time spread in a beam. These quantitites are canonical coordinates and hence by Liouville's theorem the area in $(\Delta E, \Delta t)$ space is an invariant. The area in this space corresponding to 95% of a beam whose energy and time rms widths are σ_E, σ_t respectively is

$$s = 6\pi \, \sigma_E \sigma_t$$

The synchrotron oscillation of ΔE can be described by the equation

$$\Delta E = (\Delta E)_0 \cos \Omega_s t$$

whose Ω_s is the synchrotron oscillation frequency. Then

$$d/dt \, (\Delta E) = (\Delta E)_0 \Omega_s \sin \Omega_s t$$

Over one turn,

$$(\Delta E)_{turn} = eV_{RF} \sin \omega_{RF} \Delta t$$

where V_{RF} = RF voltage, and ω_{RF} = RF frequency. For $\Delta\phi = \omega_{RF}\Delta t \ll 1$ (a small bunch),

$$(\Delta E)_{turn} \sim eV_{RF} \, \omega_{RF} \, \Delta t$$

If T_0 = period of 1 turn ($= 2\pi R/\beta c$) then

$$\frac{(\Delta E)_{turn}}{T_0} \sim \frac{d(\Delta E)}{dt} = \frac{eV_{RF}\omega_{RF}\Delta t}{T_0}$$

So

$$(\Delta E)_0 \Omega_s \sin \Omega_s t = \frac{eV_{RF}\omega_{RF}\Delta t}{T_0}$$

or

$$\Delta t = \left(\frac{T_0 \Omega_s}{eV_{RF} \omega_{RF}} \Delta E_0 \right) \sin\Omega_s t = (\Delta t)_0 \sin\Omega_s t$$
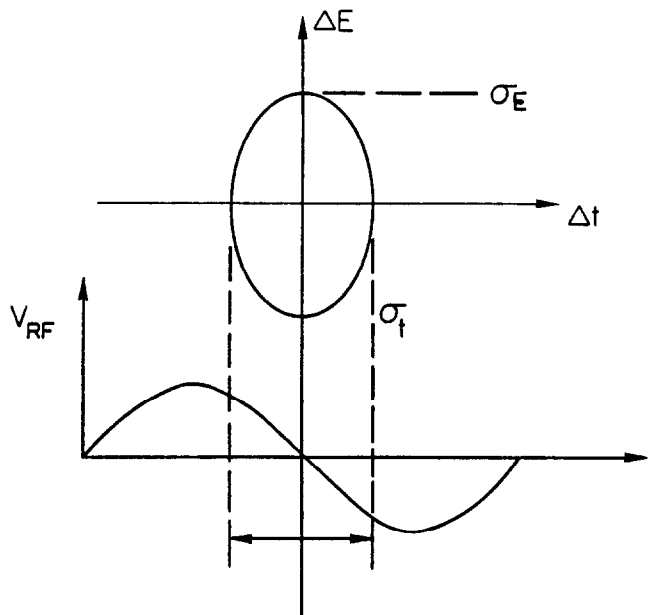
and

$$(\Delta t)_0 = \frac{T_0 \Omega_s}{eV_{RF} \omega_{RF}} (\Delta E)_0$$

As in example 2.1, we argue that σ_t and σ_E are proportional to $(\Delta t)_0$ and $(\Delta E)_0$ so

$$\sigma_t = \frac{T_0 \Omega_s}{eV_{RF} \omega_{RF}} \sigma_E$$

In this expression $\omega_{RF} = 2\pi f_{RF} = 2\pi h f_0$, where $f_0 = 1/T_0$ and $h =$ harmonic number. So

$$\sigma_t = \frac{T_0^2 \Omega_s}{2\pi eV_{RF} h} \sigma_E$$

The synchrotron oscillation frequency Ω_s is given by

$$\Omega_s = \left(\frac{eV_{RF}h|\eta|\cos\phi_s}{2\pi\beta^2 E}\right)^{1/2} \left(2\pi/T_0\right)$$

where ϕ_s is the synchronous phase angle and

$$\eta = 1/\gamma_t^2 - 1/\gamma^2 = -(df/f)/(dp/p)$$

so

$$\sigma_t = T_0 \left(\frac{|\eta|\cos\phi_s}{2\pi\beta^2 EV_{RF}eh}\right)^{1/2} \sigma_E$$

and

$$s = 6\pi\sigma_E\sigma_t = \frac{6\pi\sigma_t^2}{T_0} \left(\frac{2\pi\beta^2 EV_{RF}eh}{|\eta|\cos\phi_s}\right)^{1/2}$$

(i) Using $h = 1113$, $E = 120\times10^9$eV, $eV_{RF} = 4$ MeV, $\cos\phi_s \sim 1$, $\beta \sim 1$ and

$$\eta = 1/\gamma_t^2 - 1/\gamma^2 \sim 1/\gamma_t^2 = 1/20^2 = .0025$$

we have

$$x = \frac{2\pi\beta^2 EV_{RF}eh}{|\eta|\cos\phi_s} = \frac{2\pi(1)(120\times10^9)(4\times10^6)(1113)}{.0025}$$

$$= 1.343\times10^{24} \text{ eV}^2$$

and

$$T_0 = 2\pi R/\beta c = \frac{2\pi(10^3)}{(1)(3\times10^8)} = 2.09\times10^{-5}\text{sec}$$

and so for $s = 0.3$ eV-sec,

$$\sigma_t^2 = \frac{T_0 s}{6\pi} \frac{1}{x^{1/2}} = \frac{2.09\times10^{-5}\times0.3}{6\pi\times(1.343\times10^{24})^{1/2}} \text{ sec}^2 = 2.87\times10^{-19}\text{sec}^2$$

$$\sigma_t = .53 \text{ nsec}$$

$$\sigma_E = (\sigma_t/T_0)x^{1/2} = \frac{.53\times10^{-9}}{2.09\times10^{-5}} \sqrt{1.34\times10^{24}} = 29 \text{ MeV}$$

The bunch length is

$$\sigma_\ell = \beta c\sigma_t = (1)(3\times10^{10}\text{cm/sec})(.53\times10^{-9}\text{sec})$$

$$\sigma_\ell = 16 \text{ cm}$$

(ii) For the Tevatron, $V_{RF} = 1.4$ MV and $E = 1$ TeV so

$$x = \frac{2\pi\beta^2EV_{RF}eh}{|\eta|\cos\phi_s} = \frac{2\pi(1)(1000\times10^9)(1.4\times10^6)(1113)}{.0025}$$

$$= 3.92\times10^{24} \text{ ev}^2$$

T_0 is still 2.09×10^{-5}sec but $s = 3$ eV-sec so

$$\sigma_t^2 = \frac{T_0s}{6\pi}\frac{1}{x^{1/2}} = \frac{2.09\times10^{-5}\times3}{6\pi(3.92\times10^{24})^{1/2}} \text{ sec}^2 = 1.68\times10^{-18}\text{sec}^2$$

$$\sigma_t = 1.29 \text{ nsec}$$

$$\sigma_E = (\sigma_t/T_0)x^{1/2} = \frac{1.29\times10^{-9}}{2.09\times10^{-5}} (3.92\times10^{24})^{1/2} = 122 \text{ MeV}$$

$$\sigma_\ell = \beta c\sigma_t = 3\times10^{10}\text{cm/sec}\times1.29\times10^{-9}\text{sec} = 39 \text{ cm}$$

(iii) From the equation for s,

$$\sigma_t^2 = \frac{sT_0}{6\pi} \left(\frac{|\eta|\cos\phi_s}{2\pi\beta^2EV_{RF}eh}\right)^{1/2}$$

so

$$\sigma_t = \left(\frac{sT_0}{6\pi}\right)^{1/2} \left(\frac{|\eta|\cos\phi_s}{2\pi\beta^2eh}\right)^{1/4} \left(\frac{1}{EV_{RF}}\right)^{1/4}$$

Thus

$$\sigma_t \propto (EV_{RF})^{-1/4}$$

3. p̄ PRODUCTION

3.1. <u>Maximizing the p̄ yield</u>

In principle, if one could produce very large numbers of antiprotons, beam cooling would be unnecessary. One would simply use only that small part of phase space which fits into an accelerator, as is done for protons, which are in abundant supply. Unfortunately, although the total probability of p̄ production per interacting high-energy (>100 GeV) proton can be as high as a few percent, the produced p̄'s are spread over a huge range in energy and transverse momentum. Less than a percent of the p̄'s can be captured into even the relatively large acceptance of a conventional beam transport system. The much smaller fraction which could be captured directly into the acceptance of an accelerator is too small by orders of magnitude to be useful in a pp̄ collider. Hence the need to (1) produce and collect as many p̄'s as possible directly from the target, and (2) decrease the phase space occupied by the p̄'s (by cooling techniques) until it fits into an accelerator.

The first of these functions is carried out by the p̄ target and collection system. The system should maximize the yield of p̄'s collected into the acceptance of the first stage of the cooling (the Debuncher ring at Fermilab; the AA at CERN). The parameters available for optimization are the incident proton energy and spot size on the p̄ production target, the p̄ collection energy, the target length and material, and the details of the collection system optics.

Figure 3.1.1[15] illustrates the dependence of the 0-30 mrad p̄ production rates (per interacting proton) on the incident proton energy and the p̄ collection momentum. In general, the higher the proton energy the better: at Fermilab, a practical limit is 120 GeV. At this energy, the production peaks at ~10-12 GeV/c p̄ momentum: again, for practical reasons, a momentum of 8.9 GeV/c is selected. At CERN, the incident proton energy is 28 GeV, and the p̄'s are collected at 3.5 GeV/c.

The choice of target length and material is coupled to the characteristics of the p̄ collection system. As we will discuss below, the principal element in the collection system used at Fermilab will be a very short focal length lens (the short focal length minimizes chromatic aberrations, allowing a large momentum bite to be collected efficiently). Because of depth-of-field problems associated with the short focal length, a 6 cm long, high-density material (tungsten-rhenium) target will be used.

The effective source size seen by the p̄ collection system will depend primarily upon the proton beam size σ_x. For simplicity in the following discussion, we neglect effects due to target multiple scattering and secondary production, and assume a round beam ($\sigma_x = \sigma_y$). For a fixed polar collection angle $\theta_{\bar{p}}$, the transverse emittance of the p̄ source is proportional to $\theta_{\bar{p}}^2$ and σ_x^2:

$$\varepsilon_{\perp} = \varepsilon_x \varepsilon_y \propto \theta_{\bar{p}}^2 \, \sigma_x^2$$
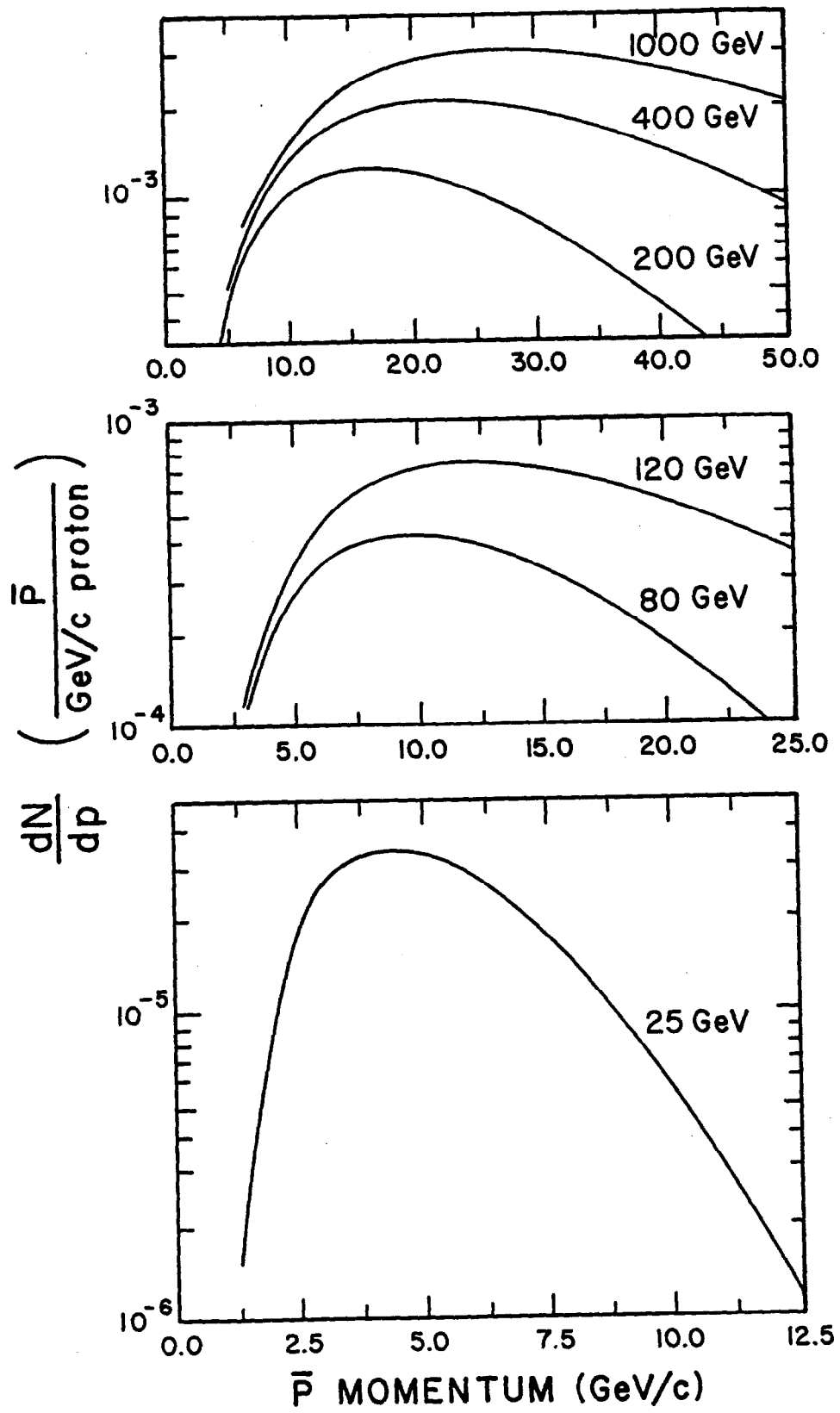
The transverse momentum dependence of the $\bar{p}$-production cross section is typically rather steep: there is not much yield above $p_\perp \sim 0.5$ GeV/c, corresponding to production angles of $(\theta_{\bar{p}})_{max} \sim p_\perp/p = 0.5/8.9 \sim 60$ mrad at Fermilab, and $(\theta_{\bar{p}})_{max} \sim 0.5/3.5 \sim 140$ mrad at CERN. For small angles $(\theta_{\bar{p}} < (\theta_{\bar{p}})_{max})$ the number of antiprotons $N_{\bar{p}}$ is proportional to $\theta_{\bar{p}}^2$:

$$N_{\bar{p}} \propto \theta_{\bar{p}}^2$$

So the transverse phase space density $N_{\bar{p}}/\epsilon_\perp \propto 1/\sigma_x^2$ grows inversely with the square of the proton beam spot size. Small proton beams maximize the $\bar{p}$ phase space density at production, and hence the $\bar{p}$ yield into a fixed acceptance.

This gain in $\bar{p}$ yield cannot be fully exploited, unfortunately. If the energy density deposited in the target by the proton beam (E_D) exceeds about 200 J/g,[16] thermal shock waves propagating through the target will result in density depletion and mechanical failure of the target material. The energy density, E_D, varies inversely with the square of σ_x.[15] For a given number of protons per pulse, this requirement of $E_D < 200$ J/g puts a lower limit on the permissible beam size. At CERN, $\sim 10^{13}$ 28 GeV protons per pulse are targeted in a spot size of $\sigma_x \sim .75$ mm, resulting in an $E_D \sim 185$ J/g. For the Fermilab project, with $\sim 2 \times 10^{12}$ protons per pulse, the requirement on E_D restricts $\sigma_x > 0.4$ mm.[2]

3.2. $\bar{p}$ collection

The collection optics for the antiprotons must transform the diverging $\bar{p}$ flux from the target into a parallel beam which can be transported to and injected into the cooling rings. To collect $\bar{p}$'s up to 0.5 GeV/c requires substantial integrated fields:

$$(BL = p_\perp/0.3 \sim 1.6 \text{T-m})$$

If the aperture is to be kept to a reasonable size, the collection lens must be relatively short and thus have high field gradients. Specialized devices are required for this purpose. At CERN, the device is a 40 cm linear horn, similar to those used to collect secondary particles for neutrino beams. The horn is a pulsed current (~ 140 kA) device in which the current is arranged so as to create a field integral for the $\bar{p}$'s which varies linearly with r, producing focusing in both planes simultaneously. At Fermilab, the device which does the $\bar{p}$ collection will be a 15 cm long lithium lens,[17] operating at a pulsed current of ~ 500 kA. The $\bar{p}$'s travel along the axis of a solid 1 cm radius lithium cylinder which carries the pulsed current; they are focused simultaneously in both planes by the resulting linear field. The lithium lens can develop substantially higher field gradients (and thus shorter focal lengths), and has better field linearity, than the horn: this allows larger $\bar{p}$ collection angles and less chromatic aberrations.
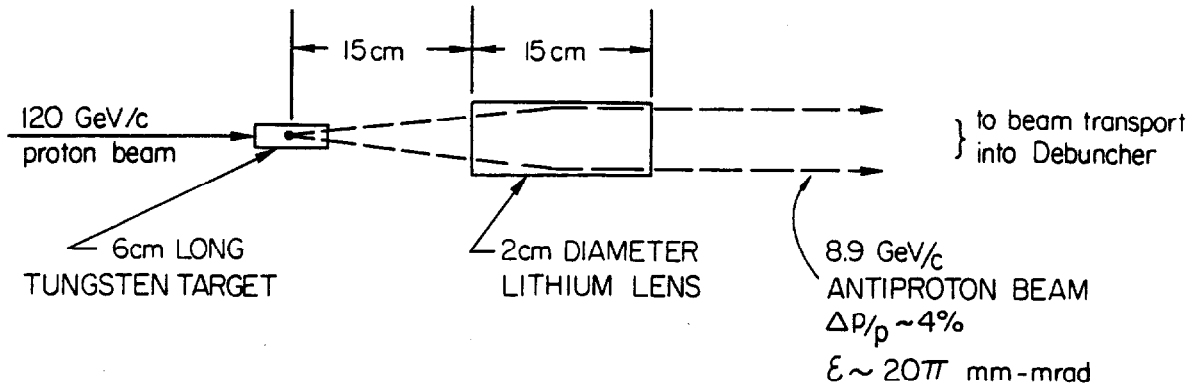
to beam transport into Debuncher

120 GeV/c proton beam

6cm LONG TUNGSTEN TARGET

2cm DIAMETER LITHIUM LENS

8.9 GeV/c ANTIPROTON BEAM
$\Delta P/p \sim 4\%$
$\mathcal{E} \sim 20\pi$ mm-mrad

Figure 3.2.1 shows the calculated $\bar{p}$ yield for the Fermilab $\bar{p}$ production collection system.[15] The plot is yield in $\bar{p}$ per incident proton vs transverse acceptance, for $\Delta p/p = 4\%$. The appropriate acceptance is that of the Debuncher ring: 20π mm-mrad. The corresponding yield is $\sim 5 \times 10^{-5}$, for $\sigma_x = .038$ cm and a 1 cm radius lens. We may compare this with a crude estimate from Fig. 3.1.1:

$$\frac{\bar{p}}{\text{incident proton}} = \frac{\bar{p}}{\text{GeV/c}\cdot\text{interacting proton}} \times (.04 \times 8.9 \text{GeV/c}) \times \frac{\text{interacting protons}}{\text{incident protons}}$$

$$= 6 \times 10^{-4} \times .356 \times (1 - e^{-4/9.6})$$

$$\simeq 7 \times 10^{-5}$$

The last factor comes from the fact that, although the target is 6 cm of tungsten (whose interaction length is 9.6 cm), only 4 cm are effective on average for $\bar{p}$ production due to depth-of-field effects.[15]

3.3. Examples

Example 3.1: (a) Estimate the number of $\bar{p}$'s delivered by the Fermilab collection system to the Debuncher on each pulse. Assume 2×10^{12} incident protons/pulse. For a pulse rate of 0.5 Hz, estimate the time required to collect 10^{11} $\bar{p}$'s. Compare this with the rate of $\bar{p}$'s available from the Accumulator ($\sim 10^{11}$ $\bar{p}$'s/hour).

(b) The Fermilab booster is capable of delivering ~ 13 batches, each of intensity $\sim 3 \times 10^{12}$ protons, to the Main Ring every 2 seconds. Assume that the technical problems of bunch rotation for multiple batches and target heating limitations are solved, allowing all these protons to be available for $\bar{p}$ production. Further assume that the $\bar{p}$ collection system can be improved to collect $\bar{p}$'s up to the maximum angle ($\theta_{\bar{p}} \sim 60$ mrad), and target depth-of-field limitations are eliminated, allowing full use of a 1-interaction-length (9.6 cm)
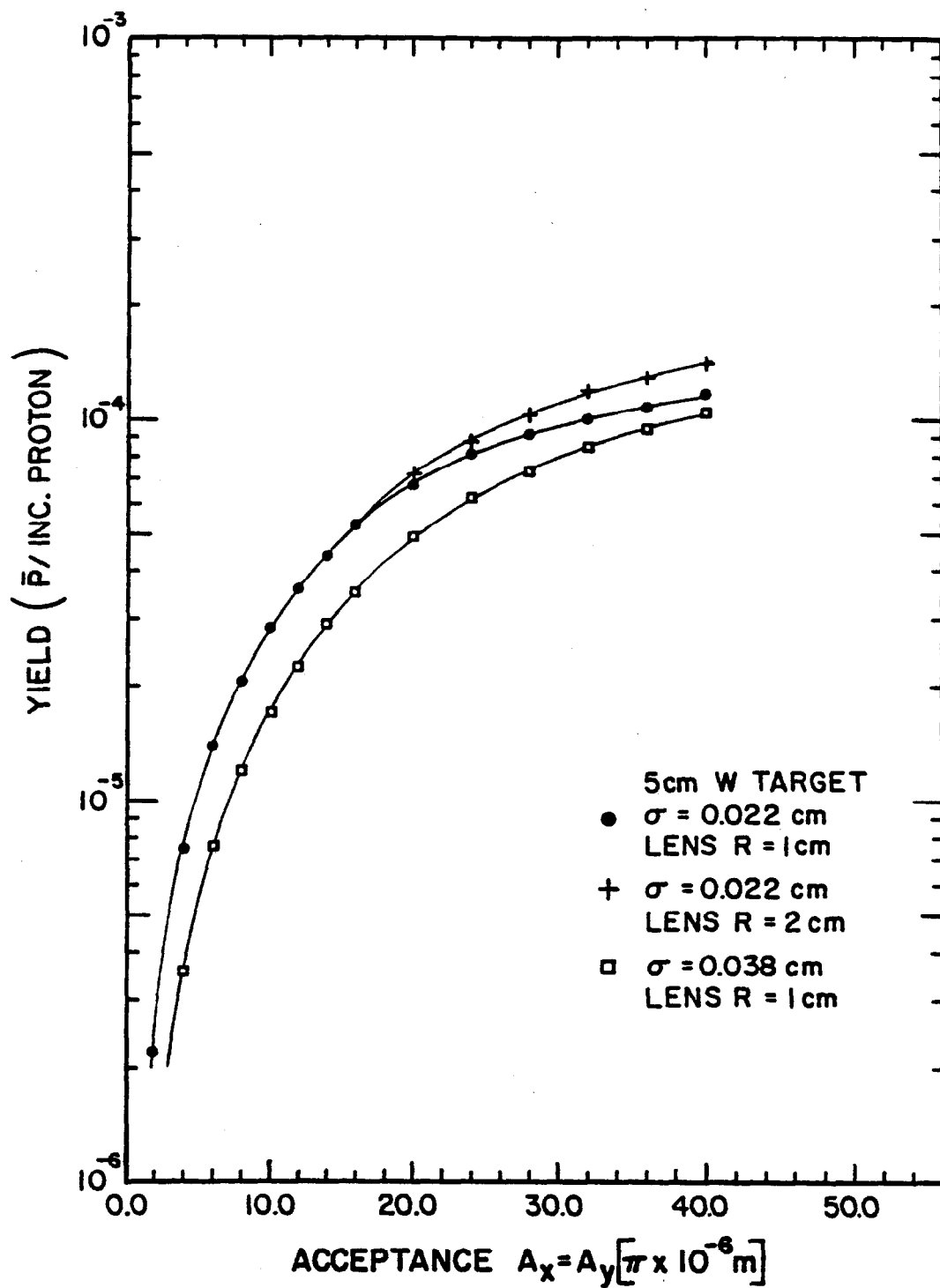
target. Under these conditions, estimate the number of $\bar{p}$'s available
on each pulse. For a pulse rate of 0.5 Hz, estimate the time
required to collect 10^{11} $\bar{p}$'s.

Solution: (a) From Fig. 3.2.1, $\bar{p}$/incident proton ~5×10^{-5} for the
Fermilab collection system. Hence

$$\bar{p}/\text{pulse} = 2\times10^{12} \text{ protons/pulse} \times 5\times10^{-5} \ \bar{p}/\text{proton} = 10^8$$

The $\bar{p}$ rate is $10^8 \times 0.5$ Hz = 5×10^7 Hz; to collect 10^{11} $\bar{p}$'s requires
$10^{11}/5\times10^7$ sec $\simeq$ 33 min. < 1 hr. Hence the rate of $\bar{p}$'s available
from the antiproton source (10^{11}/hr) is not limited by the $\bar{p}$
production rate.

(b) If all the booster protons are useable, then we have a
proton pulse of $3\times10^{12}\times13 \simeq 4\times10^{13}$. The number of $\bar{p}$'s collected
varies with $\theta_{\bar{p}}^{-2}$: for $\theta_{\bar{p}}$ = 60 mrad, we can scale from Fig. 3.1.1 by a
factor of 4. A calculation analogous to that given near the end of
the last section gives

$$\frac{\bar{p}}{\text{incident proton}} = \frac{\bar{p}}{\text{GeV/c} \cdot \text{interacting proton}} \times (.04 \times 8.9 \text{ GeV/c}) \times \frac{\text{interacting protons}}{\text{incident protons}}$$

$$= (6\times10^{-4}) \times 4 \times .356 \quad \times \ (1-e^{-1})$$

$$= 5.4\times10^{-4}$$

We then collect $4\times10^{13} \times 5.4\times10^{-4} = 2\times10^{10}$ $\bar{p}$'s per pulse. The $\bar{p}$
rate is 10^{10} $\bar{p}$/sec, so we need $10^{11}/10^{10}$ = 10 sec to collect 10^{11} $\bar{p}$'s.
In one hour, we could collect 3.6×10^{13} $\bar{p}$'s, which is a factor of 360
times the number of $\bar{p}$'s available from the present source.
Improvements in the stochastic cooling to utilize these $\bar{p}$'s would
result in several orders of magnitude increase in luminosity.

4. $\bar{p}$ SOURCES AND LIOUVILLE: THE ROLE OF THE DEBUNCHER

4.1. Transmission of phase space variables through the targeting process

We have seen in the previous section that the density of $\bar{p}$'s in
transverse phase space can be increased by decreasing the proton beam
size σ_x (subject to target heating limitations). The antiproton
phase space has some "memory" of the proton phase space: we can
transmit one of the transverse phase space variables from protons to
antiprotons through the targeting process. Howver, after the
targeting, the $\bar{p}$ phase space area is fixed, according to Liouville's
theorem. We may alter the shape of this area: this is done primarily
by the specialized $\bar{p}$ collection device discussed above, and in fact
is required to be able to transport the $\bar{p}$ beam to the cooling ring.
The $\bar{p}$ phase space ellipse at production, which is large in θ_x and
small in x, is rotated by ~90° in phase space to become narrow in θ_x
and large in x. This manipulation cannot increase the transverse
phase space density, however, which is determined at production.

A similar situation prevails for the longitudinal phase space. The energy spread of the p̄'s produced in the targeting process is independent of any characteristics of the proton beam (except total energy). However, since the time scale of the proton-nucleus interaction which generates p̄'s is much smaller than the time spread of the proton beam (σ_t), the produced p̄'s will have the same time distribution as the protons. Like the proton beam size, the proton beam time spread can be transmitted from protons to antiprotons through the targeting process. Hence, just as we could increase the transverse phase space density of the p̄'s by shrinking σ_x, so the longitudinal phase space density of the p̄'s can be increased by shrinking σ_t. After the targeting process, Liouvilles's theorem requires that the longitudinal phase space area of the p̄'s be constant. The shape of this area may be changed, however: in fact, just as for the transverse phase space, this change in shape (a 90° rotation in longitudinal phase space) is required to be able to further cool the p̄ beam. The device which accomplishes this rotation in phase space is the Debuncher. Again, this manipulation is necessary but does not increase the longitudinal phase space density, which is determined at production.

The above ideas can be summarized as follows. The number of antiprotons produced in the targeting process is roughly

$$N_{\bar{p}} \propto \Delta E \; \theta_{\bar{p}}^2$$

where ΔE and $\theta_{\bar{p}}$ are the energy and angular spreads of the p̄'s. The transverse emittance of the p̄'s is $\epsilon_\perp \propto \sigma_x^2 \theta_{\bar{p}}^2$; the longitudinal emittance is $\epsilon_\parallel \propto \Delta E \; \sigma_t$. Hence the density of p̄'s in phase space

$$d_{\bar{p}} = \frac{N_{\bar{p}}}{\epsilon_\perp \epsilon_\parallel} \propto \frac{1}{\sigma_x^2 \sigma_t}$$

increases as we decrease σ_x and σ_t. The total number of p̄'s which we can collect is the density times the transverse and longitudinal acceptances A_x, A_y, A_z of the cooling ring:

$$(N_{\bar{p}})_{collected} \simeq d_{\bar{p}} A_x A_y A_z \propto \frac{A_x A_y A_z}{\sigma_x^2 \sigma_t}$$

The transverse acceptances A_x, A_y are limited by magnet apertures. The longitudinal acceptance A_z is limited by chromatic aberrations and the cooling ring size. Increases in A_x, A_y, A_z tend to be very costly; the best way to increase $(N_{\bar{p}})_{collected}$ is to decrease σ_x and σ_t.

The decreasing of σ_x is done by a tight focus of the proton beam on the target; the subsequent manipulation of the transverse phase space for matching to the cooling ring acceptance (which amounts to increasing σ_x and decreasing σ_{θ_x} of the p̄ beam) is done by the p̄

collection device (e.g., the lithium lens). The decreasing of σ_t is done by RF manipulation in the Main Ring prior to extraction; the subsequent manipulation of the longitudinal phase space for matching to the cooling ring acceptance (which amounts to increasing σ_t and decreasing σ_E of the p̄ beam) is done by the Debuncher.

4.2. RF Bunch Rotation and Debunching

We have seen above (Example 2.2) that the time spread σ_t and energy spread σ_E of 120 GeV protons in the Fermilab Main Ring are, respectively, 0.56 nsec and 29 MeV. For adiabatic changes in RF voltage (i.e., changes in which the bunch area is invariant) the time spread σ_t varies as $(V_{RF}E)^{-1/4}$, so σ_E varies as $(V_{RF}E)^{1/4}$. The reduction in σ_t in the Main Ring is done in two steps:
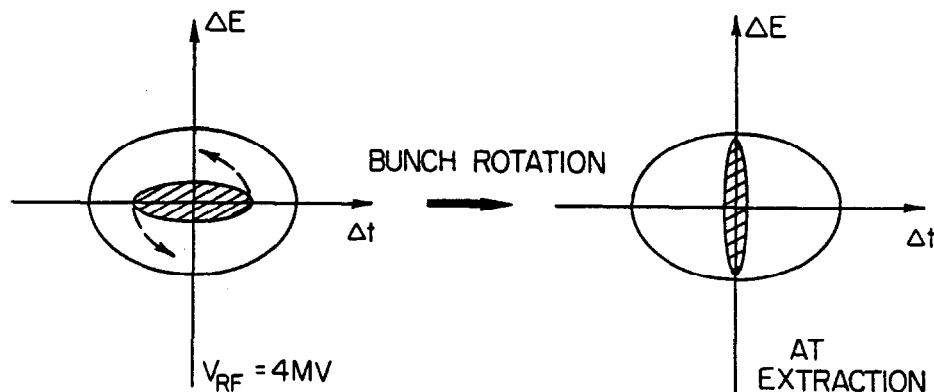
(i) V_{RF} is reduced adiabatically from V_{max} = 4MV to V_{min} = 30kV. Then

$$\sigma_t \rightarrow 0.56 \text{ nsec} \times \left(\frac{4000}{30}\right)^{1/4} = 1.9 \text{ nsec}$$

$$\sigma_E \rightarrow 29 \text{ MeV} \times \left(30/4000\right)^{1/4} = 8.5 \text{ MeV}$$
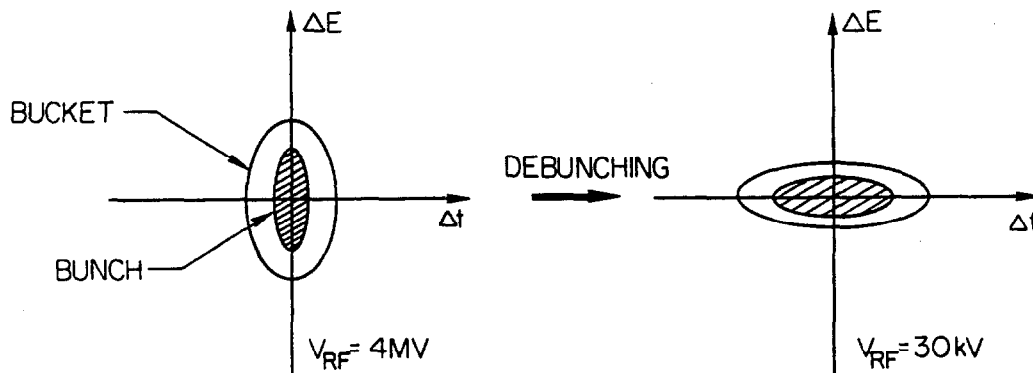
(ii) V_{RF} is suddenly raised to 4MV, increasing the bucket size. The bunch is no longer matched to the bucket and starts to rotate.

The phase space trajectory followed by the edges of the bunch, for which $\sigma_t = 1.9$ nsec, corresponds to an energy spread

$$\sigma_E = \sigma_t \, x^{1/2}/T_0 = \frac{1.9 \times 10^{-9}}{2.05 \times 10^{-5}} (1.343 \times 10^{24})^{1/2} \text{ eV} = 103 \text{ MeV}$$

(see Example 2.2). After 1/4 of a synchrotron oscillation, the bunch will have this energy spread, but its area $s = 0.3$ eV-sec is invariant; hence it has a time spread

$$\sigma_t = \frac{s}{6\pi\sigma_E} = \frac{0.3 \text{eV-sec}}{6\pi(103 \times 10^6) \text{eV}} = 0.15 \text{ nsec}$$

The time spread σ_t has been reduced from .56 nsec to .15 nsec; (a factor of $.56/.15 = 3.7 = (V_{max}/V_{min})^{1/4}$). The proton beam is now extracted and targeted.

The $\bar{p}$'s generated in the target have $\sigma_t = .15$ nsec. The energy spread at injection into the Debuncher is determined by the bandwidth of the $\bar{p}$ collection system and transport line ($\pm 2\%$ in $\Delta p/p$, which implies $\sigma_E \sim 180$ MeV). The $\bar{p}$ beam is captured into 53.1 MHz RF buckets in the Debuncher, with $V_{RF} = 5$MV. These buckets are larger than the $\bar{p}$ bunch; the bunch rotates in the large bucket. It is allowed to rotate through 1/4 of a synchrotron oscillation, so that the time spread is increased and the energy spread decreased. During the same time, V_{RF} is reduced to 122 kV to match the bucket to the rotated bunch. Then V_{RF} is reduced to 5 kV adiabatically (see Figs. 4.2.1-4.2.4). The overall result is a reduction in $\Delta E/E$ to $\sim 0.2\%$. The longitudinal $\bar{p}$ emittance is now well matched to the acceptance of the Accumulator. This scenario is worked out in the example below.

4.3. Examples

Example 4.1: The Debuncher ring, operating at $p = 8.9$ GeV/c, has a mean radius of 83 m, a harmonic number $h = 90$ and $\eta \sim .006$. Consider a $\bar{p}$ bunch with $\sigma_t = 0.15$ nsec and $\sigma_E = 180$ MeV, injected into a bucket with $V_{RF} = 5$ MV. Assume that the bucket is substantially larger than the bunch.

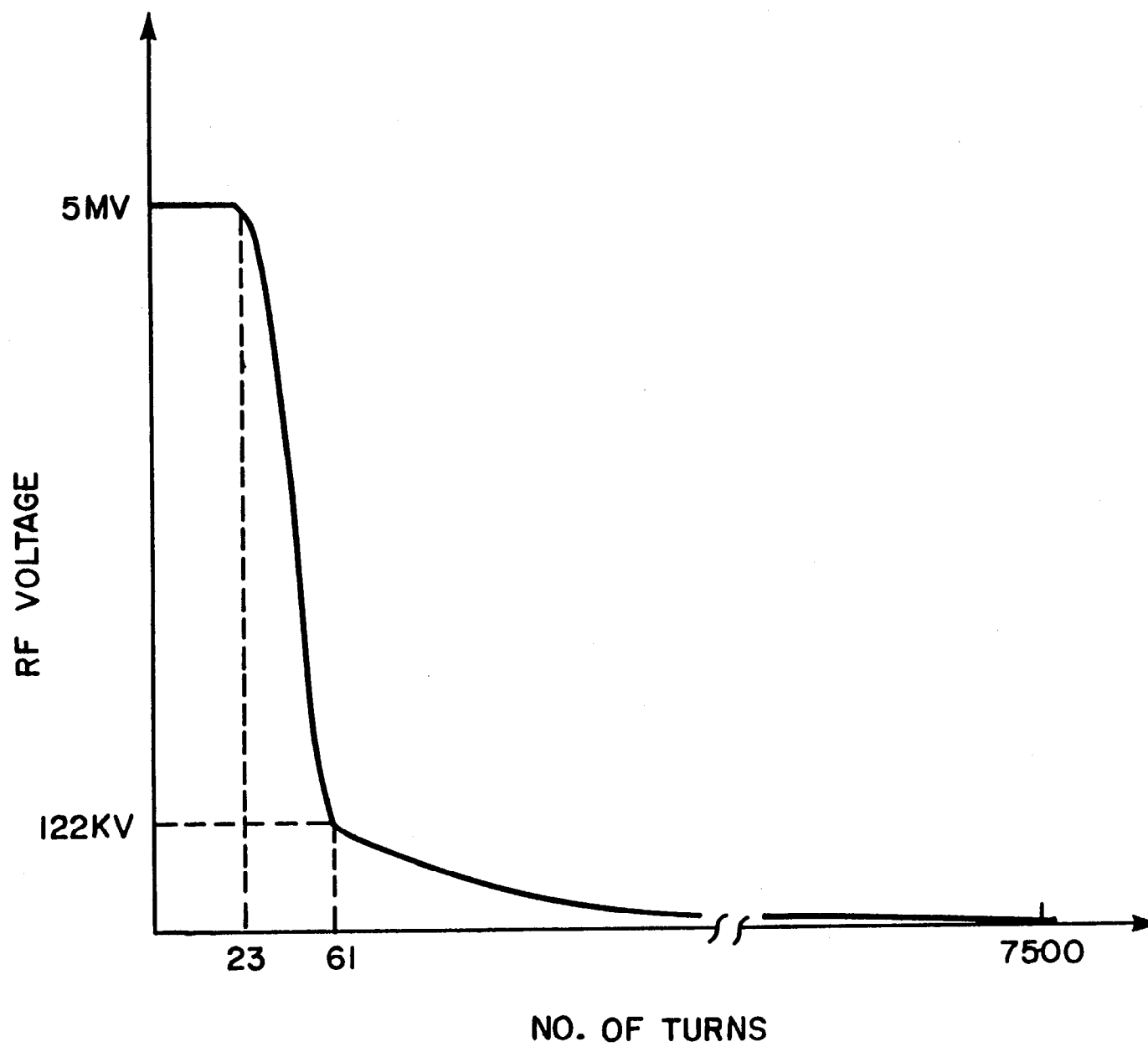(i) The bunch undergoes 1/4 of a synchrotron oscillation. Find the resulting σ_E.
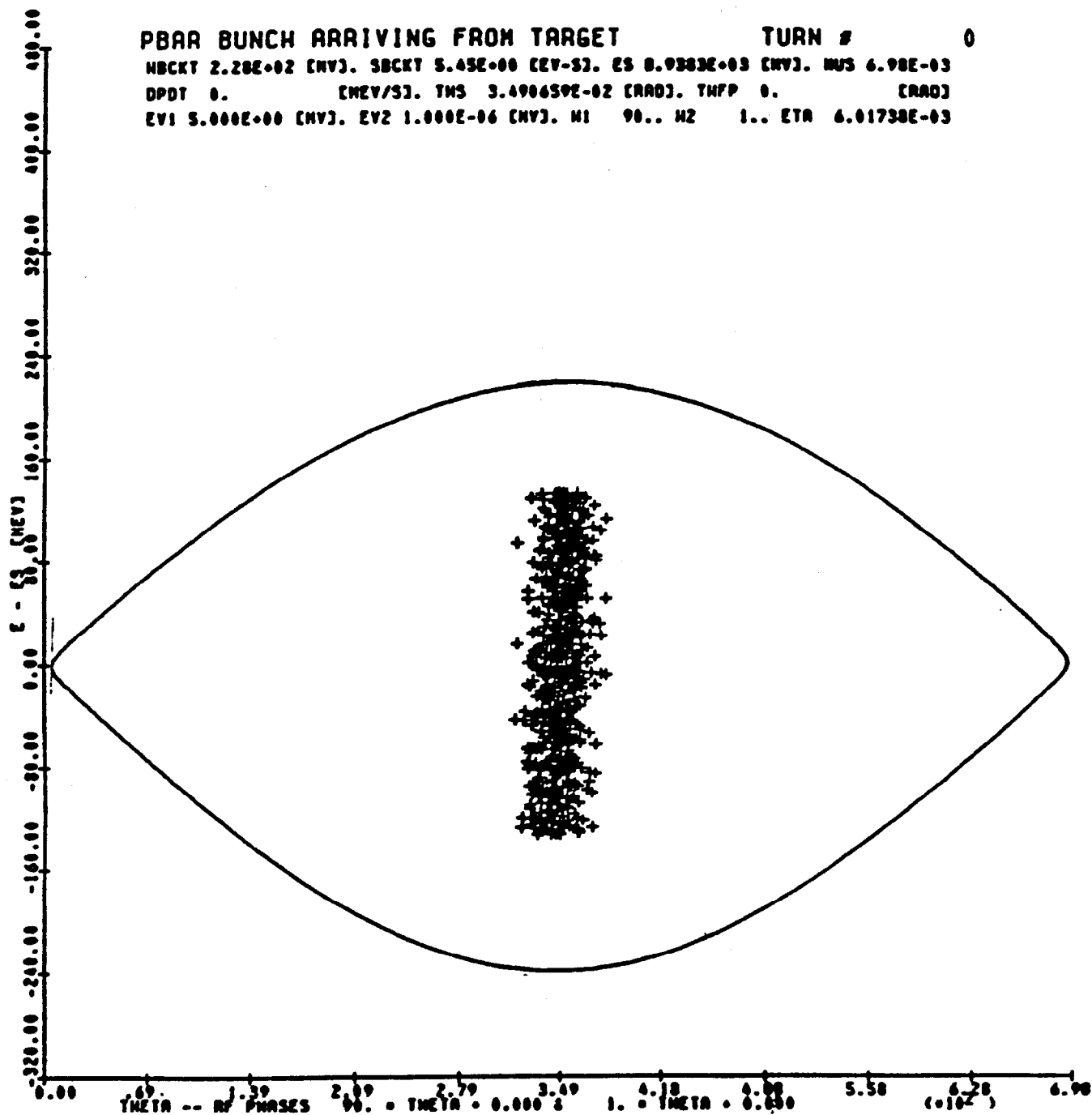
(ii) The RF voltage was reduced during the previous step to 122 kV to match the bucket to the bunch. The voltage is now adiabatically reduced to 5 kV. Find the final σ_E.
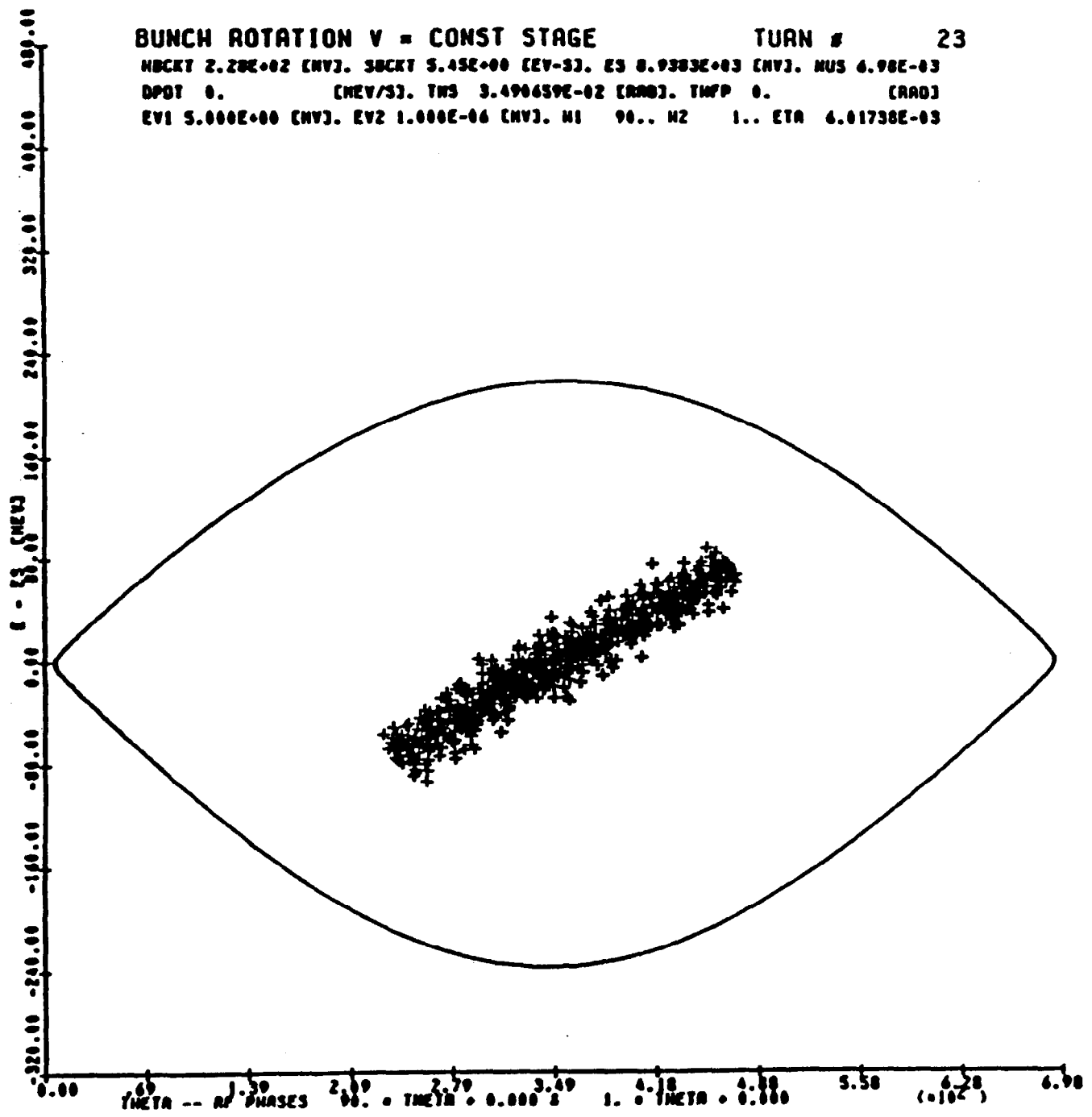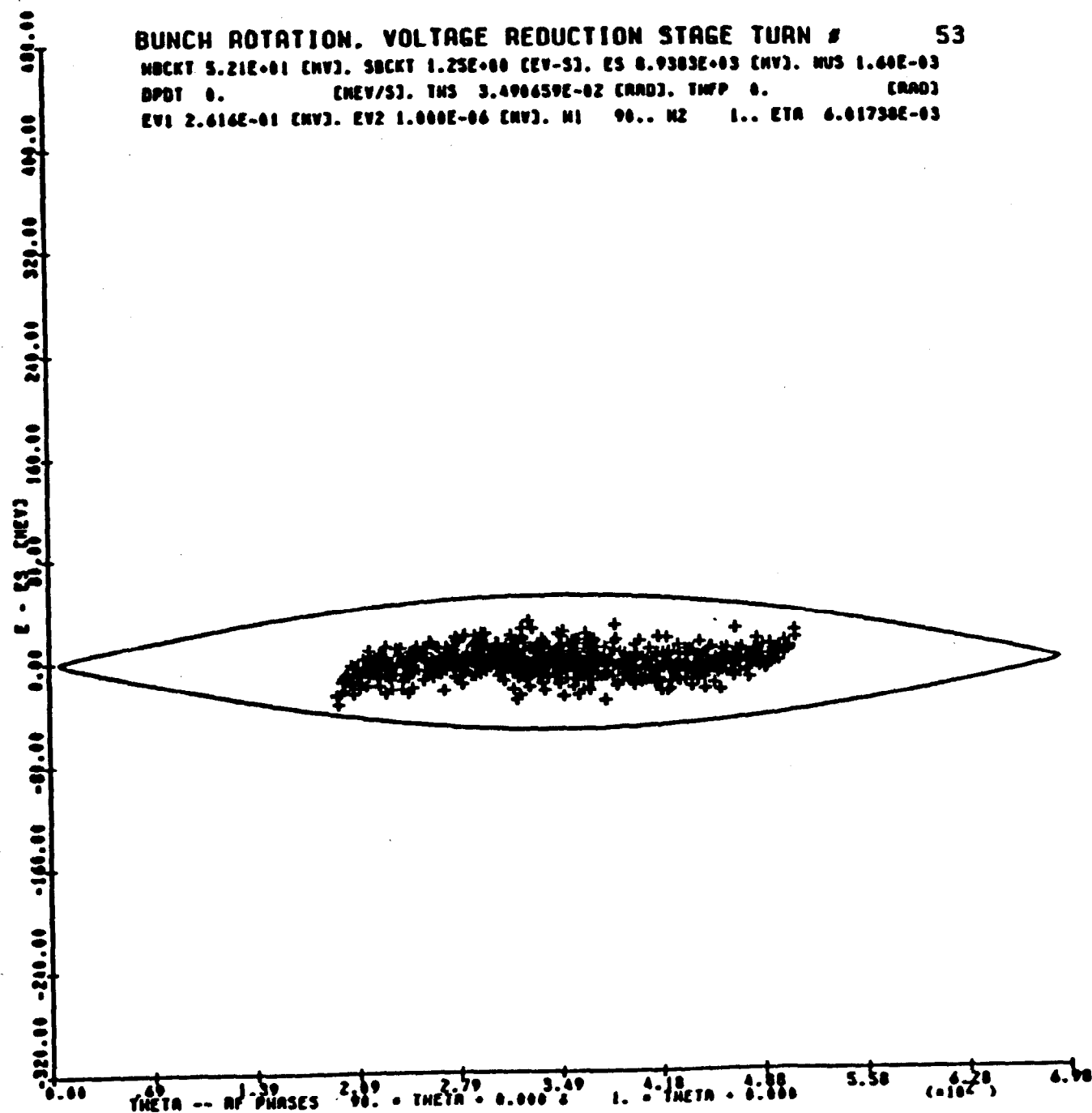
Solution: We use the equations developed in Example 3.2.

$$x = \frac{2\pi\beta^2 V_{RF} ehE}{|\eta|\cos\phi_s} \; ; \qquad E = 8.9 \text{ GeV}, \; V_{RF} = 5\text{MV}, \; \beta \sim 1$$

$$h = 90, \; |\eta| = .006, \; \phi_s \sim 1$$

$$x = \frac{2\pi(1)(5 \times 10^6)(8.9 \times 10^9)(90)}{.006} = 4.2 \times 10^{21} \text{ eV}^2$$

PBAR BUNCH ARRIVING FROM TARGET   TURN #   0

BUNCH ROTATION V = CONST STAGE   TURN #   23

BUNCH ROTATION, VOLTAGE REDUCTION STAGE TURN #   53

WBCKT 5.21E+01 [MV], SBCKT 1.25E+00 [EV-S], ES 8.9383E+03 [MV], WUS 1.60E-03

DPDT 0.   [MEV/S], TH3 3.490659E-02 [RAD], THFP 0.   [RAD]

EV1 2.616E-01 [MV], EV2 1.000E-06 [MV], N1   90.. N2   1.. ETA 6.01738E-03

E - ES [MEV]

THETA -- RF PHASES   90. ● THETA ● 0.000 S   1. ● THETA ● 0.000

The phase space trajectory followed by the edges of the bunch, for which σ_E = 180 MeV, corresponds to a time spread

$$\sigma_t' = \sigma_E T_0 / x^{1/2}$$

$$T_0 = \frac{2\pi R}{\beta c} = \frac{2\pi(8.3)}{(1)(3\times10^8)} \text{ sec} = 1.74\times10^{-6} \text{sec}$$

so

$$\sigma_t' = 180\times10^6 \times 1.74\times10^{-6} / \sqrt{4.2\times10^{21}} = 4.83 \text{ nsec}$$

After 1/4 of a synchrotron oscillation, the $\bar{p}$ bunch will have this time spread, but $s = 6\pi\sigma_E\sigma_t$ is conserved: $s = 6\pi (180\times10^6)$ $(.15\times10^{-9}) = 0.5$ eV-sec; thus,

σ_E' = energy spread after 1/4 synchrotron oscillation

$\quad\quad = s/6\pi\sigma_t = 0.5/6\pi(4.83\times10^{-9}) = 5.5$ MeV

(ii) The energy spread varies like $(V_{RF}E)^{1/4}$ during an adiabatic change. Thus

$$\sigma_E \rightarrow \sigma_E (122/5)^{-1/4} = 5.5(.450) = 2.5 \text{ MeV}$$

The energy spread is now

$$\Delta E/E \sim 2\sigma_E/E = \frac{2.5\times2}{8.9} \times 10^{-3} = 5.6\times10^{-4}$$

One may wonder why the RF manipulations described above could not have been done in the Accumulator: that is, why is a separate Debuncher ring necessary? One reason is simply that the RF system would inevitably diffuse the cooled core of the $\bar{p}$ stack to some extent. Another reason is the conflicting requirements on η which arise if the same ring is used for RF manipulations and stochastic cooling. To accomplish the required longitudinal phase space rotation, one must begin with an RF bucket which is larger than the initial $\bar{p}$ energy spread. The RF bucket half-height is

$$(\Delta E)_{bucket} = \left(\frac{eV2\beta^2 E}{h\pi|\eta|}\right)^{1/2}$$

We need h = 90 to capture the 83 $\bar{p}$ bunches; E = 8.9 GeV, β = 1, and V ~5 MV is a practical upper limit. So

$$(\Delta E)_{bucket} = 17.7/\sqrt{|\eta|} \text{ MeV}$$

For $|\eta|$ = .006, we get $(\Delta E)_{bucket}$ = 228 MeV, ~25% larger than the σ_E ~180 MeV corresponding to $\Delta p/\underline{p}$ ~4%, the largest reasonable momentum bite easily collected from the $\bar{p}$ target. Smaller values of $|\eta|$ give even larger buckets. But in the Accumulator, we need a large $|\eta|$ ~0.02, to optimize the stochastic cooling (see below). So the Accumulator bucket size is $(\Delta E)_{bucket}$ = 110 MeV, which would only accept $\Delta p/p$ ~1.8%. We would lose more than a factor of 2 in $\bar{p}$ collection without the Debuncher.

5. TRANSVERSE STOCHASTIC COOLING: TIME DOMAIN

5.1. <u>Simple statistical theory</u>

We have seen how the RF manipulations of the $\bar{p}$ beam in the Debuncher allow the narrow time spread of the $\bar{p}$'s (inherited from the protons) to be transformed into a narrow momentum spread. The second cooling ring, the Accumulator, benefits from needing only to accept this narrow $\Delta p/p$ spread. It would also benefit from a reduced demand on its transverse acceptance. If the transverse beam emittance in the Debuncher (~20π mm-mrad at injection) could be reduced without loss of beam, then the Accumulator acceptance could also be reduced. The required increase in the transverse phase space density is accomplished by a betatron stochastic cooling system in the Debuncher, which reduces the emittance to ~7π during the 2 seconds that the $\bar{p}$ beam remains in the Debuncher.

This betatron cooling system serves as a good example of stochastic cooling. We will develop a simple theory of cooling[18] and then illustrate with the Debuncher system as an example. The development is done in the time domain, and will refer to transverse cooling, although most of the equations will apply as well to longitudinal cooling when properly interpreted.

Conceptually, a transverse stochastic cooling system consists of a position-sensitive pickup located at one point in a storage ring, connected through an amplifier across a chord in the ring to a kicker.

POSITION-SENSITIVE PICKUP   PARALLEL-PLATE KICKER

$$\frac{n\lambda}{4}$$

n odd

BETATRON OSCILLATION
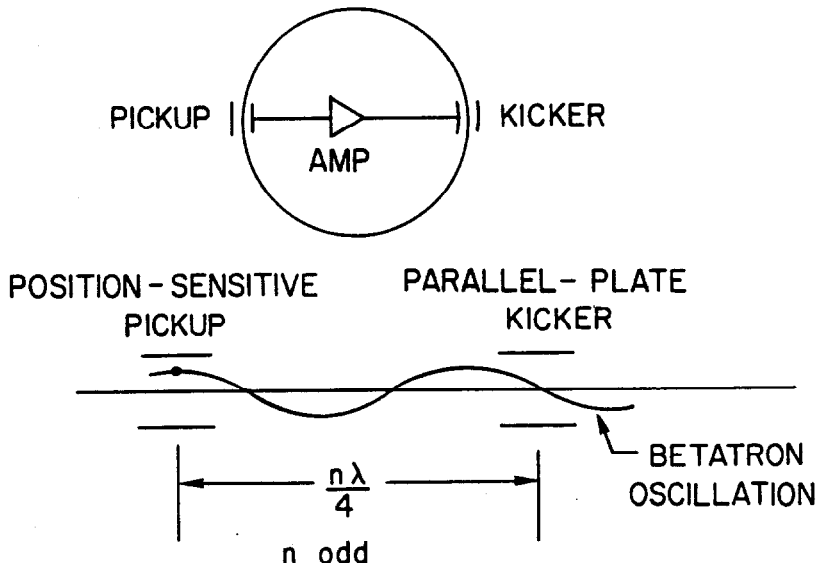
Ideally, the kicker and pickup should be located an odd number of betatron quarter-wavelengths apart. Let us imagine that there is only one $\bar{p}$ in the ring (the "test particle") and that the amplifier is perfect. Then the system "cools" the $\bar{p}$ as follows: a deviation of the test $\bar{p}$ position x_k^T on the kth turn from the center of the kicker is sensed, and a kick is applied to the test $\bar{p}$ at the kicker so that, on the next (k+1) turn, the test $\bar{p}$ is centered at the pickup:

$$x_{k+1}^T = x_k^T - g x_k^T$$

Here g is the "gain" of the system: it is a measure of the position correction at the pickup applied by the cooling system through the kicker. In this case, g = 1 gives $x_{k+1} = 0$ and the test $\bar{p}$ is "cooled" in one turn.

A real system has $N_{\bar{p}} \sim 10^8 - 10^{11}$ antiprotons in the ring at the same time, and uses real amplifiers which have thermal noise and a finite bandwidth. The inclusion of these effects leads to the basic equations for the rate of stochastic cooling. Each $\bar{p}$, passing the pickup, could be seen and corrected individually if the pickup-amplifier-kicker system had infinite time resolution. Actually, the finite time resolution σ_T results in a finite sampling time $T_s = 2\sigma_T$ for the system: $T_s = 1/2W$, where W = system bandwidth.
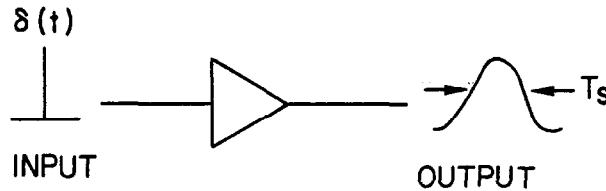
The finite sampling time means that the system responds not to one $\bar{p}$, but to a sample of size $N_s = (T_s/T_0) N_{\bar{p}}$, where T_0 = rotation period of a single $\bar{p}$. On the kth turn, the pickup senses the centroid of this entire sample (which we take to include our "test" $\bar{p}$):

$$\bar{x}_k = \frac{1}{N_s} \left[\sum_j x_k^j + x_k^T \right]$$

Here x_k^j is the coordinate of the jth particle in the sample; j is summed to $(N_s - 1)$. The kick delivered to the test particle now results in a new position on the next turn:

$$x_{k+1}^T = x_k^T - g [\bar{x}_k + \xi_k(N_s)]$$

Here $\xi_k(N_s)$ is the amplifier thermal noise seen by the N_s particles (including the test particle) on the kth turn, expressed in terms of the particle displacement at the input to the amplifier.

The change in the square of the test particle position at the pickup on the k→k+1 turn is

$$(x_{k+1}^T)^2 - (x_k^T)^2 = \Delta(x_k^T)^2$$

$$= (x_k^T - g(\bar{x}_k + \xi_k(N_s)))^2 - (x_k^T)^2$$

$$= -2g(\bar{x}_k + \xi_k(N_s))x_k^T + g^2(\bar{x}_k + \xi_k(N_s))^2$$

Expanding, we have

$$\Delta(x_k^T)^2 = -2g\left[\frac{x_k^T}{N_s}\sum_j x_k^j + \frac{1}{N_s}(x_k^T)^2 + x_k^T\xi_k(N_s)\right]$$

$$+ g^2\left\{\frac{1}{N_s^2}\left[\sum_j(x_k^j) + x_k^T\right]\left[\sum_i(x_k^i) + x_k^T\right]\right.$$

$$\left. + 2/N_s\left[\sum_j(x_k^j) + x_k^T\right]\xi_k(N_s) + \xi_k^2(N_s)\right\}$$

We now consider the result of averaging over a large number of samples. Each sample contains the test particle, together with a statistically independent collection of (N_s-1) other particles. Although the samples are statistically independent, they are identical in the sense that they all have the same mean (0) and the same $\sigma = x_{RMS}$. The average over samples of each term in the above expression gives

$$\overline{\Delta(x_k^T)^2} = \Delta(x_{RMS}^2)$$

$$\overline{x_k^T\sum_j x_k^j} = 0 \qquad \text{since the individual particles in the samples are statistically independent (there are no two-particle correlations)}$$

$$\overline{(x_k^T)^2} = x_{RMS}^2$$

$$\overline{x_k^T\xi_k(N_s)} = 0 \qquad \text{since the noise is statistically independent of the particles (there is no noise-particle correlation)}$$

$$\overline{\sum_j(x_k^j)\sum_i(x_k^i)} = \overline{\sum_j(x_k^j)^2} \qquad \text{since the particles are statistical independent, so all cross terms average to zero}$$

$$= (N_s - 1)x^2_{RMS}$$

$$\overline{\xi_k(N_s)\sum_j x^j_k} = 0 \quad \text{since the noise is statistically independent of the particles}$$

$$\overline{\xi^2_k(N_s)} = \xi^2(N_s), \text{ the mean-square thermal amplifier noise}$$

So, putting everything together, we have

$$\Delta(x^2_{RMS}) = -2g \ [0 + x^2_{RMS}/N_s + 0]$$

$$+ g^2 \left[\frac{1}{N_s{}^2} \ [(N_s-1)x^2_{RMS} + 0 + 0 + x^2_{RMS}] + 0 + \xi^2(N_s) \right]$$

$$= -2gx^2_{RMS}/N_s + g^2 \ [x^2_{RMS}/N_s + \xi^2(N_s)]$$

The time rate of change of x^2_{RMS} can be written as

$$\frac{dx^2_{RMS}}{dt} = \frac{\Delta x^2_{RMS}}{T_0} = \frac{-2gx^2_{RMS}}{N_s T_0} \left[1 - g/2 \left(1 + \frac{\xi^2(N_s)N_s}{x^2_{RMS}} \right) \right] \qquad (5.1.1)$$

The first term represents the coherent self-force (the "single particle cooling"). The second term results from noise due to other particles in the sample. The third term is due to the amplifier thermal noise.

To understand this fundamental result for the cooling rate, let us consider two limiting cases:

1. No amplifier noise. In this case the relative cooling rate of the RMS beam size x_{RMS} is

$$\frac{1}{\tau} = \frac{1}{x_{RMS}} \frac{dx_{RMS}}{dt} = \frac{1}{2} \frac{1}{x^2_{RMS}} \cdot \frac{dx^2_{RMS}}{dt}$$

$$\frac{1}{\tau} = - \frac{g}{N_s T_0} \ (1 - g/2)$$

This is a maximum for $g = 1$:

$$(1/\tau)_{max} = \frac{1}{2N_s T_0} = \frac{1}{2T_0} \left(\frac{T_0}{T_s N_p} \right) = \frac{1}{2T_s N_p}$$

$$= \frac{W}{N_{\bar{p}}} \quad \text{in terms of bandwidth}$$

For example, a bandwidth $W = 1$ GHz can cool $N_{\bar{p}} = 10^9$ with an optimal rate of $(1/\tau)_{max} \sim 1$ sec^{-1}. The larger the bandwidth, the faster the cooling rate.

2. All noise

    (a) all thermal amplifer noise

$$\frac{dx^2_{RMS}}{dt} = \frac{g^2 \xi^2(N_s)}{T_0}$$

Here x^2_{RMS} grows linearly with a slope $g^2 \xi^2(N_s)/T_0$

    (b) all Schottky noise

$$dx^2_{RMS}/dt = \frac{g^2 x^2_{RMS}}{N_s T_0}$$

Here x^2_{RMS} grows exponentially with a slope

$$\frac{g^2 x^2_{RMS}}{N_s T_0}$$

The ratio of these two slopes at any time is

$$R = \frac{\xi^2(N_s)}{(x^2_{RMS}/N_s)},$$

which is the "amplifier noise" term in our fundamental Eq. (5.1.1). This ratio is also just

$$R = \frac{\text{thermal noise power}}{\text{Schottky noise power}} \quad .$$

Since

$$R = \frac{\xi^2(N_s)}{x^2_{RMS}} N_s = \frac{\xi^2(N_s) T_s N_{\bar{p}}}{x^2_{RMS} T_0} = \frac{\xi^2(N_s)}{2W} \frac{N_{\bar{p}}}{x^2_{RMS} T_0}$$

and $\xi^2(N_s)$, being a white noise source, is proportional to W, we see that R is independent of the bandwidth. Hence, even in the presence of amplifier noise, larger bandwidth increases the cooling rate.

The complete cooling rate in Eq. (5.1.1) can be integrated by substituting $y = x_{RMS}^2$. We have

$$dy/dt = - \frac{2gy}{T_0 N_s} \left(1 - g/2 \left(1 + \frac{N_s \xi^2 (N_s)}{y}\right)\right) = -Ay + B$$

with

$$A = 2g/T_0 N_s (1 - g/2), \quad B = \frac{g^2 \xi^2 (N_s)}{T_0}$$

Then

$$\int_{y_0}^{y} \frac{dy}{-Ay + B} = \int_0^t dt$$

$$- \frac{1}{A} \ln(B - Ay) \Big|_{y_0}^{y} = t$$

$$\frac{B - Ay}{B - Ay_0} = e^{-At}, \quad Ay - B = (Ay_0 - B)e^{-At}.$$

For $A > 0$ (which requires $g < 2$), $Ay - B$ goes to zero exponentially so

$$y \to B/A = \frac{g \xi^2 (N_s) N_s}{2(1 - g/2)} = (x_{RMS}^2)_\infty$$

If the beam size is initially less than $(x_{RMS}^2)_\infty$, it grows due to thermal amplifier noise; if it is initially greater, it can be reduced. If g is too large ($g > 2$) it will always grow exponentially. The optimum gain for a maximum cooling rate at $t = 0$ can be obtained from Eq. (5.1.1), written as

$$\frac{1}{y} dy/dt \Big|_{t=0} = \alpha g (1 - \beta g)$$

with

$$\alpha = - \frac{2}{T_0 N_s}, \quad \beta = \frac{1}{2} \left(1 + \frac{N_s \xi^2}{y_0}\right)$$

This is a minimum for

$$g = 1/2\beta = \frac{1}{1+N_s\xi^2/(x^2_{RMS})_0} < 1 \text{ for } \xi^2 \neq 0$$

The optimum cooling rate for y at t = 0 is

$$\frac{1}{\tau} = \frac{-1}{y} \left. dy/dt \right|_{t=o} = -\alpha/2\beta(1-1/2) = -\alpha/4\beta = \frac{1}{T_0 N_s} \frac{1}{1+N_s\xi^2/(x^2_{RMS})_0}$$

5.2. Computer model

Many of the above ideas can be illustrated, and the important concept of mixing can be introduced, in a simple computer model of stochastic cooling. This model is easy to implement on any computer for which a random number generator is available: experimenting with the parameters of the model can provide useful insights into the stochastic cooling process. In this model, we start with a collection of N— particles, randomly distributed in x over the range ± 1, and in ϕ^p(which corresponds to the phase angle in a ring) over the range 0 to 360°. The range of ϕ is divided into 10 bins; on average, each bin contains N—/10 = N_s particles. These bins correspond to the samples in our^{p}previous analysis.
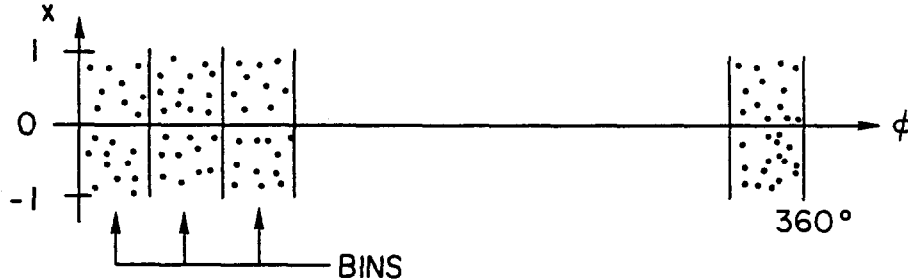
We implement the cooling in x by the following steps:
 (1) We calculate $\bar{x}$ for each bin.
 (2) We cool the particles in each bin $x_i \rightarrow x_i -g\bar{x}$. This constitutes one "turn" of cooling. If we now repeat the process on the next "turn", nothing further will happen, since all the bins have $\bar{x} = 0$ exactly. To continue cooling, we must introduce "mixing" after step (2):
 (3) We mix the samples (bins) by shifting the phase of each particle.

$$\phi_i \rightarrow \phi_i + \delta\phi + \gamma x_i$$

This redistributes the particles in the bins: a complete redistribution on each turn results in complete statistical independence of the bin populations on subsequent turns, which corresponds to the condition of statistical independence of the samples made in our derivation of the cooling rate above.

For a real stochastic cooling system, the $\delta\phi$ mixing term, corresponding to a direct phase shift on each turn, has no physical analog. However, in momentum cooling, there is a physical realization of the γx_i term. If we interpret x_i as the fractional momentum deviation from a central momentum, then x_i and $\Delta\phi_i$ per turn are related through η:

$$\Delta\phi = \omega_o \Delta t = \omega_o T_o \frac{\Delta p}{p} |\eta| = 2\pi x |\eta|$$

Thus γ corresponds physically to $2\pi |\eta|$.

After mixing, we return to step (1) for another turn. A simple BASIC program which implements this model is the following:

```
1 REM N1=#PARTICLES;N2=#TURNS BETWEEN PRINTOUTS;N3=#PRINTOUTS;
  W=#BINS/TURN
2 REM A=#DEGREES PHASE ADVANCE/TURN FOR DELTA R=1
3 REM G=GAIN I.E.  DELTA R=G*(FIRST MOMMENT)
4 REM E0= BIAS ON DELTA R;
10 N1=200
11 N2=20
12 N3=50
13 A=0
14 G=1
15 W=10
16 E0=0
17 A0=3.1
50 DIM P(1000,4),S(100),N(100),S2(100)
55 DIM H(200)
90 MAT P=ZER(N1,4)
91 MAT S=ZER(W)
92 MAT N=ZER(W)
93 MAT S2=ZER(W)
100 FOR I=1 TO N1
110 P(I,1)=I
120 P(I,2)=2*RND(0)-1
130 P(I,3)=360*RND(0)
140 NEXT I
200 PRINT "#PARTICLES=";N1
210 PRINT "#TURNS=";N2*N3
220 PRINT "#TURNS/PRINTOUT=";N2
230 PRINT "AZIMUTHAL BINS=";W
240 PRINT "GAIN=";G
250 PRINT "PHASE/TURN=";A
255 PRINT"CONSTANT PHASE/TURN";A0
260 PRINT"B1AS=";E0
```

```
300 PRINT"TURN NO.","MEAN R","SIGMA SQRD"
4999 REM FNA SORTS PHI INTO W BINS
5000 DEF FNA(X)
5010 FOR I=1 TO N1
5030 Y=P(I,3)
5040 Y=Y-360*INT(Y/360) ' SETS PHI IN RANGE 0 TO 360
5042 P(I,3)=Y
5045 FOR K=1 TO W-1 ' SORTS ON PHI
5050 IF Y=>K*360/W THEN 5100
5060 P(I,4)=K
5070 GO TO 5200
5100 NEXT K
5110 P(I,4)=K
5200 NEXT I
5400 FNEND
5500 Z9=FNA(1)
5510 GO TO 9000
5999 REM FNB FINDS AVERAGE RADIUS IN W PHI BINS
6000 DEF FNB(X)
6010 FOR K=1 TO W
6015 S2=0
6016 S=0
6020 S(K)=0
6021 N(K)=0
6022 S2(K)=0
6030 NEXT K
6040 FOR I=1 TO N1
6050 B=P(I,4)
6060 S(B)=P(I,2)+S(B)
6070 N(B)=N(B)+1
6071 S2(B)=S2(B)+P(I,2)**2
6080 NEXT I
6090 FOR K=1 TO W
6100 S(K)=S(K)/N(K)
6101 S2(K)=S2(K)/N(K)
6102 S2(K)=S2(K)-S(K)**2
6110 S2=S2+S2(K)
6120 S=S+S(K)
6130 IF ABS(S(K))>E0 THEN 6160
6140 H1=H1+1
6150 S(K)=0
6160 NEXT K
6170 S=S/W
6180 S2=S2/W
6200 FNEND
6499 REM FNC MOVES RADIUS BY AVERAGE OF S(W)
6500 DEF FNC(X)
6510 FOR I=1 TO N1
6516 C=S(P(I,4))
6520 P(I,2)=P(I,2)-G*C 'CHANGES RADIUS
6530 P(I,3)=P(I,3)+A*P(I,2) ' CHANGES PHI
6535 P(I,3)=P(I,3)+A0
6540 NEXT I
```

```
6550 FNEND
9000 FOR L=1 TO N3
9005 FOR J=1 TO N2
9010 Z9=FNA(1)
9020 Z9=FNB(1)
9030 Z9=FNC(1)
9100 NEXT J
9300 GO TO 9500
9400 FOR J1 =1 TO W
9410 PRINT S(J1),
9420 NEXT J1
9430 PRINT
9440 FOR J1=1 TO W
9450 PRINT N(J1),
9460 NEXT J1
9470 PRINT
9480 FOR J1=1 TO W
9490 PRINT S2(J1),
9495 NEXT J1
9500 REM
9520 PRINT L*N2,S,S2,H1
9530 H1=0
9600 NEXT L
9700 PRINT"NUMBER OF TIMES  BIAS";H1
10000 END
```
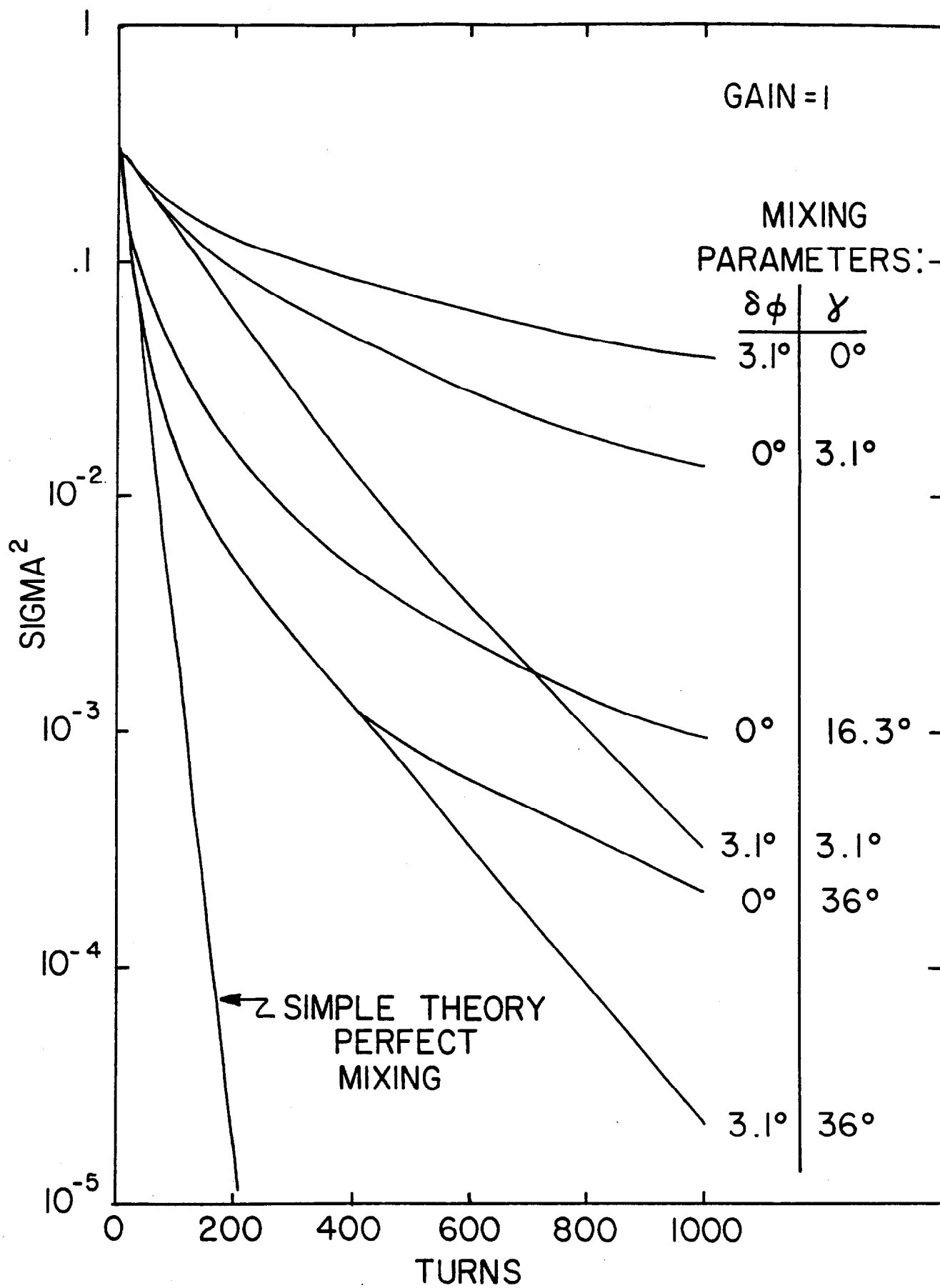
If our cooling rate theory applies, we would expect that, for $g = 1$, the rate of cooling of σ^2 would be

$$\frac{1}{\tau} = \frac{1}{T_0 N_s} \, , \; \sigma^2 = \sigma_0^2 e^{-t/T_0 N_s}$$

If $N = t/T_0 =$ turn number, then $\sigma^2 = \sigma_0^2 e^{-N/N_s}$. Figure 5.2.1 shows the results of the cooling of σ^2 vs N, for $N_{\bar{p}} = 200$ ($N_s = 20$). The curves are labelled by the values of the mixing parameters $\delta\phi$ and γ. We would expect a variation of σ^2 like $e^{-N/20}$; typically, the cooling is considerably slower, except for $\gamma \sim 36°$. This is because, except in this latter case, the bin populations are not completely redistributed on each turn: there is substantial coherence in the bins from turn to turn, which of course slows down the cooling. For $\gamma \sim 36°$, we essentially redistribute randomly each entire bin population into neighboring bins: this tends to destroy all coherence, and (at least initially) we observe the cooling rate predicted by our simple theory, which assumes perfect mixing.

5.3. Mixing

In a real cooling ring, we will have both "good" and "bad" mixing. To get statistical independence of the samples, we want to loose all coherence between turns: but losses of order in the half-turn between pickup and kicker will result in the wrong population being kicked. This is "bad" mixing. We thus have contradictory requirements: we want to keep all order between pickup and kicker, but loose all order between kicker and pickup. One must make some compromise between these demands in the design of a cooling ring.
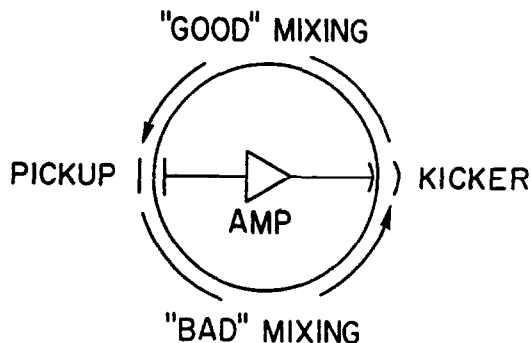
Mixing results from the finite momentum spread and the dependence of revolution time on momentum. The correct inclusion of the effects of both good and bad mixing in stochastic cooling theory is best done in the frequency domain analysis. However, a simple argument which illustrates the basic idea of good mixing can be made in the time domain. The time spread of a $\bar{p}$ sample, seen by a system

of bandwidth W, is T_s = 1/2W. The mixing of samples between turns is determined by the ratio of this sample time width to the time spread $(\Delta T)_p$ which occurs in one turn due to the finite momentum spread $\Delta p/p$?

$$|\eta| = (\Delta f/f)/(\Delta p/p) \text{ so } (\Delta T)_p = T_0(\Delta p/p)|\eta|$$

Thus the ratio

$$M = T_s/(\Delta T)_p = \frac{T_s}{T_0|\eta|(\Delta p/p)} = \frac{f_0}{2W|\eta|\Delta p/p}$$

is a measure of the mixing. If M ~ 1, the mixing is good; but if M >> 1, then T_s >> $(\Delta T)_p$, there is substantial coherence of samples from turn to turn, and the cooling rate is reduced from the optimum for perfect mixing (as in the computer model above). For that part of the sample which is coherent from turn to turn, the single particle cooling effect is essentially zero; but the beam shot noise still contributes on each turn to beam heating. Inclusion of mixing in the cooling results effectively in the beam noise term being enhanced by the factor M. The cooling rate in Eq. (5.1.1) then becomes

$$\frac{1}{x^2_{RMS}} \frac{dx^2_{RMS}}{dt} = \frac{-2g}{N_s T_0}(1-Mg/2) + \frac{g^2\xi^2(N_s)}{T_0 x^2_{RMS}}$$

For cooling we require Mg < 2.

5.4. Examples

Example 5.1: The transverse cooling in the Debuncher takes place with $\eta \simeq$ .006, $\Delta p/p$ ~.2%, and utilizes a bandwidth of W ~2 GHz.

(a) Estimate the mixing factor M, using the simple expression derived above.

(b) Assuming negligible amplifier noise contributions, find the optimum gain.

(c) Estimate the cooling rate of the betatron emittance ϵ at the optimum gain, for $N_{\bar{p}}$ = 10^8. If the initial emittance is 20π mm-mrad, find the emittance after 2 sec, when transfer to the Accumulator takes place.

Solution: (a) Using

$$M = \frac{f_0}{2W|\eta|\Delta p/p}$$

and

$$f_0 = \frac{1}{T_0} = \frac{1}{1.74 \times 10^{-6}} \text{ Hz} = .575 \text{ MHz (from Example 4.1)}$$

we have

$$M = \frac{.575 \times 10^6}{2 \times 2 \times 10^9 \times 6 \times 10^{-3} \times 2 \times 10^{-3}} \simeq 12$$

Since M > 1, we have a poor mixing situation. This is related to the small value of $|\eta|$ which is necessary for the RF bunch rotation in the Debuncher.

(b) For no amplifier noise, the cooling rate for x^2_{RMS} is

$$1/\tau = \frac{2g}{N_s T_0} (1 - Mg/2)$$

this peaks at g = 1/M, so we need g = 1/M $\simeq$ 0.083 for optimum cooling in the Debuncher.

(c) The betatron emittance $\epsilon = 6\pi\sigma_x^2/\beta$. Here σ_x is the RMS betatron amplitude. The betatron oscillations reduce the cooling rate of the mean-square amplitude σ_x^2 by a factor of 2 relative to the rate of x^2_{RMS}. Thus

$$\frac{1}{\epsilon}\frac{d\epsilon}{dt} = \frac{1}{\tau_\epsilon} = \frac{g}{N_s T_0}(1-Mg/2) = \frac{1}{MN_s T_0}\left(\frac{1}{2}\right) \text{ for } g = \frac{1}{M}$$

$$1/\tau_\epsilon = \frac{1}{2T_s}\frac{1}{M}\frac{1}{N_{\bar{p}}} = \frac{W}{N_{\bar{p}}}\frac{1}{M}$$

$$= \frac{2 \times 10^9}{10^8}\frac{1}{12} = 1.7 \text{ HZ}$$

After 2 seconds, ϵ is reduced by a factor $e^{-t/\tau_\epsilon} = e^{-2(1.7)} = 0.03$ to $20\pi(0.03) = .6\pi$.

The expected transverse cooling in the Debuncher is shown in Fig. 5.4.1.[2]

6. THE ACCUMULATOR

We have now considered the role of the Debuncher and a simple time domain picture of cooling. We must next pass on to the Accumulator whose primary role is to accept and collect particles from the Debuncher. In the FNAL Source the Debuncher supplies 7×10^7 $\bar{p}$ with an energy density of 5 $\bar{p}$/eV every two seconds to the Accumulator. However, it is necessary to collect 10^{11} $\bar{p}$ at a density
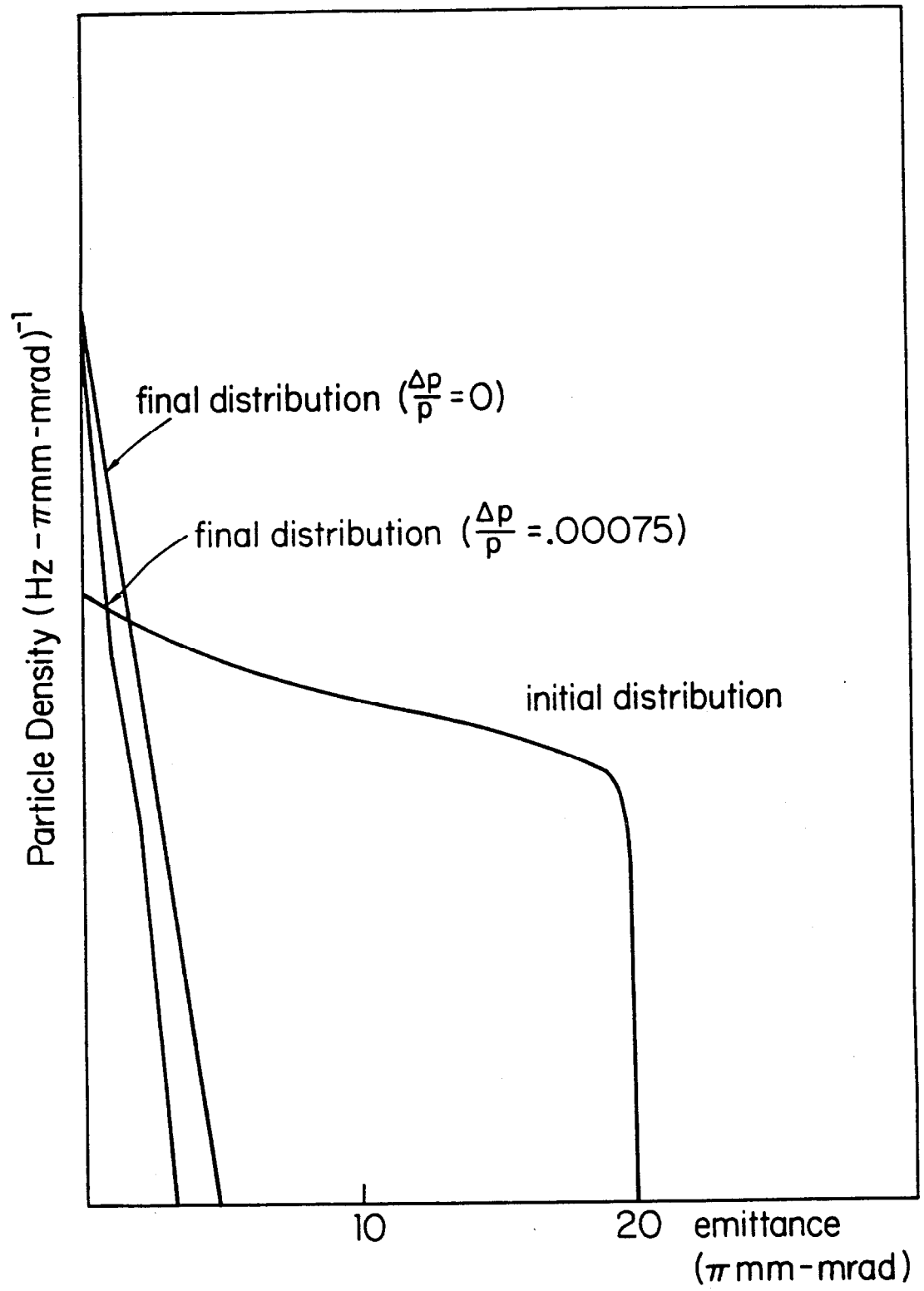
of 10^5 $\bar{p}$/eV in order to achieve a $\mathscr{L} = 10^{30}$. It was the cleverness of Van der Meer that taught us how to accomplish this feat.

6.1. Momentum stacking

We consider a simple example to explain the basic idea of the system. Suppose we have particles with an initial distribution of energies $\psi(E)$ as shown circulating in a machine.
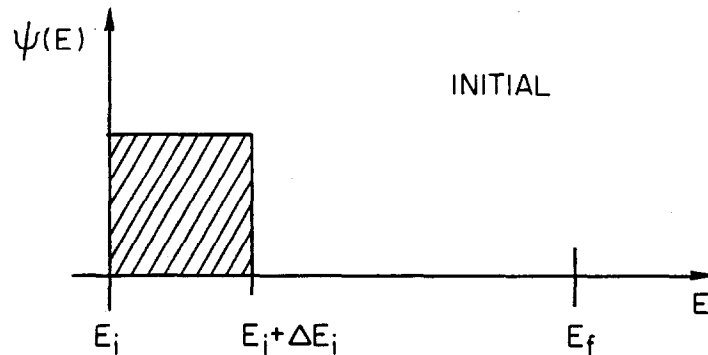

Now suppose we turn on a momentum cooling system whose central energy is E_f, i.e., if a particle is at E_f, it receives no correction. This system will move the group of particles from E_i, $E_i + \Delta E_i$ to $E_f \pm \delta$ as shown below
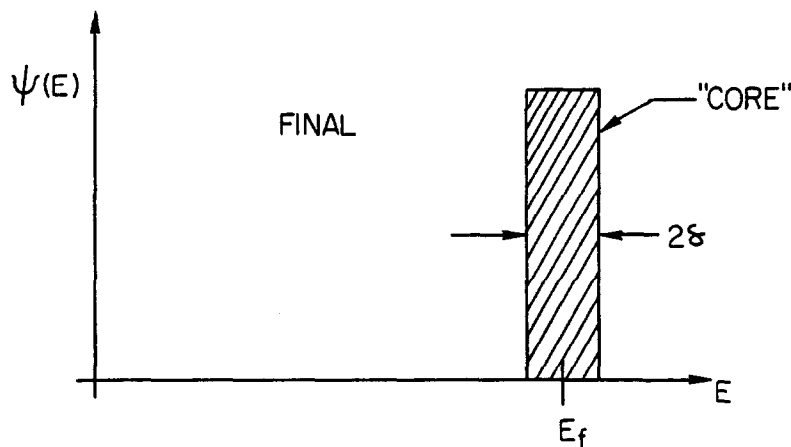
If we inject a second group of particles between E_i, $E_i + \Delta E_i$, these too will be moved to E_f and added to the core. Now consider the case where this becomes a continuous process. Every two seconds particles are injected at E_i and start to move to E_f. The cooling must be strong enough at E_i to move each batch of particles out of the way before the next is injected so that the injection process will not destroy the previous batch.

The above picture is simple minded but conveys the essence of the idea of stacking. The batches are not moved from E_i to E_f in a short time, but rather the core has an exponential tail toward injection and the density change is actually as shown below.

$\psi(E)$

$10^5 \ \bar{P}/eV$

INJECTION

TAIL   CORE

$7 \ \bar{P}/eV$

$E_i \longleftarrow \quad \sim 100 \quad \longrightarrow E_f$

MeV

E
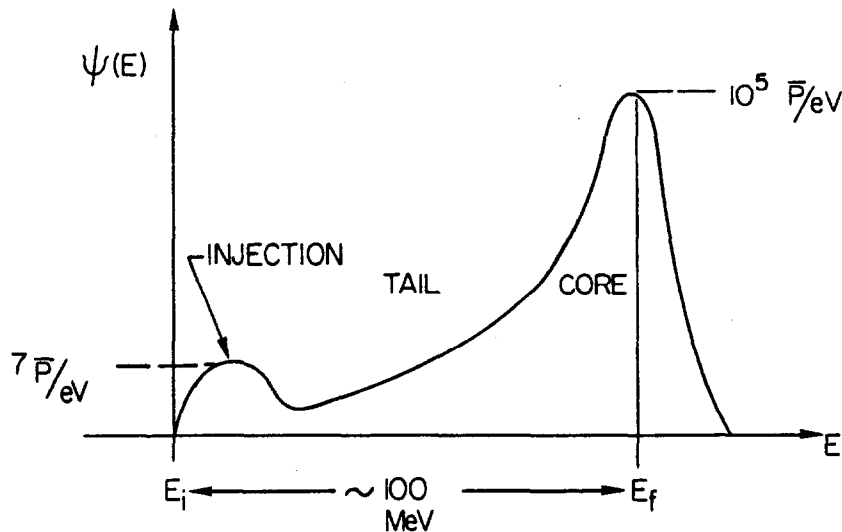
The momentum system consists of two parts: a stacking system and a core system which operate at different frequencies (FNAL stacker 1-2 Ghz, core 2-4 Ghz). In addition, it is necessary to have transverse cooling in both planes to further compress transverse phase space and to counteract any forces that would tend to blow up the beam during its long stay in the Accumulator (up to 24 hours).

6.2. Injection and extraction

It is now clear that the Accumulator must also have ways to inject beam into it and extract beam from it. The injection process is a simple one turn injection at either an outer or inner radius depending on which way the stack grows. The extraction is done by means of a very low level RF system. This system is centered on the core frequency and non-adiabatically turned on to capture particles in the core. The frequency is then adiabatically changed to move the particles to an extraction orbit where they are removed with a one turn extraction system well shielded from the core. The details of this process, which is an interesting subject in its own right, will not be pursued further in this article.

We must now develop more sophisticated mathematical techniques to describe the above complicated processes. To proceed we will have to develop our understanding of these processes in the frequency domain rather than the simplified picture presented in Section 5 for

the time domain. We must also understand how to treat pickups and kickers and finally we need the mathematical apparatus to handle a particle density function $\psi(E)$ instead of just the moments of the distribution. These subjects are treated in turn in the following sections.

7. FREQUENCY DOMAIN

The discussion in Section 5 has all been based on the time domain. The ideas are easy to understand intuitively, but more extended analytical development is easier if we now make use of the frequency domain. We will first obtain the Fourier spectrum of a single particle rotating in a machine. Next, we will derive the response of pickup electrodes to such a particle, and finally we will explore the response of a beam of particles to signals applied to kicker electrodes. We will then be in a position to derive the Fokker-Planck equation for an ensemble of particles in a storage ring. This is the mathematical tool that enables us to discuss the Accumulator ring, which takes many bunches of pre-treated particles from the Debuncher and increases their density in phase space sufficiently to be used in a collider.

7.1. Spectrum of a single particle

Consider a single particle of charge e rotating in an orbit at frequency f_0. This represents a current which is a periodic delta function. If the particle crosses $\phi = 0$ at $t = 0$, we can write its current as

$$I(t) = ef_0 + 2ef_0 \sum_{n=1}^{\infty} \cos n \omega_0 t$$

A second particle at a different phase ϕ_1 and the same period f_0 will generate no new frequencies, but will simply modify the amplitudes of the various components $n\omega_0$ already present.

However, suppose we have a particle with a different momentum. Its frequency will be different by an amount determined by the machine lattice function

$$\eta = \frac{p}{T} \frac{dT}{dp} = - \frac{p}{f} \frac{df}{dp}$$

If the second particle differs by δp from the first, then

$$\omega = \omega_0 - \eta \omega_0 \frac{\delta p}{p} .$$

This particle will then generate a second set of frequencies which are all multiples of ω.

7.2. Schottky spectrum

Now consider an ensemble of particles of all different phases and energies. We can compute the rms average of the current and in this process, all of the interference terms between particles at the same energy but different phase as well as between those at different energies will average out to zero. As a result, the beam power spectrum is simply proportional to the number density of particles per unit frequency. We can specify a distribution function of the beam by

$$dN = \psi(E)dE$$

where E is the energy. This can be converted to a frequency spectrum by the use of η which relates frequency and energy

$$dE = p/E \; dp = \beta \; dp$$

$$d\omega = -\eta\omega_0 dp/p = - \frac{\eta\omega_0 EdE}{p^2}$$

$$\psi(\omega) = \psi[E(\omega)] \left(\frac{p\beta}{\eta\omega_0}\right) d\omega \quad .$$

The spectrum $\psi(\omega)$ is the spectrum of fundamental rotation frequencies. The power spectrum of a set of particles is called the "Schottky spectrum." Consider a case where this spectrum is rectangular and extends from ω_0 to $\omega_0 + \Delta\omega$. The complete power spectrum of the beam will then look as follows:
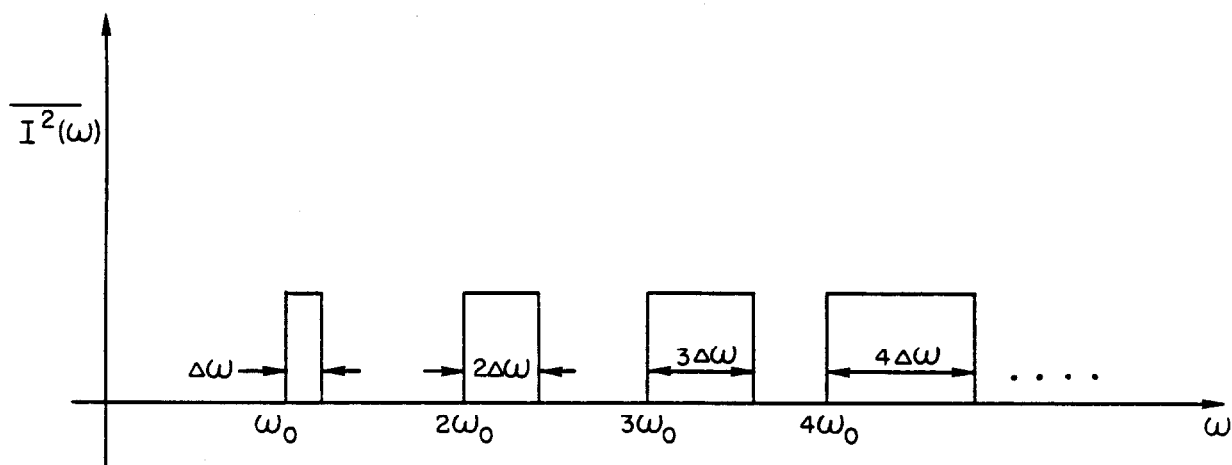
The spectral density in each Schottky band is a reproduction of that in the fundamental. A spectrum analyzer can be used to observe the power spectrum and the momentum spectrum of the particles can be

derived from such a measurement. This procedure is called a "Schottky scan" and is an extremely powerful diagnostic tool.

We observe a second feature of the spectrum shown above. When the harmonic number is great enough, the bands begin to overlap, and the simple single valued relation between the power spectrum and the particle density spectrum is lost. This occurs when

$$n \, \Delta\omega = \omega_o$$

or

$$n \geq \frac{\omega_o}{\Delta\omega} = \frac{p\beta}{\eta\Delta E}$$

8. PICKUPS AND KICKERS

We must now consider how one couples energy out of and into a circulating beam--i.e., pickups and kickers. By means of reciprocity theorems, it can be shown that there is a close relationship between the way an electrode exposed to the beam behaves as a pickup or as a kicker. An electrode that efficiently extracts energy from a beam can also couple energy into such a beam.

8.1. Ferrite transformers

There are three types of electrodes in common use. The first and easiest to understand is a ferrite core beam transformer shown schematically below:
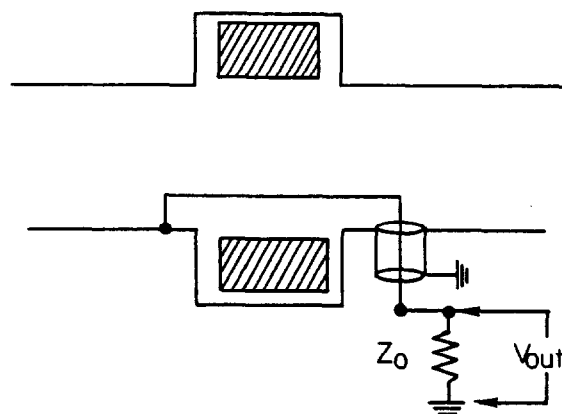
This can be viewed as a one-to-one current transformer. The ferrite must have adequate high frequency response, and the enclosure carefully designed for good transient response. The equivalent circuit of such a transformer is:
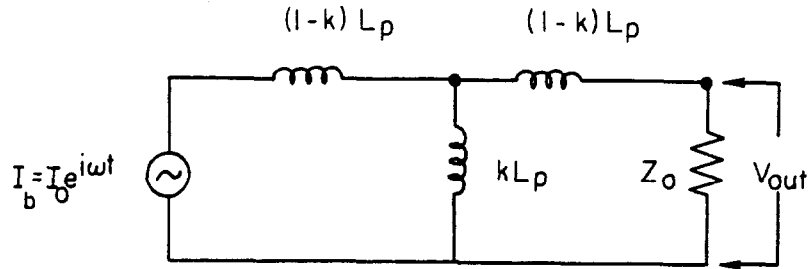
By making k very close to 1 the leakage inductance $(1-k)L_p$ becomes small and if good high frequency ferrite is used, the transient response can be extended to rise times of the order of one nanosecond. The shunt inductance is the one turn inductance of the core, and it must be large enough so that

$$\omega L_p > Z_o$$

for the lowest frequency that is required to be measured. In the mid-band range, we have

$$V_{out} = Z_o I_b$$

The transient response for transit by a single particle is
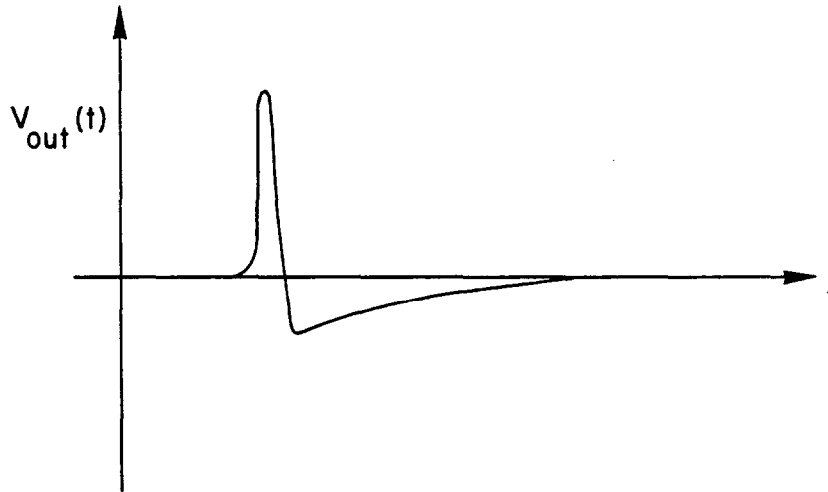
The width is determined by the ferrite high frequency response, and the tail has a time constant $\tau = L_p/Z_o$. The area must be zero, of course.

The transformer couples to longitudinal variations in the beam charge density. We have idealized this by dealing with a single Fourier component, $I_o \sin\omega t$. The analysis of the beam response to a voltage applied to the transformer (i.e., kicker) is a little tricky and will be treated in the section on beam feedback.

8.2. Loop couplers

Next we consider electrodes in the form of a transmission line whose one conductor is exposed to the beam, as shown below.


SIDE VIEW
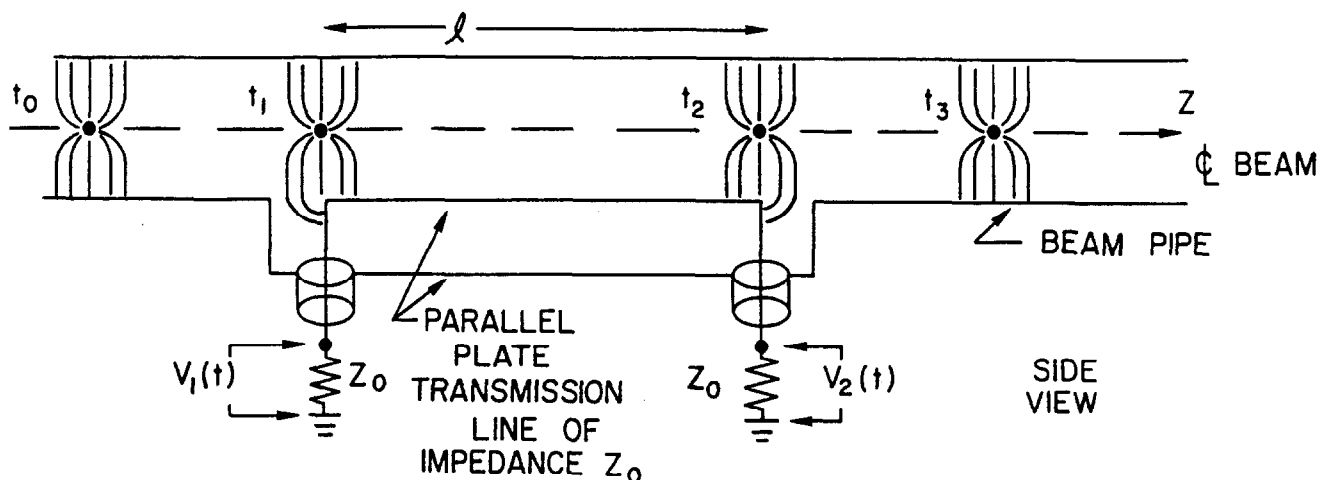
A charged particle, its field relativistically contracted, is shown at various times t_0 to t_3 as it traverses the structure. The end view shows a cross section of the electric field.

END VIEW
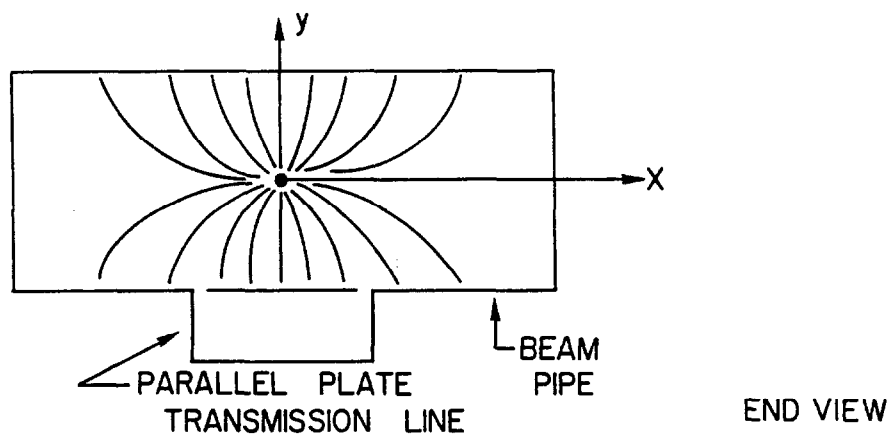
The configuration of this electric field in the xy plane closely approximates a two-dimensional distribution -- particularly when we consider the low frequency Fourier components. Remember that as a beam of particles in a grounded conductor becomes relativistic, the field configurations approach closely those of the TEM modes of a transmission line with the charge and current of the beam playing the role of one of the conductors of the two conductor system. Indeed, the response of these structures can be approximately measured by

replacing the beam by a small wire carrying a current $I_o \sin \omega t$. This approximation must break down for the higher order modes and is certainly wrong for TE and TM moes. It is nevertheless a useful measuring technique.

We now analyze the time response. At time t_1 when the lines of flux jump onto the plate (and the magnetic field lines cut the end conductor and, hence, loop the coupler), a voltage pulse $V(t)$ must appear on the line, $V(t) = \alpha I_b(t) Z_o$, where α is a geometrical coupling factor.
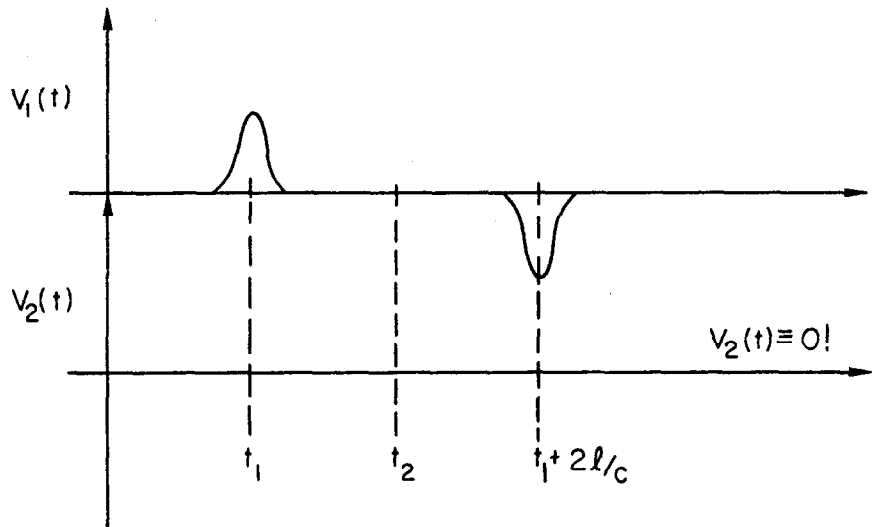
This pulse splits into two equal pulses:

$$V(t_1) = V^+(t) + V^-(t)$$

$$V^+(t_1) = V^-(t_1) = 1/2 \, \alpha I_b(t_1) Z_o$$

The pulse $V^-(t)$ travels down the output line and appears across Z_o. The pulse $V^+(t)$ travels down the line with the beam and arrives at the end approximately in phase with the beam particle (we assume a particle with $\beta \sim 1$ and a line with velocity of propagation $\sim c$). As the particle passes the end, the action is the reverse of the upstream end. A pulse $-V(t_2)$ is induced which splits into two waves. The negative wave into Z_o cancels the positive going wave $\alpha/2 \, Z_o I_b(t)$ giving $V_2(t) = 0$ at the terminating resistor Z_o. The negative traveling wave appears at $V_1(t)$ at $t = t_1 + 2\ell/c$. Thus, the output signal is always from the upstream end of the line and is independent of the termination at the downstream end. The downstream end is usually terminated so that any waves from impedance mismatches at the amplifier will be absorbed and not reflected.

We express these results mathematically. Let the origin be at $t_1 = 0$.

$$I_b(t) = \int I_b(\omega) e^{i\omega t} d\omega$$

$$I_b(\omega) = \frac{1}{2\pi} \int I_b(t) e^{-i\omega t} dt$$

$$I_b(\omega) = \frac{1}{2\pi} \, e/c: \quad \text{A flat spectrum for a delta-function beam.}$$

$$V_1(\omega) = \frac{1}{2\pi} \int e^{-i\omega t} \left[e/c \; \delta(t) - \frac{e}{c} \delta\left(t - \frac{2\ell}{c}\right) \right] \frac{\alpha Z_o}{2} \, dt$$
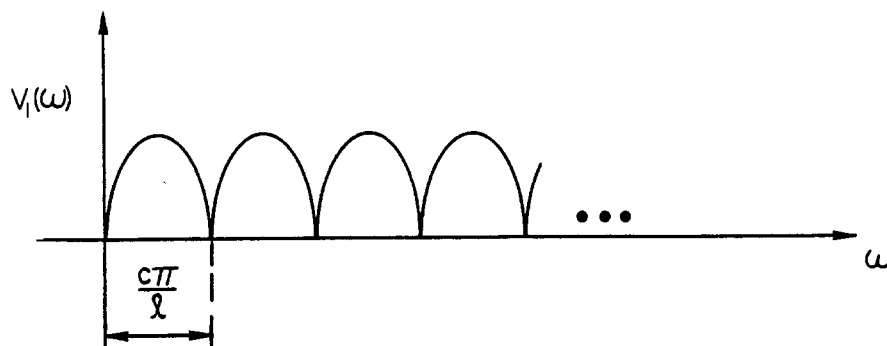
$$V_1(\omega) = \frac{\alpha}{2\pi} \frac{e}{c} Z_o \, i e^{-i\omega\ell}/c \; \sin \frac{\omega\ell}{c}$$

$$= \alpha I_b(\omega) Z_o \, i e^{-i\omega\ell/c} \sin^{\omega\ell}/c$$

Combining ±ω terms to get real currents and voltages, we get for the time-dependence of the Fourier component of V_1 at frequency ω:

$$V_1(\omega,t) = -\alpha \, I_b(\omega) \, Z_o \, \sin \omega\ell/c \, \sin \omega(t-\ell/c)$$

Note: t is measured from the point that the particle crosses the upstream end of the line. The frequency response at t = 0 is:


The first dip occurs when the line is a half wave length. The length is usually picked so that the line is $\lambda/4$ long at the center of the operating band. Note that from the equation for $V_1(t)$ we see that this results in a voltage that is in phase with the beam current (I_b cosωt) at this frequency and that the phase is a function of the reference point.

8.2.1. <u>Transverse spacial sensitivity</u>. We next consider the factor α in the above equations. This is clearly a function of the position of the beam relative to the plates of the transmission line. In fact we will make use of this feature in designing electrodes that are sensitive to the x or y coordinates of the beam. Two configurations are of interest:
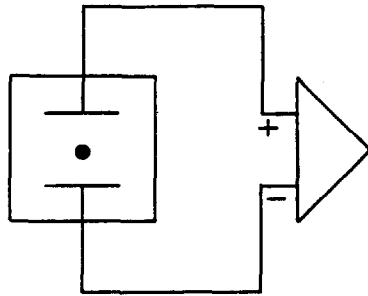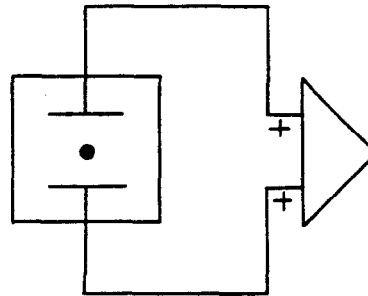
DIFFERENCE MODE   SUM MODE

In (A) the difference signal yields a sensitivity to the y coordinate of the beam. In (B) the vertical sensitivity is not large, but as the beam moves in x, the signal decreases. Indeed, it falls off exponentially after a gap width or so past the edge of the plates. We will use this fact later when we discuss momentum stacking.

To calculate the sensitivity to the beam position, we fix the frequency and use the TEM approximation for the fields. We must make some approximation to the actual geometry to derive results in analytical form, but these results are a good approximation to measurements made on actual structures.

The induced charge is related to the two-dimensional potential distribution. Consider the two charge and potential distributions:
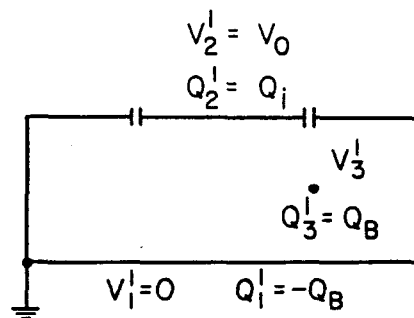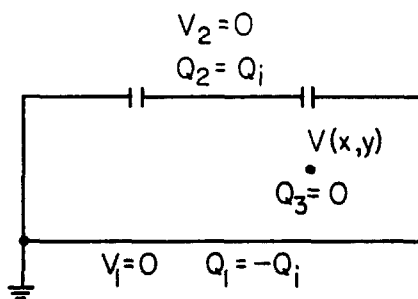
Reciprocity theorem gives:

$$\Sigma \; Q_i \; V_i' \; = \; \Sigma \; Q_i' \; V_i \qquad Q_i = \text{induced charge with all electrodes at } V = 0$$

Hence:

$$-Q_i \cdot 0 + Q_L \cdot V_0 + 0 \cdot V'_3 = -Q_B \cdot 0 + Q_L \cdot 0 + V(x,y) \cdot Q_B$$

or

$$Q_i = \frac{V(x,y)}{V_0} Q_B .$$

Thus, if we solve the two dimensional problem with an appropriate potential distribution on the electrodes, the ratio $V(x,y)/V_0$ gives the fraction of the beam charge induced on the plates for the beam at (x,y). The two-dimensional potential function is given in Ref. 2 (TeV I Design Report) for the case of the two configurations below:
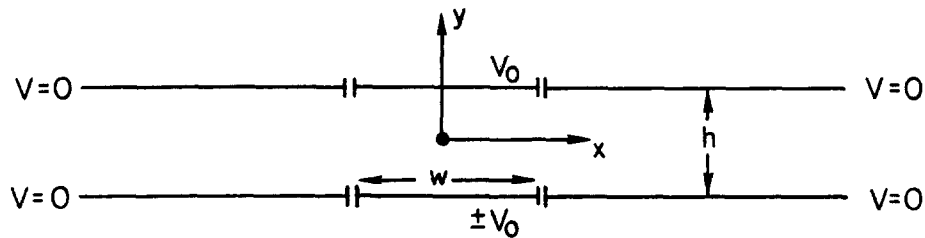
For the symmetrical case, the potential outside the plates approaches the form

$$\cos \frac{\pi y}{h} e^{-\pi x/h}$$

and for the difference mode,

$$\sin \frac{2\pi y}{h} e^{-2\pi x/h}$$

The exact form for $\alpha(x,y)$ in the y = 0 plane is

$$\alpha(x,0) = \frac{2}{\pi} \tan^{-1} \frac{\sinh \pi w/2h}{\cosh \pi x/h} \quad \text{Symmetric case}$$

For pickups with w = h, $\alpha(0,0)$ = 0.74. $\alpha(0,0)$ would equal 1 for very wide plates. Thus, we collect most of the charge with w = h.

    8.2.2. <u>Loop Kickers</u>. We must now consider how this configuration can work as a kicker. The difference mode described above operates in a straightforward way to deflect the beam in the transverse direction. The amplitude of this deflection is twice that calculated from the electric field. Remember that in a TEM mode, $|H|$ = $|E|$ Z_0, with $Z_0 = \sqrt{\mu_0/\epsilon_0}$ and the force is:

$$F = e(E+VB) = e(E+c\mu_o H)$$

$$= eE(1+c\ \mu_o/Z_o^*) = 2eE$$

$$Z_o^* = \sqrt{\mu_o/\epsilon_o} \quad c = 1/\sqrt{\mu_o\epsilon_o}$$

Also notice that for E and H to operate with the same sign, the wave on the transmission line must move <u>opposite</u> to the beam, i.e., the feed is from the <u>downstream</u> end of the electrode.

To understand how the kicker works to change the energy, we must look at the longitudinal fields at the end of the transmission line. Consider the situation at the central frequency, where the electrode is $\lambda/4$ long.
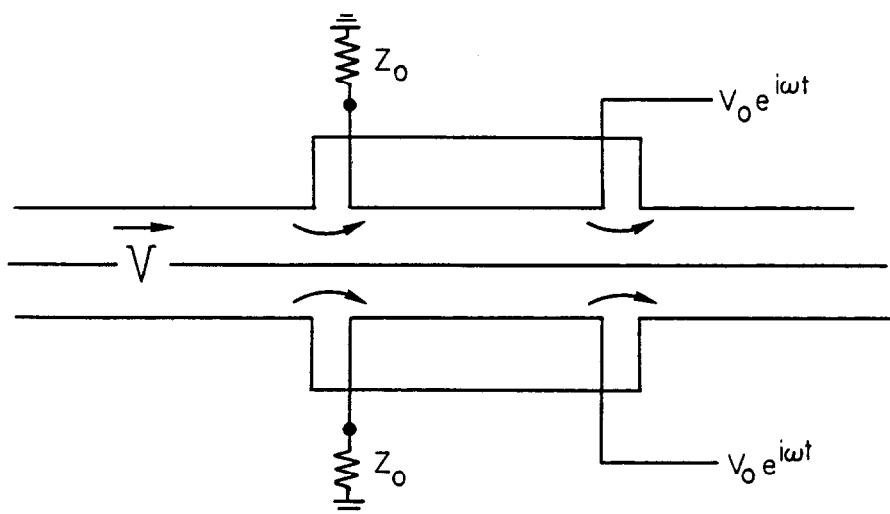
If the particle crosses the gap when the phase is $+45°$, it will get a positive kick of $0.7\ V_o$, and when it crosses the exit gap $90°$ later, the fields will have reversed and an equal kick will be received. This is very similar in action to a drift tube in a linear accelerator.

8.2.3. <u>Combiners and Signal to Noise Ratio</u>. Finally, we must discuss how the signal from a number of pickups is combined. Since the signals are on transmission lines, it is necessary that the system be matched throughout. Since no waves are reflected, all of the power is transmitted. Thus, if we are combining n pickups on a system of lines with characteristic impedance Z_o, and if P_o is the power picked up from the beam by a single electrode, then the total signal after combining signals will be:

$$P = n\ P_o$$

And the amplitude increases like $\sqrt{n}$.

We must now ask why if power is simply added does the signal to noise ratio improve with more pickups. The answer is found in Example 8.1. It works out the signal combiner operates differently for coherent signals and for incoherent signals such as the thermal noise from the back terminating resistors at each pickup.

After combining n pickups and converting back to the standard impedance Z_o, the noise is just $P_n = kT$, not nkT. Thus, n pickups improve the S/N by n. This is obviously true also for the noise inherent in the amplifier. To reach satisfactory signal-to-noise levels in practical systems, several hundred pickups may be necessary. A great improvement can be achieved by cooling both the amplifier as well as the terminating resistors.

Example 8.1: A signal combiner is constructed by joining n lines of impedance Z_o at a common point to a line of impedance Z_o/n. Show that, if a voltage pulse of magnitude V_n (and power $P_n = V_n^2/Z_o$) is transmitted down one of the n lines, the power transmitted into the Z_o/n impedance is P_n/n.

Solution: The arrangement is
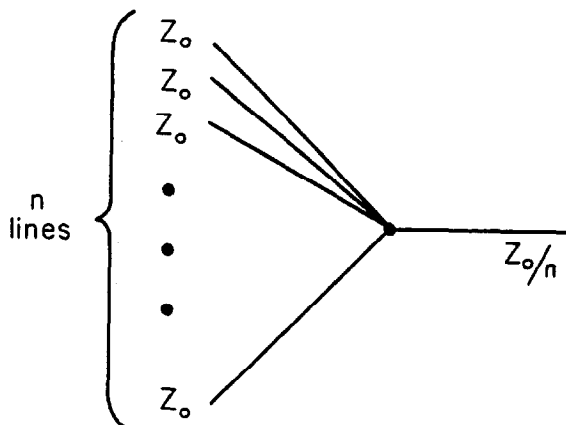
A voltage generator connected to one of the n lines sees a circuit:
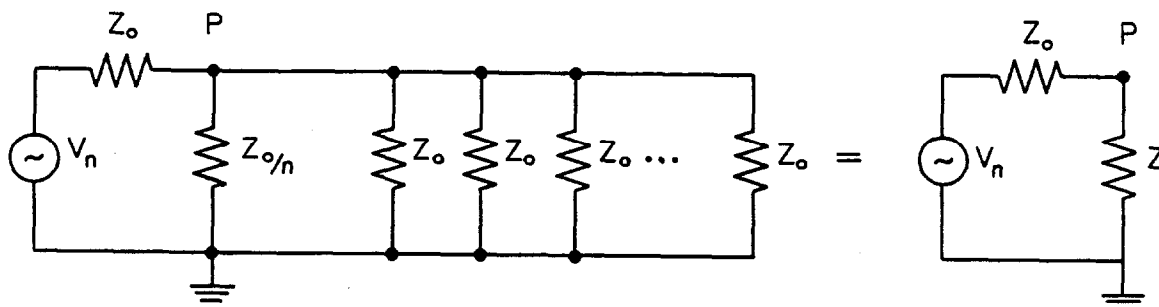
The effective impedance Z is just Z_o/n in parallel with (n-1) lines of impedance Z_o:

$$Z = \frac{(Z_o/n)(Z_o/n-1)}{Z_o/n+Z_o/n-1} = \frac{Z_o}{(2n-1)}$$

The reflection factor at point P is

$$\rho = \frac{V_{rel}}{V_n} = \frac{Z-Z_o}{Z+Z_o}$$

Hence

$$V_{rel} = \text{reflected voltage} = V_n \frac{Z-Z_o}{Z+Z_o} = V_n \frac{((1/2n-1)-1)}{((1/2n+1)+1)} = -V_n \frac{(n-1)}{n}$$

The reflected voltage pulse is inverted. The transmitted voltage pulse is

$$V_{TR} = V_n - |V_{rel}| = V_n \left(1 - \frac{n-1}{n}\right) = V_n/n.$$

The reflected power is

$$P_{rel} = V_{rel}^2/Z_o = V_n^2/Z_o \frac{(n-1)^2}{n^2} = P_n \frac{(n-1)^2}{n^2}$$

The transmitted power into Z_o/n is

$$P_{TR} = V_{TR}^2/(Z_o/n) = \frac{V_n^2}{n^2}\frac{n}{Z_o} = \frac{V_n^2}{nZ_o} = \frac{P_n}{n}$$

If we superimpose n coherent voltage generators (such as signals from a beam in a matched system), the total transmitted voltage is $V_{TR} = (V_n/n)n = V_n$, and the transmitted power is $P_{TR} = V_{TR}^2/(Z_o/n) = (V_n^2/Z_o)n = nP_n$: all the power is transmitted into the Z_o/n impedance. But for n <u>incoherent</u> generators (such as noise sources), the transmitted voltages add in quadrature so

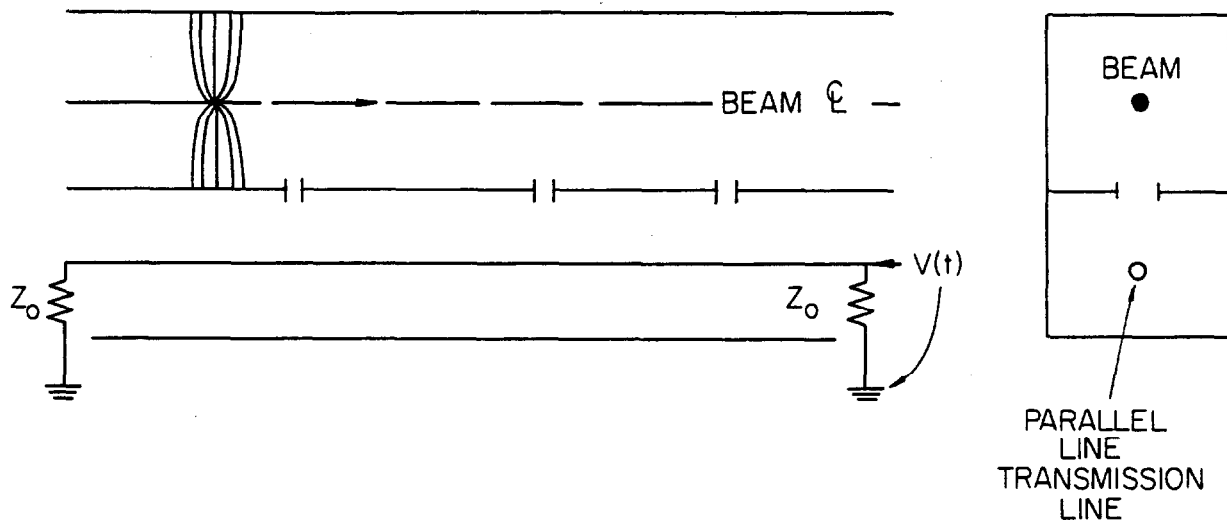$$V_{TR}^2 = n(V_n/n)^2 = V_n^2/n$$

and

$$P_{TR} = V_{TR}^2/(Z_o/n) = (V_n^2/n)(n/Z_o) = P_n.$$

8.3. Slot couplers

The final type of coupler we will discuss is the so-called "slot coupler". For this system, we consider the beam in its pipe traveling parallel to a TEM line in an adjacent pipe. The two are coupled by slots periodically:

BEAM £ —

V(t)

Z_O Z_O

BEAM

●

○

PARALLEL
LINE
TRANSMISSION
LINE

Unlike the loops, the wave induced in the structure travels in the same direction as the beam. Consider a particle in the beam. Its field is traveling along the surface of the guide, and encountering a slot, couples some energy into the transmission line below. The field restores itself between slots and at the next opening coherently adds to the wave on the transmission line. The voltage on the line is

$$V = n \, V_o \qquad P \sim n^2 \, P_o$$

where n = number of slots, and V_o is voltage coupled in one slot. This assumes the velocity of the line matches that of the beam. The shape of the slots control the coupling to the electric and magnetic fields of the beam. Big openings increase the coupling but load the transmission line and make the propagation velocity slower than the particle velocity.   Thus, the number of sections which can be used before encountering large phase differences between the wave and the beam is limited.   Short sections of these lines can be combined by combiners in the same manner as for the loops but then the n^2 dependence applies only to the substructures.

This behavior is unfortunate, because in an RF sense, the slot structure is much cleaner with fewer parasitic modes to interfere

with its operation than is the case for loops. Thus, one is tempted
to use this scheme when the frequencies of interest exceed 2 GHz.
However, its sensitivity falls off with beam energy like $1/\gamma^2$.

Much work remains to be done in developing beam couplers. They
are the very heart of the system and in a real sense limit the
performance by their small bandwidth and poor signal-to-noise ratio.
It should also be obvious that if very high frequency systems are
desired the beam must necessarily be small and the size of the
electrode structures as well as their spacing to the beam must be
less than a wavelength. At present the tremendous amount of
information available in the beam signal is not being used. An 8
GeV/c proton passing 1 in. from an electrode has spectral components
up to 50 GHz, but our present cooling systems only work up to 4 GHz.
This indicates the challenge of designing a better coupling system.

8.4. Measuring pickup response

We have discussed the physical ideas behind pickups and kickers.
It should be clear that the actual hardware will behave in a much
more complicated way than indicated by the simple model we have been
using. We have neglected all of the complicated higher order modes
that exist for any real structure, and these modes can modify the
behavior of the system. Consequently it has been imperative that
methods be developed to measure the response of prototypes. We will
discuss two methods briefly.

The first makes use of the fact that the lowest order TEM mode
of a relativistic beam in a pipe can be approximated by replacing the
beam by a wire carrying a current of frequency ω_o. This system has
for its lowest mode the simple TEM transmission line mode which
closely approximates the fields of a beam current modulated at ω_o.
The disadvantage, of course, is that the higher modes are completely
different. Nevertheless, this is a simple and expedient way to make
prototype measurements.

By positioning the wire at various points in the pipe one can
measure the transfer impedance of the electrode. The transfer
impedance is defined by

$$V_{PU} = I_b \, Z_T(\omega)$$

where V_{PU} is the signal measured in the terminated pickup system and
I_b is the amplitude of the current in the wire.

Figure 8.4.1[19] shows the response of a simple loop coupler
during its development by the LBL group for the FNAL Source. This
coupler is designed to operate in the 1-2 GHz band, and indeed we see
its predicted sinusoidal response in this band. (Note that at low
frequencies the fact that $Z_T \sim \omega$ is just what one would expect from
simple inductive coupling). However, outside this band (see
Fig. 8.4.3) we see a very complicated response, and it is possible
for the resonant dip in the response above 2 GHz to move down in
frequency until it completely obliterates the response in the desired
band.

RESPONSE OF ONE LOOP PAIR

• LBL WIRE MEASUREMENTS

—— MEASURED WITH 1.8 MeV BEAM

△ CALCULATED
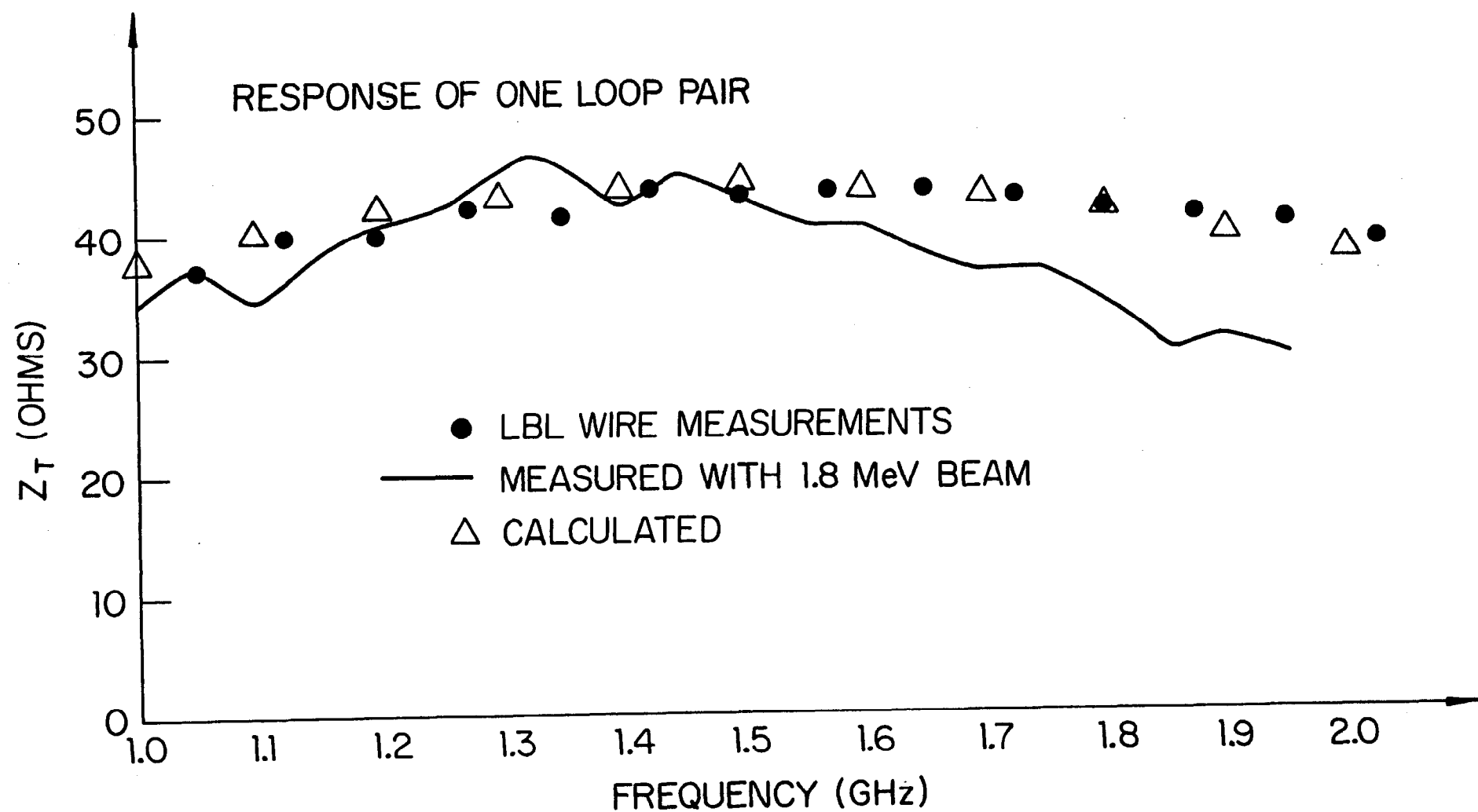
These details are very sensitive to the smallest details of the shape of the plates, the fields at the two ends, the spacing of the edges of the pickup from the beam tube, etc. Much patience and intuitive understanding of Maxwell's Equations are necessary to achieve a good electrode design.

There is one more limitation to the wire method that must be mentioned. If Z_T becomes very large, then the coupling of energy from the wire to the loop becomes very effective. This, of course, is the goal of a good pickup design. However, if we wish to measure the response of an array of pickups, this can cause real difficulties in that the attenuation length may be only a few electrodes long. It becomes impossible to measure long arrays by this technique without modifications. This is a serious difficulty since one is really interested in the response of arrays that may have as many as 200 elements. Note that this represents a difference between the wire and the beam in that the beam represents a real current source.

An elegant solution to this problem has been developed at ANL for measuring the large arrays of pickups being developed for the TeV I Source. This technique uses a 20 MeV linac beam that has been bunched in a single bucket so that it is only 20 psec long. This beam is shot through the electrode structure under investigation at a repetition rate of 800 hz and the output voltage is recorded on a sampling oscilloscope. The output of the sampling head is digitized for each pulse and the information stored in memory. The scope displays the transient response of the electrode to the very short current spike which is almost a δ function. This is shown in Fig. 8.4.2[20] and should be compared with our simple interpretation in Section 8.2. The digitized points are then fourier transformed by an FFT and the frequency response along with phase is shown in Fig. 8.4.3.[20] The spacial response at a fixed frequency is shown in Fig. 8.4.4[20] for an electrode being developed for the momentum stacking system. The desired exponential fall off is clearly visible. This technique is not limited to single electrodes but can readily measure large arrays. Its only limitation is that the pulse from the linac must be short enough to have a high harmonic content at the frequency being studied. Corrections for the spatial response can be made as necessary.

8.5. Higher order modes

A glance at Fig. 10.7.1 showing the block diagram of a cooling system reveals a high gain amplifier whose input and output are coupled to the beam by means of electrodes. These same electrodes also couple to the beam pipe as well, and if it is possible to propagate energy around the ring by either the beam or the beam pipe, it is possible for instabilities to develop that will result in oscillation of the electronics. The beam coupling is called beam feedback and will be treated later. Feedback via the beam pipe is also possible and we will now examine a simple possibility.
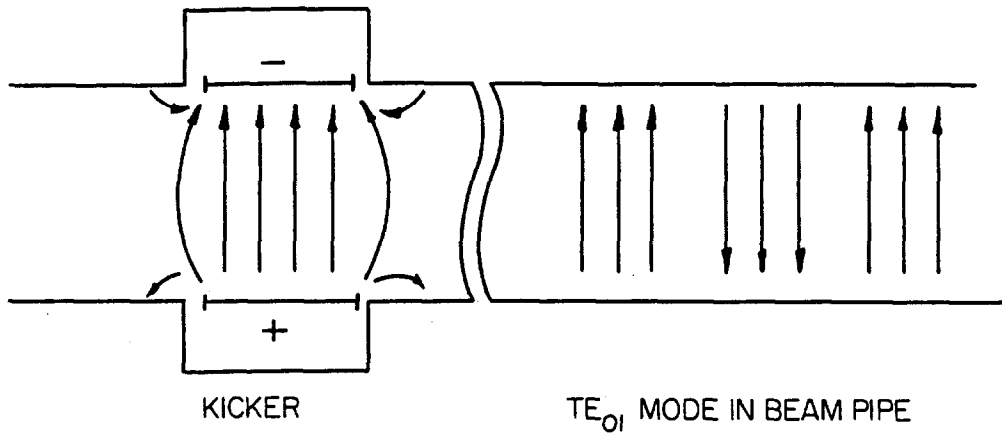
Consider for simplicity a transverse kicker or coupler operating in the difference mode such as would be used in a transverse cooling system. A side view of the kicker looks like:
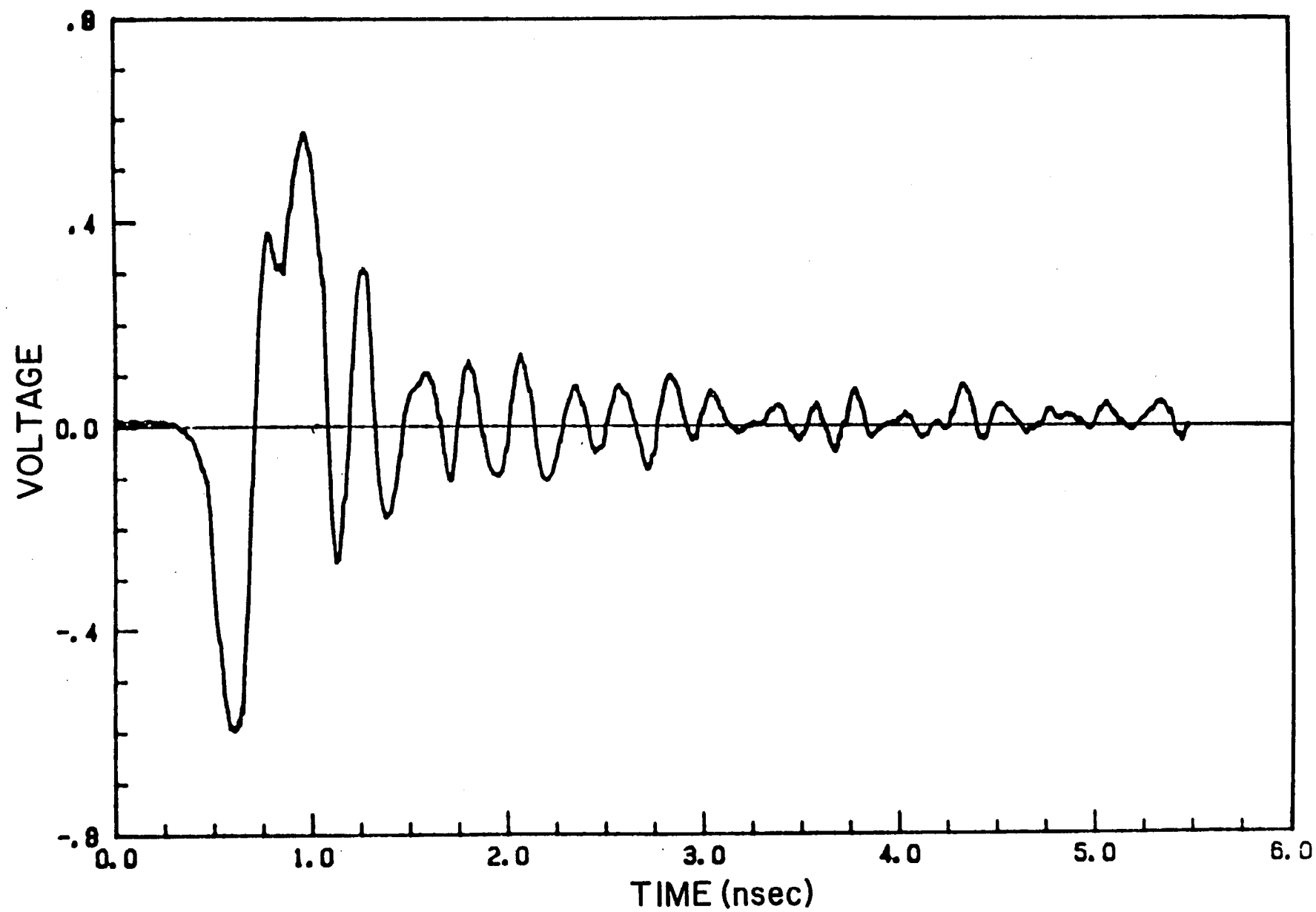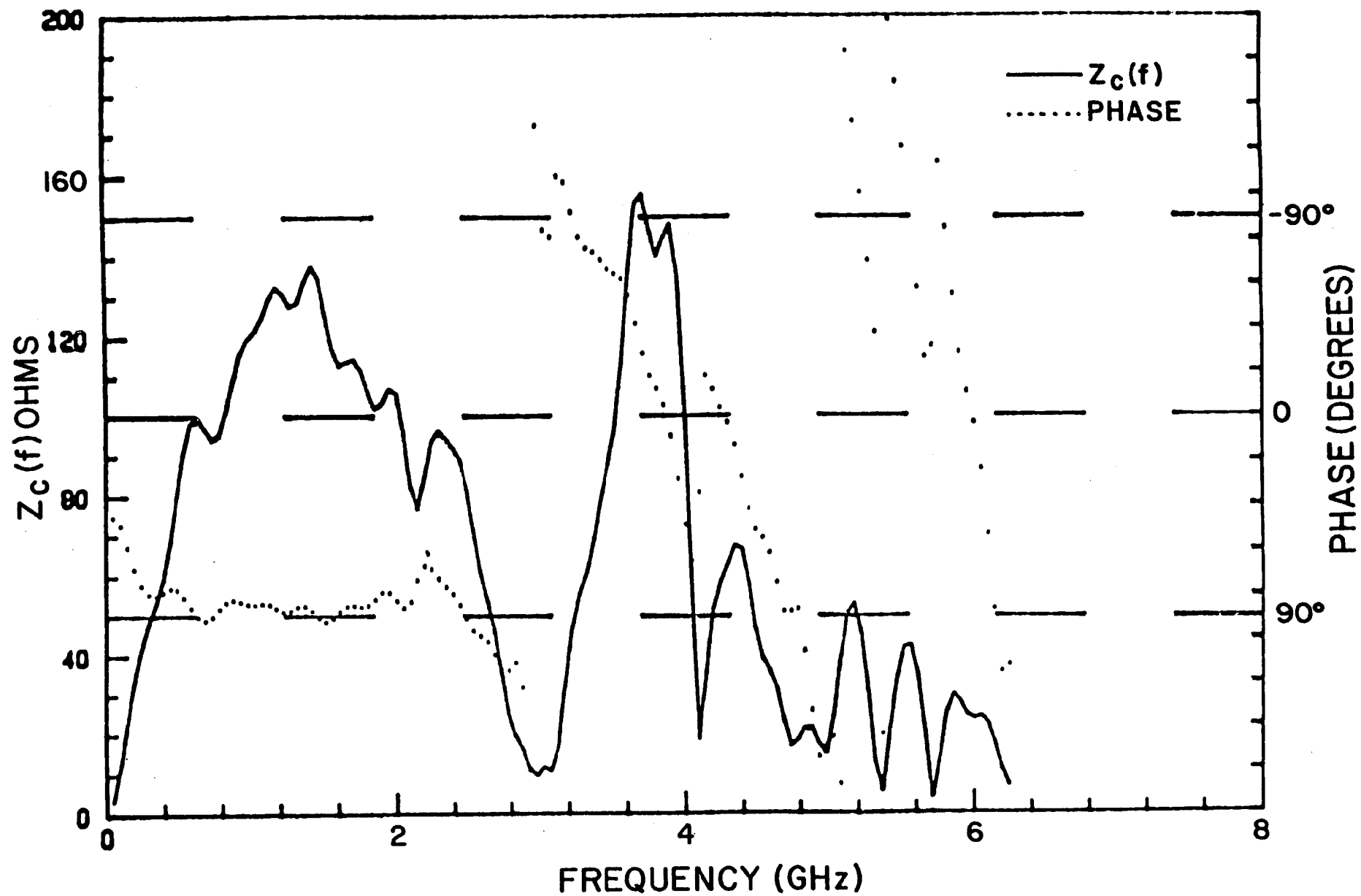
Pickup Sensitivity at 1.5 GHz

KICKER TE_{01} MODE IN BEAM PIPE
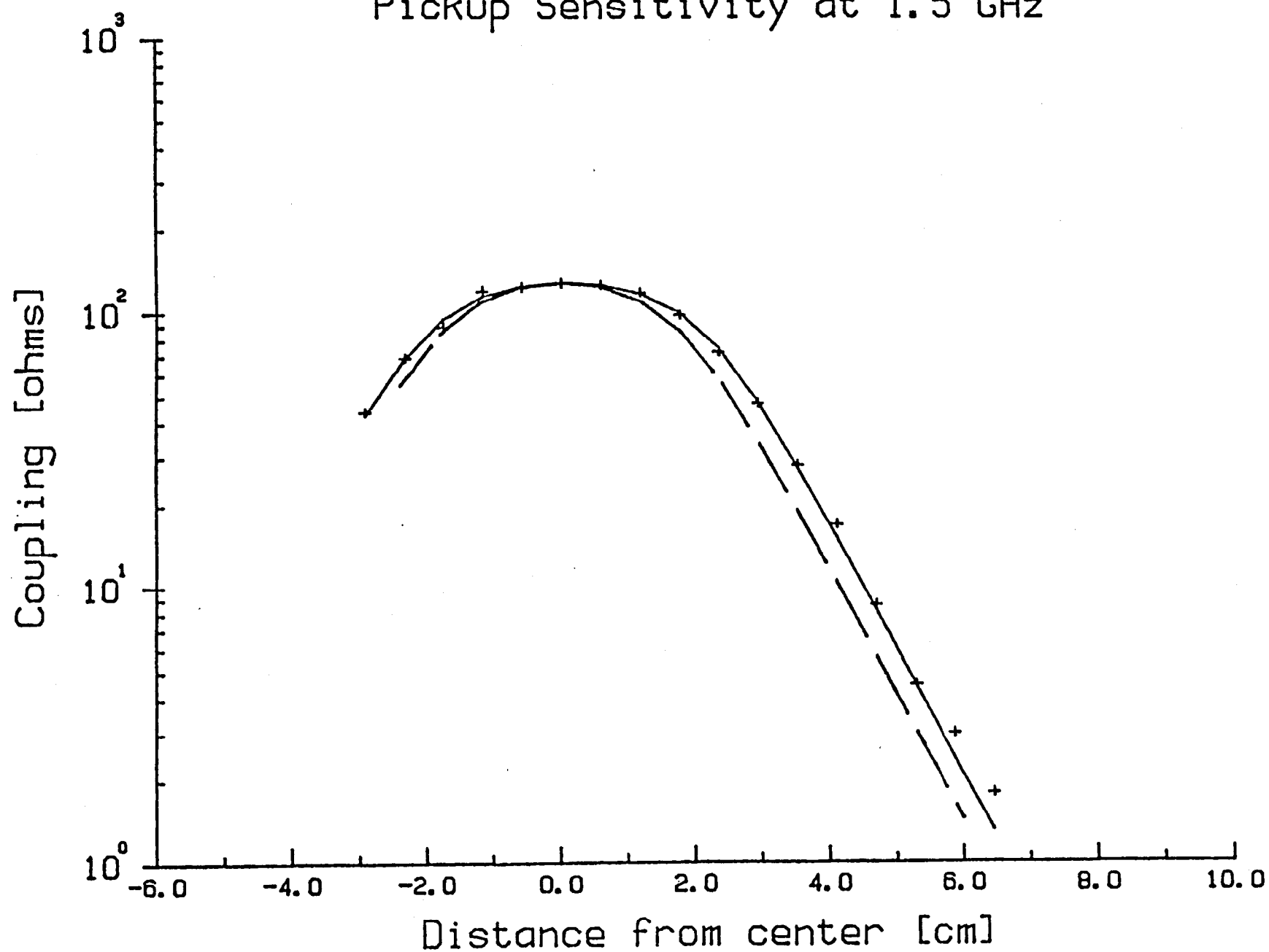
It is obvious that if the width (perpendicular to the page) is more
than $\lambda/2$ that the TE_{01} mode will propagate down the beam tube as
shown to the right. It is also obvious by symmetry that such a TE_{01}
wave will couple with difference mode pickups. With the very high
gain systems necessary for effective cooling (>100 db) it is not
unlikely that the system will oscillate if this feedback path is not
broken. The most effective way to decouple sections of the beam pipe
is to make a section of the pipe small enough in transverse
dimensions so that it is beyond cutoff in the band where there is
appreciable gain. If this is not possible then one has recourse to
lossy materials that can absorb the propagating wave. Special RF
materials are available for this purpose such as lossy ferrites and
special resistive coatings.

9. FOKKER-PLANCK EQUATION

9.1. Discussion of the equation

We now wish to discuss the time evolution of the particle density function, $\psi(E)$. In Section 5 we treated cooling theory by calculating the moments of the distribution, but as will soon become apparent, this technique is no longer appropriate to the problem we wish to treat. The equation that $\psi(E)$ obeys is the Fokker-Planck equation. We will not derive the equation, but rather make it seem plausible that this is the correct equation to use.

If we focus our attention on one particle, as we have seen, it receives random kicks from other particles in the machine. It also has a coherent "self force" acting on it through the chain: pickup, amplifier, kicker. The random kicks result in diffusion and the coherent kicks force a directed motion onto the particle. The situation is the same as Brownian motion of a particle in a gas under the influence of gravity. The gravitational force $+m\vec{g}$ is always in the same direction--the kicks from other gas molecules are randomly directed.

However, once we talk about a distribution of particles, this random motion results in a flux away from regions of high density to those of low density. This is described by means of a diffusion coefficient D, such that

$$\vec{\phi} = -D\vec{\nabla}\psi$$

where $\vec{\phi}$ is the flux of particles per second and is proportional to the slope of the density function. In our case, since energy is the only dimension, we have

$$\phi(E) = -D(E) \frac{\partial \psi}{\partial E} .$$

Note that we write D(E) because the diffusion coefficient may vary with energy. We assume it depends only locally on the energy distribution. We do not prove this--it is an assumption. Now we can also invoke the conservation of particles. If the density of particles in a small volume is increasing, it is because there is a larger flux into the volume than out. We thus have

$$\frac{\partial \psi}{\partial t} = \vec{\nabla}\cdot\vec{\phi} = -\frac{\partial}{\partial E}\left(D(E) \frac{\partial \psi}{\partial E}\right)$$

This now looks like a standard diffusion process, but we must next add coherent forces. Suppose we have a distribution $\psi(E)$ and in a time Δt we add at E an energy ΔE. Then the flux of particles crossing E will be

$$\phi = \frac{dN}{dt} = \psi(E) \frac{\Delta E}{\Delta t}$$

Let the term $\Delta E/\Delta t$, the energy gain per second of a particle at energy E, be F(E). Then we will have
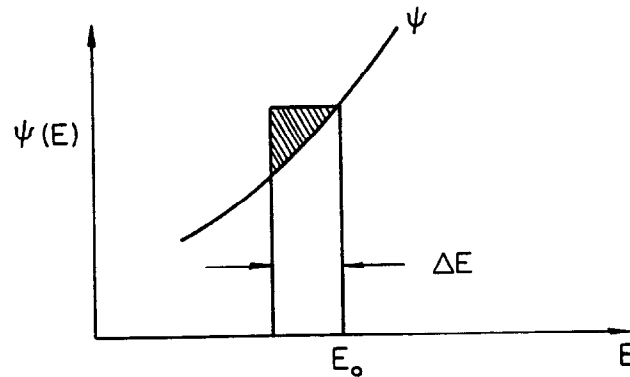
$$\phi = \psi F(E) - D(E) \frac{\partial \psi}{\partial E} \qquad (9.1.1)$$

and

$$\frac{d\psi}{dt} = \frac{\partial}{\partial E} \left[F(E) \ \psi(E) - D(E) \frac{\partial \psi}{\partial E} \right] \qquad (9.1.2)$$

There is a second way we can proceed that gives additional insight into the situation.[21] Consider $\psi(E)$ expanded around some energy E_0

$$\psi(E) = \psi(E_0) + \frac{\partial \psi}{\partial E} \bigg|_{E_0} \Delta E + \ldots$$

Suppose now we add ΔE_k through the kicker system in a short time Δt. Then the flux is given by

$$\phi = dN/dt = \frac{\psi(E_0) \ \Delta E_k - (1/2 \ (\partial \psi / \partial E) \ \Delta E_k) \ \Delta E_k + \ldots}{\Delta t}$$

The second term corrects for the shaded area in the sketch above which is an overestimate with only the first term

$$\phi = \psi(E_o) \frac{\Delta E_k}{\Delta t} - 1/2 \frac{\partial \psi}{\partial E} \frac{\Delta E_k^2}{\Delta t} + \cdots$$

If now the ΔE_k is a noise spectrum of the kicker pulses and in particular has no coherence within its structure, the short time average of the first term will be zero. If there is a small coherent term in it, such as <u>an individual</u> particle generating its own correcting voltage, then $\overline{\Delta E_k/\Delta t} = F(E)$.

Now consider the second term. With random voltage $(1/2)\overline{\Delta E_k^2}/\Delta t$ becomes $1/2\ d/dt\ (\overline{E_k^2})$. We assume this is large compared to the second order coherent term. (i.e., a linear system in the first approximation). Thus we have

$$\phi = \psi(E)\ F(E) - 1/2 \frac{d}{dt} \overline{E_k^2} \frac{\partial \psi}{\partial E} \tag{9.1.3}$$

Comparing with Eq. (9.1.1) we have the important relationship:

$$D(E) = \frac{1}{2} \frac{d}{dt} \overline{E_k^2} \tag{9.1.4}$$

This tells us that we may evaluate D by examining the mean square voltage that the kickers apply to a particle in the beam at energy E.

We now have the equation that describes the behavior of the density of the beam in time and energy. The spacial dependence is determined by the lattice of the machine, i.e., its dispersion or in more detail, its off momentum orbits. We will now apply this to momentum cooling and stacking.

9.2. <u>Static core</u>

Suppose we apply this equation to a simple example. Set $F(E) = -\alpha(E-E_o)$ so that there is a coherent force proportional to the deviation from the central energy E_o. Let's consider the static case where there is no flux across any point and $D(E) = D_o$, a constant diffusion force. Then we have from Eq. (9.1.1)

$$\phi(t) = 0 = -\alpha(E-E_o)\ \psi - D_o \frac{\partial \psi}{\partial E} \tag{9.2.1}$$

The solution is

$$\psi = \psi_o\ e^{-\alpha/2D_o(E-E_o)^2} \tag{9.2.2}$$

In this case the coherent force is just counteracted by diffusion at each point and a gaussian distribution results. If the initial distribution were not this shape we would have to solve Eq. (9.2.1) as a boundary value problem but for long times we would achieve the above distribution. If the noise is small and the restoring force large, the density will be high. Suppose now that we introduced a small group of particles at some energy $E >> E_o$. Then the coherent force would dominate over diffusion and the particles would be collected into the core after a lapse of time. It is just this action that constitutes stacking in momentum, i.e., the continuous injection of a flux of particles at E_i and their collection into a central core at E_o
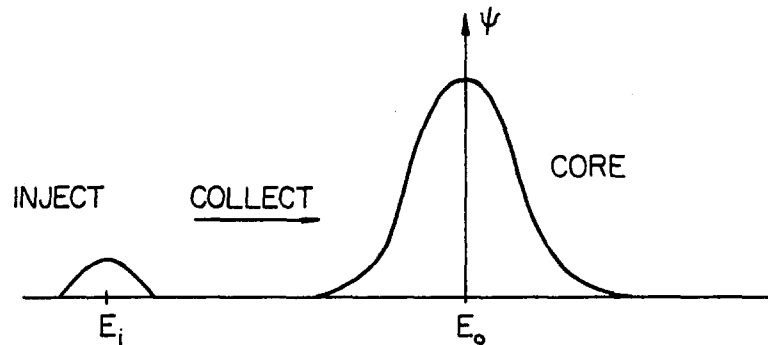
We also see from this simple example that somehow a central energy E_o must be established. There are two ways of achieving this.

a) Palmer Cooling

   In this case, the pickup electrodes are split and operated in a difference mode.
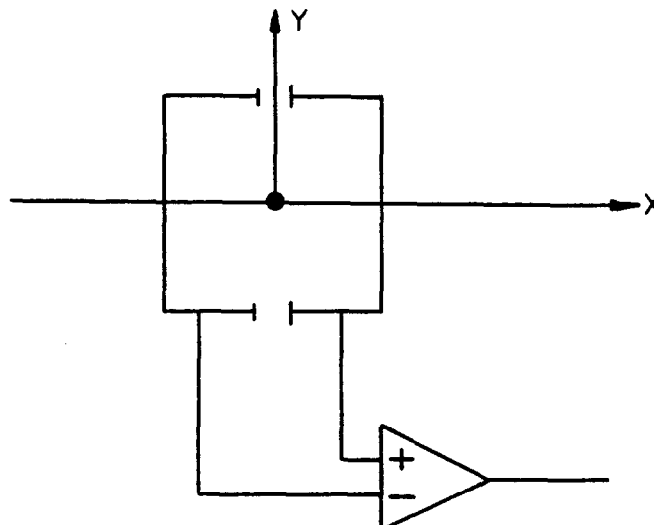
The split in the electrodes is placed at a radius in the machine that defines E_o. The dispersion function α_p must not be zero at the pickup.

b) Filter Method

Here the central energy is determined by time. The signal is picked up by a sum electrode. It is then subtracted from itself shifted in time by T_o. A shorted delay line of length $T_o/2$ can accomplish this and is the "filter". This signal is identically zero if the particle takes just T_o to travel around the ring. If this corresponds to an energy E_o, then there will be no signal at the kicker for this particular energy. Other energies will result in a positive or negative voltage at the kicker depending on whether the rotation period is greater or less than T_o.

It should be noted that these two methods produce quite different properties of the system in which they are incorporated. The difference is that in the first method the electrodes couple less strongly to the beam as the core is approached and at E_o only the amplifier noise is passed on to the kickers. The second method using sum electrodes may be a little easier to implement and has tighter coupling, but filters (the shorted delay line) become increasingly difficult to construct as the frequency spectrum becomes higher due to increased losses in the transmission line from the skin effect. As we will see, both systems are used in machines.

9.3. Momentum stacking

We now go back and follow Van der Meer's development of momentum stacking.[1] Suppose we wish to have a flux ϕ that is constant above an energy of injection E_i. Let $V(E)$ be the volts per turn applied by the kicker, and set $D = A V^2 \psi$ where A is a constant of the equipment. Remember that $D = 1/2 \, d/dt \, E_k^2$. The square of the fluctuations will be proportional to the number of particles (remember Section 5) and E_k^2 will be proportional to $V(E)^2$. (Don't panic—we will derive exact equations later). To summarize

1. $\phi = \phi_o$

2. $F = eV/T$ $\qquad\qquad\qquad\qquad\qquad\qquad\qquad$ (9.3.1)

3. $D = AV^2 \psi$.

Then we can use (9.1.1) to give

$$\phi_o = \frac{eV}{T} \psi - AV^2 \psi \frac{\partial \psi}{\partial E}$$

Solve for $\partial\psi/\partial E$

$$\partial\psi/\partial E = -\frac{\phi_o}{AV^2\psi} + \frac{e}{AVT} \qquad (9.3.2)$$

We now wish to make the gradient of ψ as steep as possible. This will happen if

$$V = \frac{2\phi_o T}{e\psi} \qquad (9.3.3)$$

Substitute into 9.3.2 and integrate

$$\psi_o = \psi_o e^{(E-E_i)/E_D} \qquad (9.3.4)$$

$$E_D = 4A\phi_o T^2/e^2 \qquad (9.3.5)$$

and using Eq. (9.3.3) we get

$$V = \frac{2\phi_o T}{e\psi_o} e^{-(E-E_i)/E_D} \qquad (9.3.6)$$

To summarize, we can inject a constant flux at energy E_i which then builds up an exponential stack to higher energies. The volts per turn must decrease exponentially as the density increases. The time evolution of such a stack showing the injected pulse and the core build up is shown in the figure below.[2]
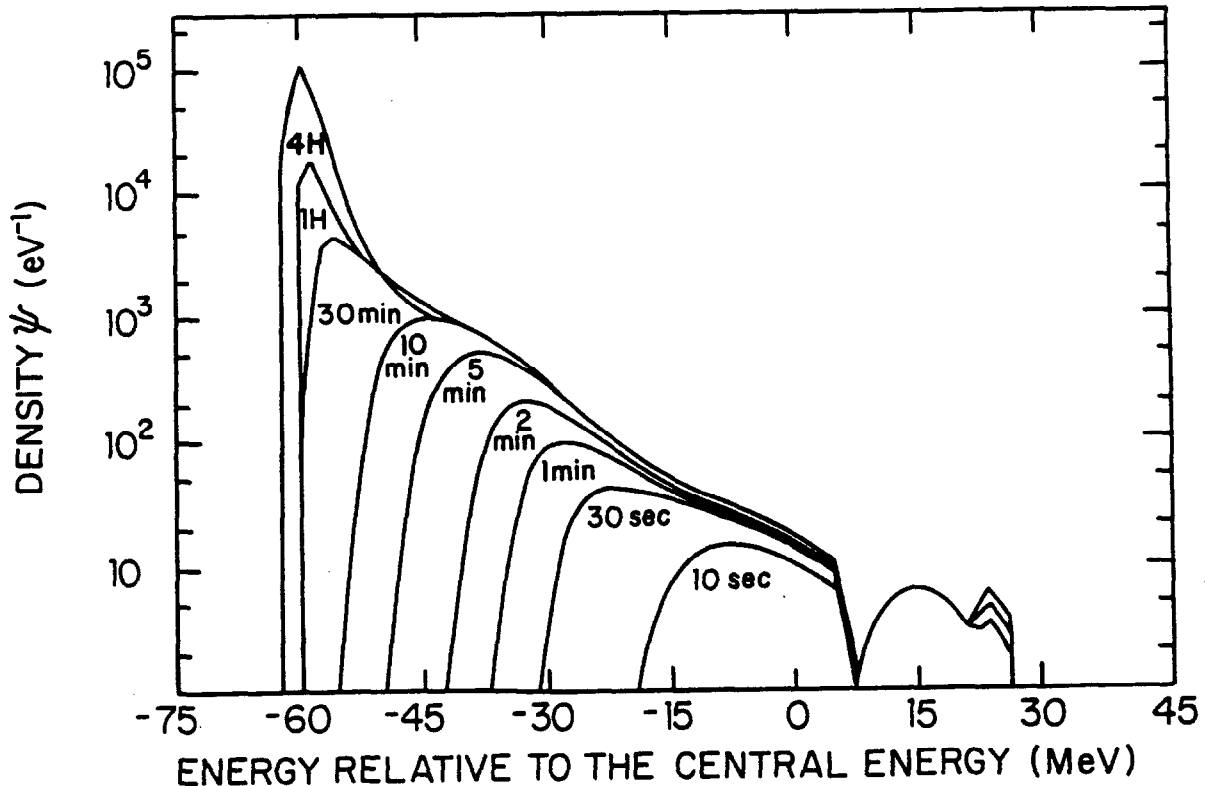
We now see the broad outline of the system. We must next calculate F(E) and D(E) for a real system.

10. CALCULATION OF CONSTANTS IN THE FOKKER-PLANCK EQUATION

For this section, we consider the block diagram below.

$$I_b e^{i\omega t} \left(\left(\frac{Z_o}{V_{Pu}} \rhd \frac{Z_o}{V_K} \right) \right)$$
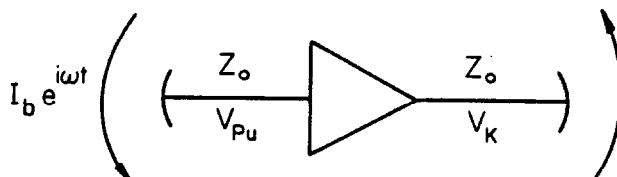
The necessary constants are listed.

1. Amplifier Gain
   $G(\omega) = A(\omega)$ A is a complex number.
2. Input, output impedance of Amplifier = Z_o
3. Pickup transfer impedance is defined by

$$V_{PU} = I_b\, e^{i\omega t}\, Z_{PU}$$

   when the beam is in the center at the central frequency.
4. $\dot{S}_{PU}(E)$ = Energy dependence of pickup. We will ignore the energy dependence of the kicker assuming it is at a point of zero dispersion.
5. $f_{PU}(\omega)$, $f_K(\omega)$ pickup and kicker frequency sensitivity over the Shottky bands being used.
6. $\omega_o(E)$: Rotation freq at energy E
   β: v/c of particle
   T_o: central rotation period
   $\eta = -(df/f)/(dp/p) = (dT/T)/(dp/p)$
   p,E: momentum, energy of particle
   k: Boltzman constant
   n: harmonic number of Schottky band
   N.F.: Noise figure of the amplifier in db

$$NF = 10 \log \left(\frac{\text{Noise Power From Amp. with } R_o \text{ at input}}{\substack{\text{Noise Power from perfect Amp.} \\ \text{with } R_o \text{ at input}}} \right)$$

A word about frequency spectra is in order. f_o is the fundamental rotation frequency. Due to the spread in momentum and

dispersion in the machine, if we have a spread of momentum in the stack there will be a spread of frequencies given by

$$\Delta f = \eta \, f_o \, \frac{\Delta P}{P_o} = \frac{\eta f_o}{\beta^2} \frac{\Delta E}{E_o}$$

Now the rotation period for the FNAL Accumulator Ring is about 1.6 µsec so $f_o \simeq 600$ kHz. We have $\eta = .02$ and $\Delta E \sim 90$ MeV at 8 GeV. Thus $\Delta f = 135$ hz. The cooling system will work with amplifiers covering the band 1-2 GHz or for n from 1600-3200.

We sketch the spectra below.
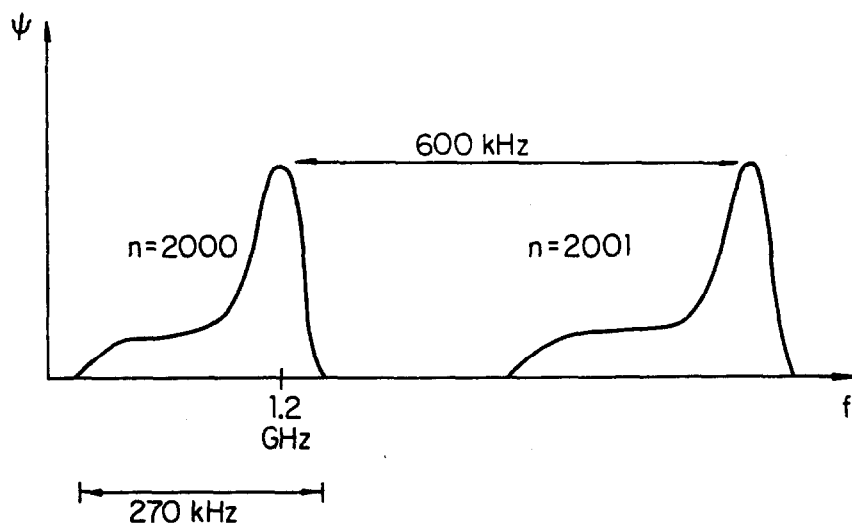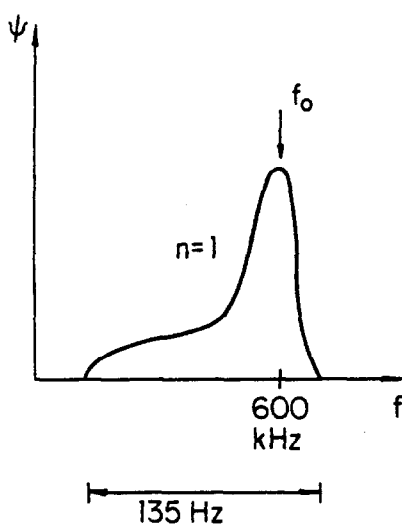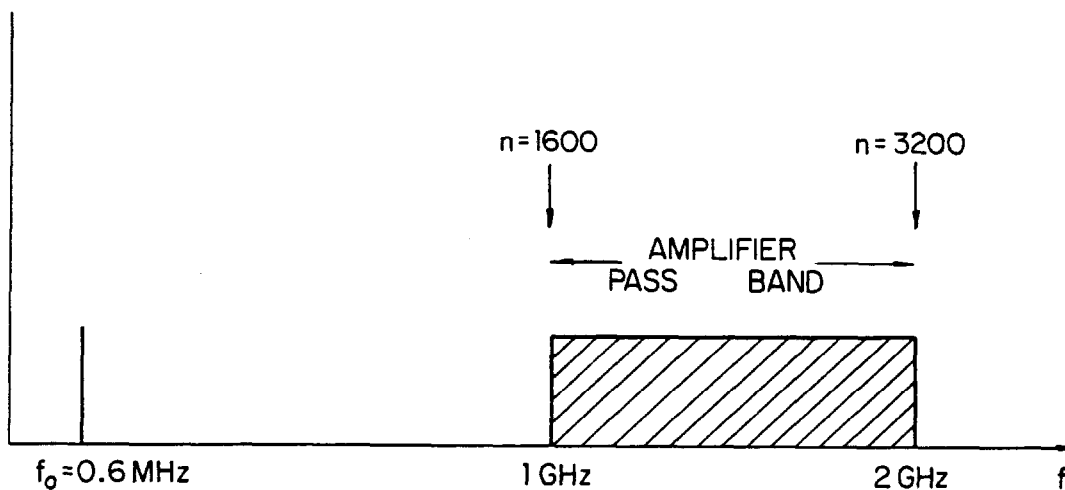
Notice that each Schottky band reflects the stack momentum spectrum and also at n = 4400 the bands just start to overlap.

10.1. Calculation of F(E)

We can now calculate F(E) easily. The beam current is Fourier analyzed and each component amplified by the amplifier and applied to the kicker. F is the energy gain per second, hence we must multiply by f_o. For a single particle

$$I(t) = \frac{2e}{T_o} \sum_n \cos n\omega_o t$$

$$V_{PU}(n) = \frac{2e}{T_o} Z_{PU} S_{PU}(E) f_{PU}(n\omega_o)$$

$$V_K(n) = \frac{2e}{T_o} Z_{PU} f_{PU}(n\omega_o) S_{PU}(E) A(n\omega)$$

Energy to beam per second:

$$E_K(n) = \frac{2e^2}{T_o^2} Z_{PU} S_{PU}(E) f_{PU}(n\omega_o) A(n\omega) f_K(n\omega_o)$$

$$F = \frac{2e^2}{T_o^2} Z_{PU} S_{PU}(E) \sum_n \text{Re} [f_{PU}(n\omega_o) A(n\omega) f_K(n\omega_o)]$$

We notice we have written $A(n\omega)$. This is because the amplifier may have a gain that varies within a Schottky band such as a periodic filter would provide. Thus the exact position of the particle in the stack can be important. We indicate this situation by writing

$$A(n\omega) = A_n(E)$$

which says all Schottky bands are modified by the same gain profile. The real part must be taken since we only wish the in phase component. This then gives

$$F(E) = 2e^2 f_o^2 Z_{PU} S_{PU}(E) \sum_n \text{Re} [f_{PU}(n\omega_o) A_n(E) f_K(n\omega_o)]$$

To emphasize again--E is used here to indicate any frequency dependence within the range of stack frequencies. Notch filters used with the amplifier are included in $A_n(E)$. Spacial dependence of the beam relative to the pickup shows up in $S_{PU}(E)$. The terms f_{PU} and f_K include any phase shifts over the overall cooling band.

10.2. A Useful Theorem

To evaluate the diffusion terms, we need to study the beam response to random noise. Consider the situation below where we break the feedback loop and study the open loop system.

test particle
period T_o
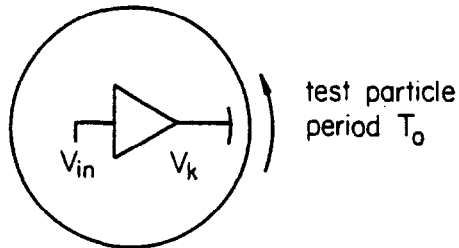
Consider applying a sinusoidal voltage to V_{in} so that the test particle receives an energy kick of $E_o \cos \omega t$ each time it crosses the kicker. After M_o turns,

$$E = E_o \sum_{m}^{M_o} \cos \omega (mT_o - t_o)$$

where t_o is the initial time.

$$E = \frac{E_o}{2} \sum_{m}^{M_o} e^{-i\omega t_o} e^{im\omega T_o} + e^{i\omega t_o} e^{-im\omega T_o}$$

This geometric series may be summed to give

$$E = E_o \cos \omega \left(\frac{M_o}{2} T_o - t_o \right) \frac{\sin (M_o+1)\omega T_o/2}{\sin(\omega T_o/2)} .$$

We now wish to consider the response of the beam to a noise spectrum. Set

$$E_o^2(f) \, df = \text{noise signal at } f \text{ (proportional to noise power}$$
$$\text{per unit frequency)}$$

$$\omega = n\omega_o (1+\epsilon) , \quad \epsilon \ll 1$$

n: harmonic number

$$f_o T_o = 1$$

The beam gets

$$dE^2 = E_0^2(f) \, df \, \cos^2 \left(\pi(M_0 n)\epsilon - \omega t_0\right) \frac{\sin^2 n(M_0+1)\pi\epsilon}{\sin^2 n\pi\epsilon}$$

Let

$$df = nf_0 \, d\epsilon.$$

Next let M_0 become large, i.e., many crossings and integrate over $d\epsilon$. The term involving sines approximates a delta function

$$\frac{\sin^2 nM_0\pi\epsilon}{\sin^2 n\pi\epsilon} \to M_0/n \; \delta(\epsilon).$$

The total time is $M_0 T_0$ and so

$$\frac{dE^2}{dt} = \int \frac{dE^2 df}{M_0 T_0} = \frac{E_0^2(nf_0)\cos^2 n\omega t_0 \, nf_0}{M_0 T_0} \frac{M_0}{n}$$

We now average over initial phases t_0 and obtain

$$\frac{\overline{dE^2}}{dt} = \frac{\overline{E_0^2(nf_0)}}{T_0^2} \tag{10.2.1}$$

This says that a particle at rotation frequency f_0 only responds to those components of noise that are harmonics of f_0! We will use this little theorem now to evaluate the diffusion coefficients.

10.3. Thermal Noise

Thermal noise is generated at the input to the amplifier and dominates the situation when there are few particles present. As the beam density grows, statistical noise from the particles can become dominant.

For thermal noise we have the circuit
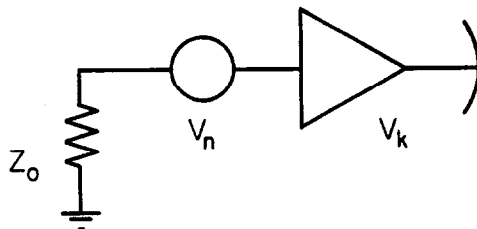
$$V_n^2 = 4k \ T \ Z_o \ \Delta f$$

This noise of the input resistance is amplified by the amplifier with the addition of its own noise and applied to the kicker. Using our theorem in Eq. (10.2.1), and the definition of D in Eq. (9.1.4), we have

$$D_1(E) = \frac{1}{2} \overline{\frac{dE_K^2}{dt}} = \frac{1}{2} \frac{e^2 \overline{V_K^2(E)}}{T_o^2}$$

$$D_1(E) = 2 \frac{(kTZ_o)e^2 \ 10^{(NF/10)}}{T_o^2} \ \sum_n \ |A_n(E)|^2 \ |f_K(n\omega_o)|^2 \qquad (10.3.1)$$

We assume the amplifier is linear and so does not add any distortion of its own.

10.4. Stochastic Noise

The beam current for one particle is

$$I(t) = \frac{2e}{T} \ \sum_n \ \cos n\omega t$$

For a collection of particles at various frequencies and phases,

$$I(t) = \int dN(f) \ 2ef \ \sum_{t_i} \ \sum_n \ \cos n\omega \ (t-t_i)$$

Square and average this over time and phases. The result is

$$\overline{I^2} = \int \ \sum_n \ dI_n^2(f)$$

$$dI_n^2(f) = \frac{4e^2}{2T_o^2} \ dN(f)$$

which is independent of harmonic number and where $dN(f)$ is the number of particles at frequency f. Using:

$$dN(f) = \psi(E) \frac{dE}{df} df$$

$$df/dp = \eta f_o / p \qquad dE = \beta dp$$

$$dE/df = \beta p / \eta f_o$$

we get:

$$dN(f) = \frac{\psi(E) \beta p}{\eta f_o} df .$$

Thus the beam current at harmonic n and for rotation period corresponding to E induces on the input to the amplifier

$$\overline{dV_{in}^2} = \frac{2e^2}{T_o^2} \frac{\psi(E)\beta p}{\eta f_o} df \; Z_{PU}^2 \; S_{PU}^2(E) \; | \; f_p(n\omega)|^2$$

Now df refers to the rotation frequency. If we wish the spectral density at $n\omega$, we write

$$f' = nf$$

$$df = \frac{1}{n} df'$$

Finally we pass the above power through the amplifier and couple it to the beam: Again using Eq. (9.1.4) and the theorem Eq. (10.2.1), we get

$$D_2(E) = \psi(E) \; \frac{e^4 Z_{PU}^2 S_{PU}^2(E)\beta p}{T_o^3 \eta} \; \sum_n \frac{1}{n} | \; f_{PU}(n\omega_o) \; A_n(E) \; f_K(n\omega_o)|^2$$

We have now related all of the constants in the Fokker-Planck equation to the hardware.

10.5. The Exponential Stack

We can now review the discussion of momentum stacking in Section 9.3. Consider that the amplifier is perfect over the band f_1 to f_2, i.e., constant gain G and no phase shift. Neglect noise and hence D_1. Eq. (10.1.1) then can be summed and gives

$$F(E) = 2e^2 r_o^2 Z_{PU} \, S_{PU}(E) \left[\frac{f_2 - f_1}{f_o}\right] G \qquad (10.5.1)$$

Set $f_2 - f_1 = W$, the bandwidth. Equation (10.4.1) gives, under the same condition,

$$D(E) = \frac{\psi(E) \, e^4 Z_{PU}^2 S_{PU}^2(E) \beta p}{T_o^3 \eta} \ln \left(\frac{f_2}{f_1}\right) G^2$$

where the log term comes from replacing the sum by an integral. Now

$$V = FT_o/e = 2e Z_{PU} \, S_{PU}(E) \, W \, G \qquad (10.5.2)$$

Comparison with D(E) gives

$$D(E) = \frac{\beta p \ln(f_2/f_1)}{4T_o^3 \eta W^2} \, e^2 V^2 \, \psi \qquad (10.5.3)$$

Thus A in Eq. (9.3.1) is

$$A = \frac{e^2 \beta P}{4T_o^3 \eta W^2} \ln (f_2/f_1) \qquad (10.5.4)$$

giving

$$\psi = \psi_o e^{(E-E_1)/E_D}$$

$$V = \frac{2\phi_o T_o}{e\psi_o} e^{-[E-E_1/E_D]} \qquad (10.5.5)$$

$$E_D = \frac{4A\phi_o T^2}{e^2} = \frac{\beta p \phi_o}{T_o W^2 \eta} \ln \left(\frac{f_2}{f_1}\right)$$

As an example consider the case with $\beta p = 8$ GeV, $\phi_o = 5 \times 10^7$ particles/sec, $W = 1$ GHz and $\eta = .02$ such as is found at FNAL. Then we find

$$E_D = \frac{8000 \times 5 \times 10^7}{1.6 \times 10^{-6} (10^9)^2 \times .02} \ln 2 = 8.7 \text{ MeV}$$

To obtain an increase in particle density from 5/eV to 10^5/eV would take

$$\frac{E_f - E_i}{E_D} = \ln 20000 = 9.9$$

or

$$E_f - E_i = 86 \text{ MeV}$$

$$\frac{E_f - E_i}{E_O} = 1.1\%$$

Thus it would appear that high density gradients are possible but in actual fact we cannot do so well for practical reasons.

The most difficult task is to achieve the rapid change in V with energy. The gain profile can be shaped by placing the pickups in the lattice where there is a large momentum dispersion, α_p. We illustrate this below:
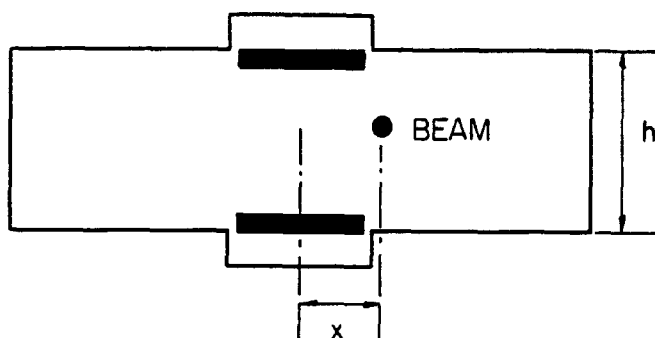
The pickup sensitivity then is (see Section 8.2.1)

$$V_{PU} \sim e^{-\pi x/h} \tag{10.5.6}$$

and x is related to ΔE by

$$x = \alpha_p \frac{\Delta p}{p} = \alpha_p \frac{\Delta E}{\beta^2 E} .$$

To achieve a factor of 20000, we must have

$$\frac{\pi \Delta x}{h} = 9.9$$

or

$$\Delta x = \frac{9.9}{\pi} h = 3.2h$$

We now come to the point at which the lattice design and the pickup
design interact. It is not hard to achieve a design where, for
instance, the beam height will fit comfortably in h = 3 cm leading to
a Δx = 10 cm. However, one must add space to this for the core and
for injection and extraction. In practical cases, the magnet
aperture can become rather large and hence it would be nice if there
were an additional way to control the gain profile. There is such a
method and it uses frequency filters which we now discuss.

10.6. The Use of Frequency Filters

Consider the frequency spectrum of the signal for several
Schottky bands.
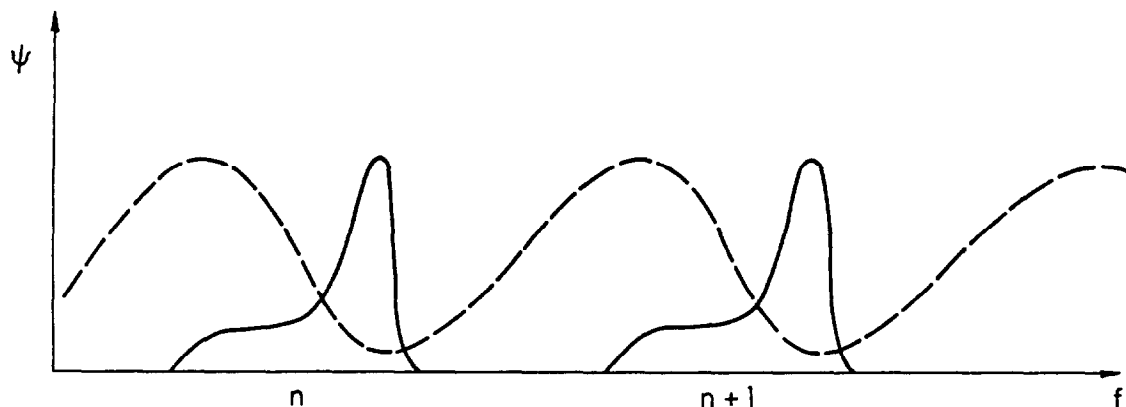
Suppose we had an amplifier with a gain vs frequency as shown by the
dotted line. This gain profile, if it is repeated over the entire
spectrum, would provide an additional method of controlling the V(E)
since E and f are related by η. Such periodic filters exist and are
called comb filters. A simple realization of such a filter is
provided by a shorted delay line whose length is just $T_0/2$.
Electrically this is equivalent to
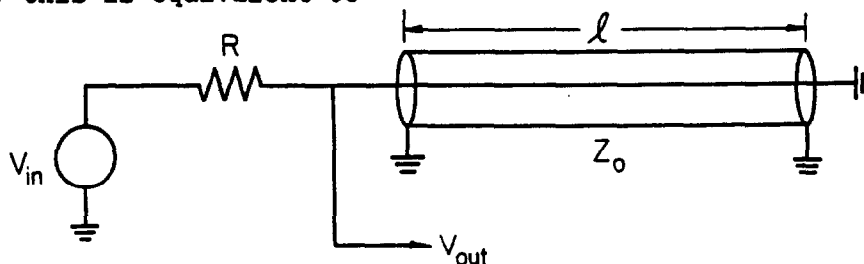
The delay line has an impedance given by

$$Z_{in} = Z_o \tanh(\alpha+j\beta)\ell \qquad\qquad (10.6.1)$$

$$V_{out}/V_{in} = \frac{Z_{in}}{Z_{in}+R} \qquad\qquad (10.6.2)$$

Here the propagation constant is

$$\gamma\ell = (\alpha + j\beta)\ell$$

with α the attenuation per unit length and β the phase shift per unit length. The length of the line is picked so that it is $\lambda/2$ at f_o.

$$\ell = \frac{v}{2f_o}$$

v is the propagation velocity along the line.

This gives a gain function that repeats with a periodic spacing equal to f_o. The shape of the frequency response and phase shift curves depends on the ratio of R/Z_o and $\alpha\ell$, the attenuation. The maximum and minimum impedance of the shorted transmission line for small $\alpha\ell$ is given by:

$$Z_{max} = Z_o/(\alpha\ell)$$

$$Z_{min} = (\alpha\ell)Z_o$$

giving

$$V_{out}/V_{in}|max \sim 1$$

$$V_{out}/V_{in}|min \sim (\alpha\ell) Z_o/R .$$

There is a phase reversal at nf_o, making this technique suitable for "filter" cooling systems.

The value of α is determined mainly by the skin effect in the conductors of the transmission line and is proportional to $\sqrt{\omega}$. Large cross section lines have small attenuation, but then it is also necessary that the frequency spectrum not excite higher propagation modes of the cable. These modes show up when the circumference of the cable is $\sim\lambda$ and result in erratic propagation and phase shift characteristics.

It is also possible to reduce α by increasing the conductivity since:

$$\alpha \sim \sqrt{\omega/\sigma}$$

If the temperature of the cable is lowered, σ will increase until the anomalous skin effect becomes important. (The classical formulas for skin effect break down when the mean free path of the electrons in the metal becomes comparable to the skin depth).

Shorted delay lines have been used very successfully at the CERN AA. However, the FNAL system requires longer lines, $T_o = 1.6$ μsec compared to $T_o = 0.8$ μsec and higher frequencies, 1-2 GHz compared to 250-500 MHz. As a result, even cooling the lines to low temperatures was not effective in making the $\alpha\ell$ less than 0.1 (compared to .02 to .05 for CERN.) Consequently, FNAL has had to develop superconducting delay lines[22] and the design uses such lines extensively.

There is an additional use for filters. The gain of the amplifier in the momentum system is very high: between 10^8 and 10^9. Thus thermal noise at the output is very large and includes frequencies overlapping the core. The voltage gain at the core is low (inversely proportional to density) and hence if all of the gain shaping were done by means of the exponential response of the pickups, the core would be completely overwhelmed by thermal noise. Hence filters to reduce the gain at the core are an absolute necessity.

10.7. A Complete System for Momentum Stacking

To finish this section, we give a brief description of the FNAL Accumulator design. The relevant parameters are

$$\psi_i = 5 \ \bar{p}/eV$$

$$\psi_f = 10^5 \ \bar{p}/eV$$

$$E_{core} = 8 \ GeV$$

$$E_{inj} = -75 \ MeV \text{ (all energies relative to core)}$$

Core width $= \pm 5$ MeV

$$T_o = 1.6 \ \mu sec$$

Frequency Momentum Stacker $= 1-2$ GHz
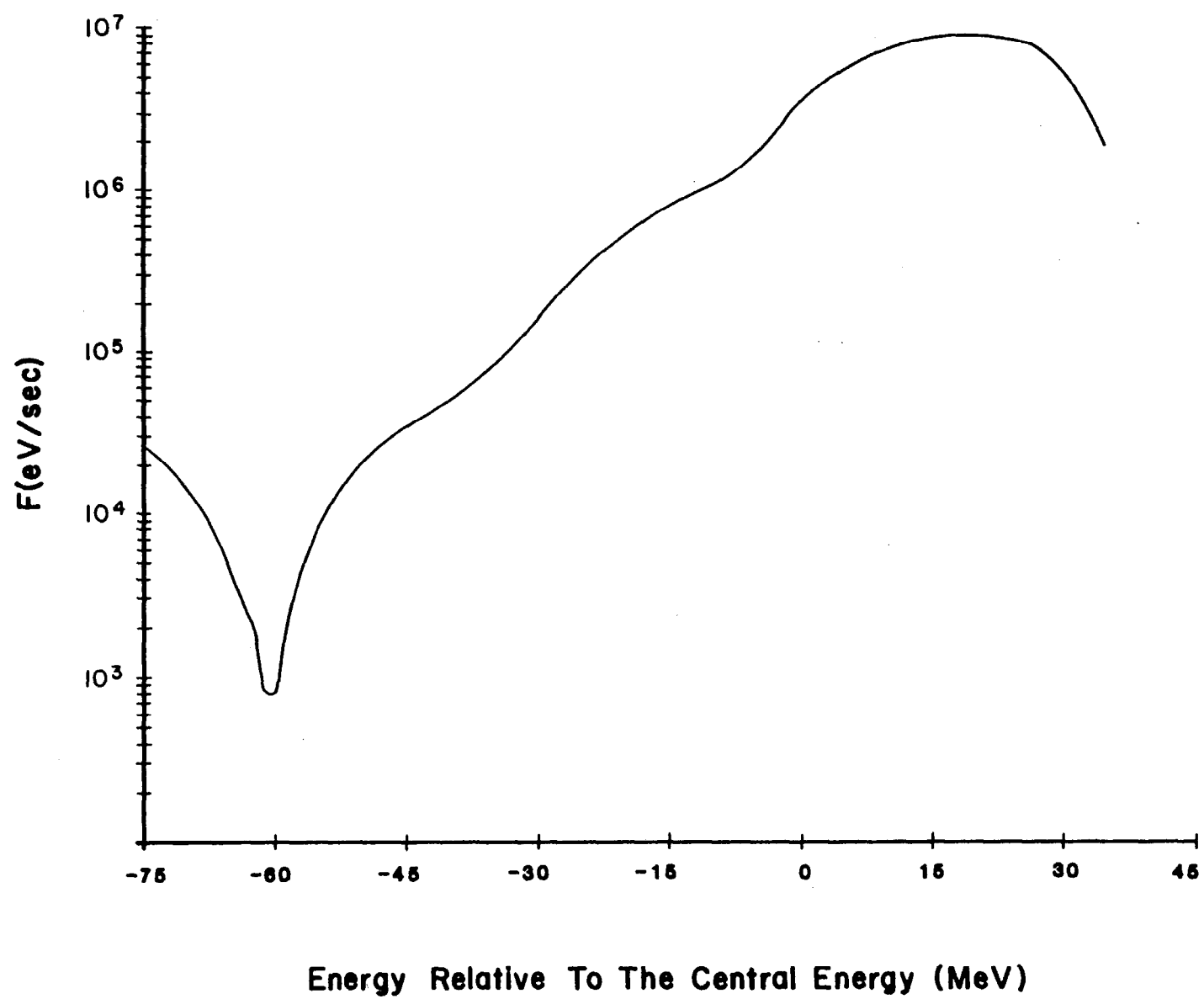
Frequency Core System $= 2-4$ GHz

Figure 10.7.1 shows a block diagram of the system. As can be seen, it is considerably more complicated than we have indicated before now. The stack density as a function of time was illustrated in Section 9.3. Figures 10.7.2, 10.7.3 and 10.7.4 shows $F(E)$, $D_1(E)$, and $D_2(E)$ at the time the stack is full. The CERN AA has a similar block diagram.
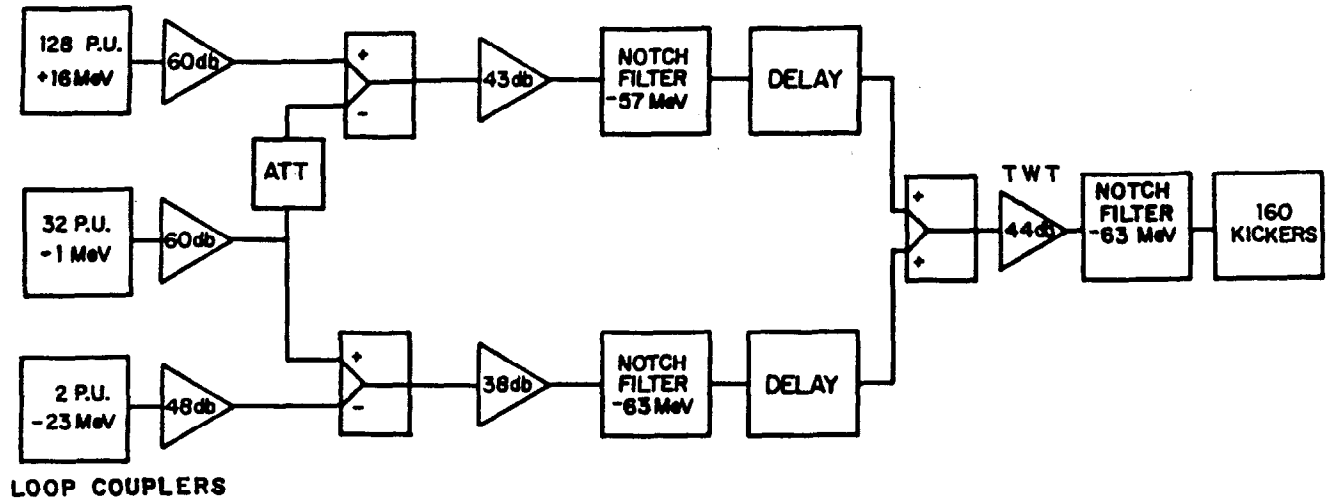
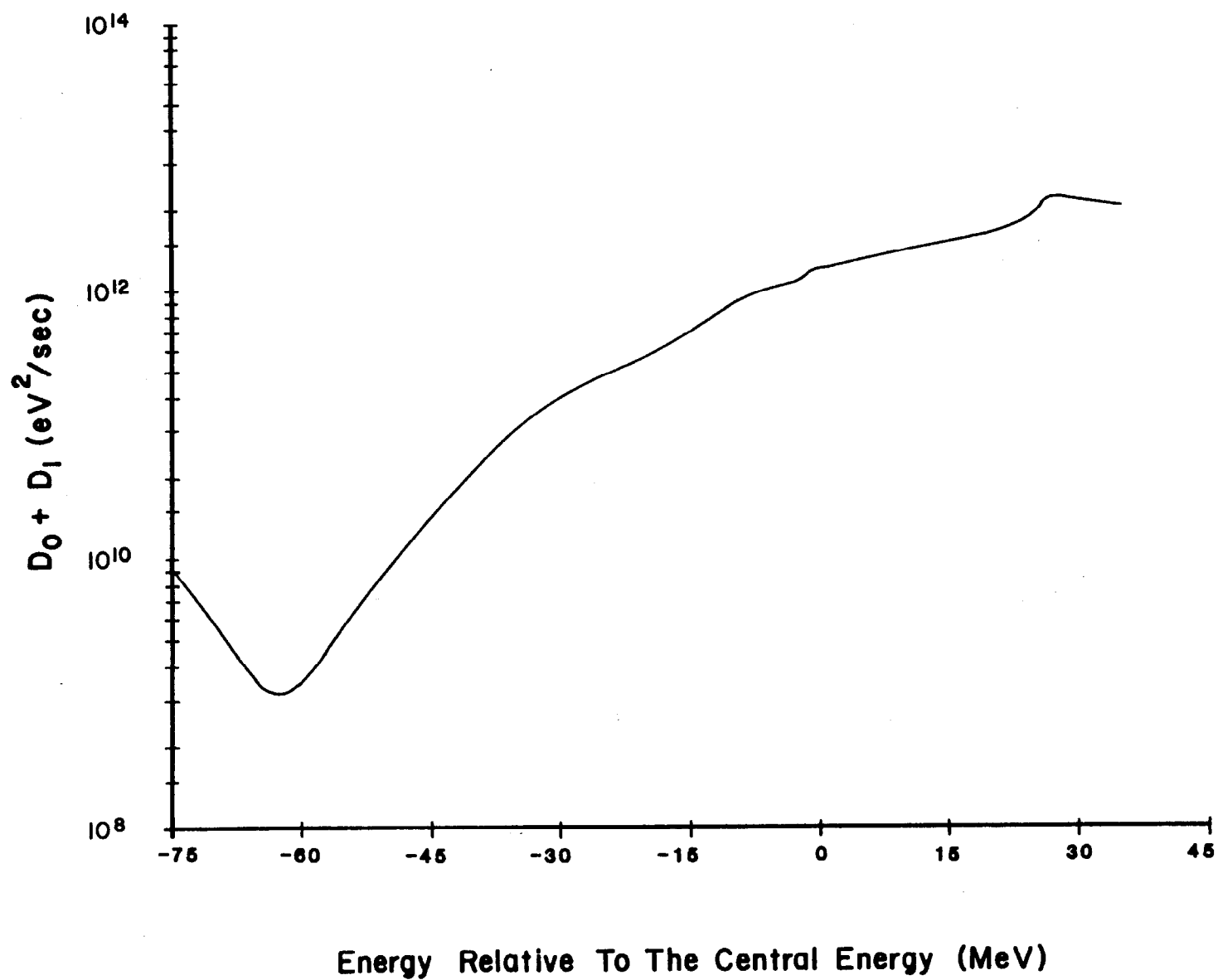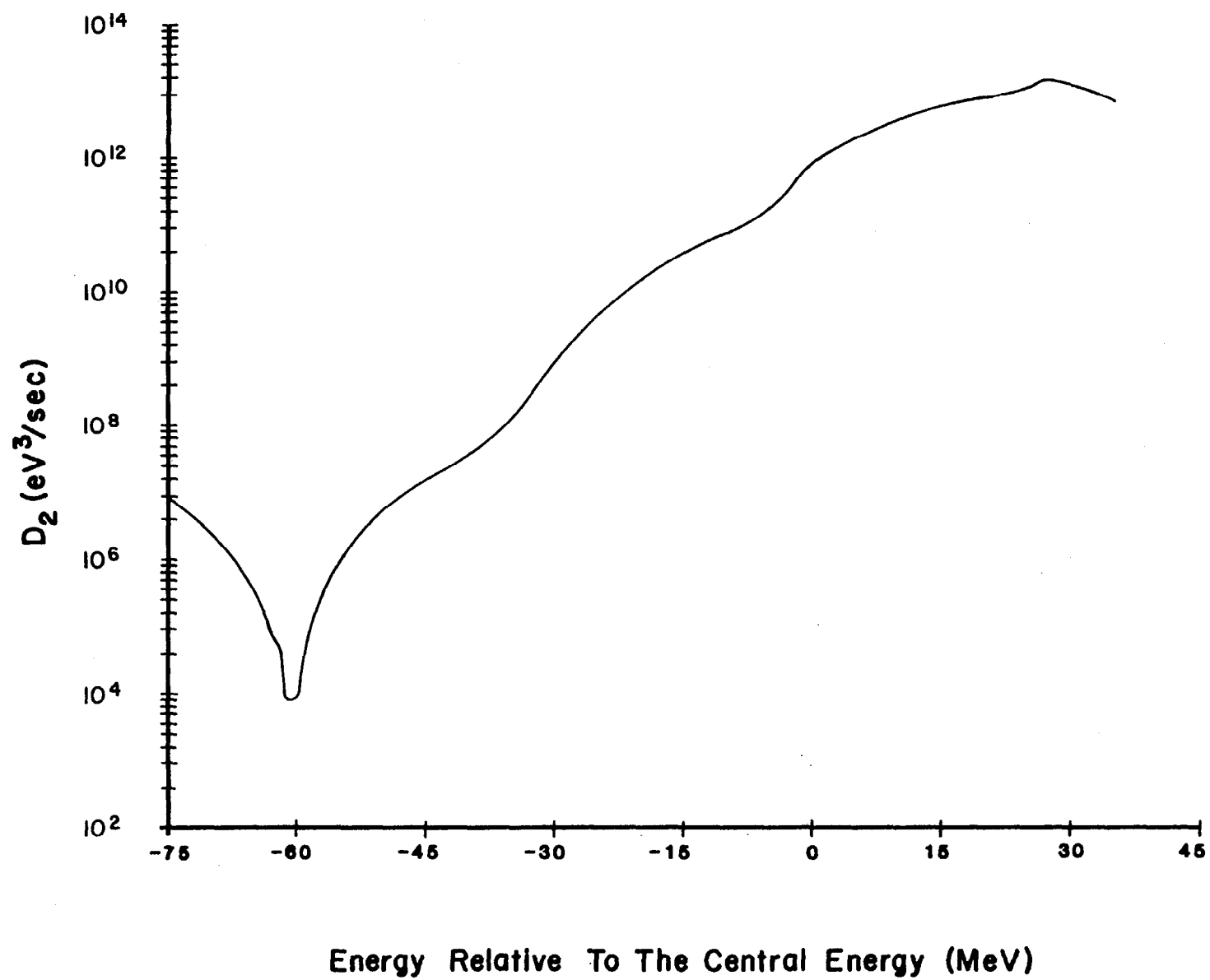STACK TAIL MOMENTUM COOLING SYSTEM   1-2 GHz
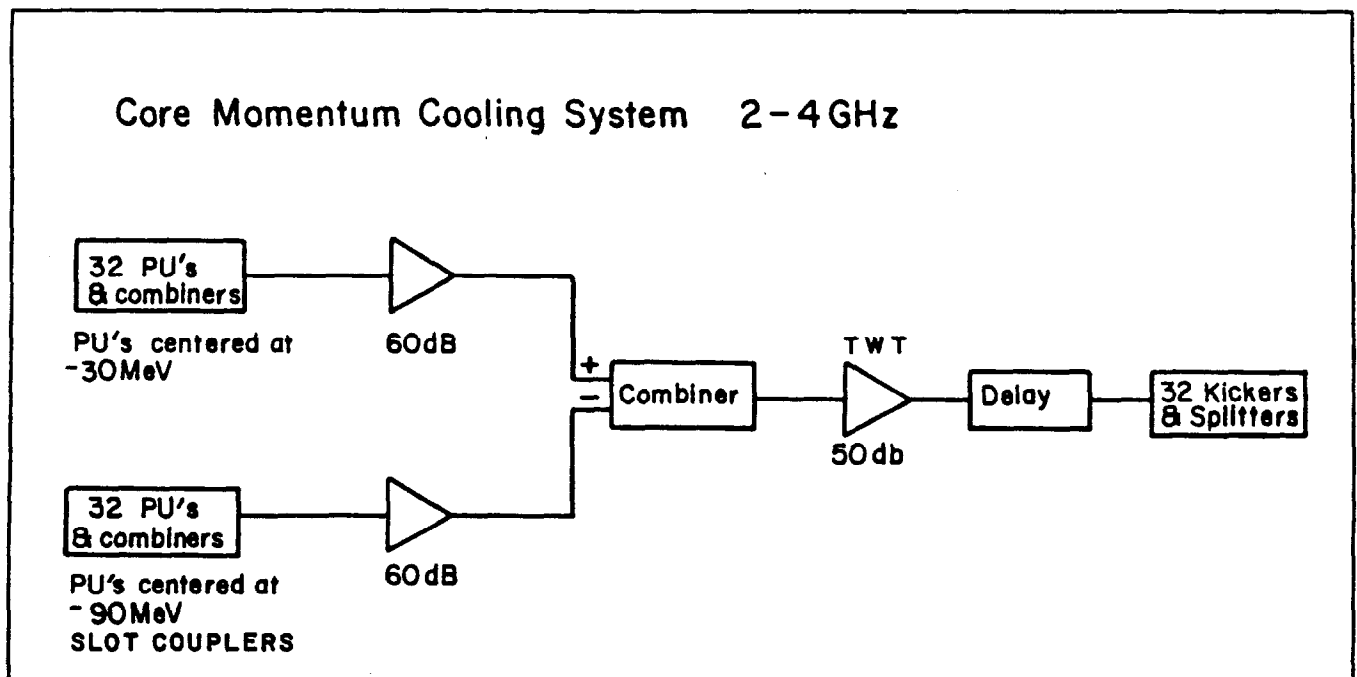
Core Momentum Cooling System   2-4 GHz

Energy Relative To The Central Energy (MeV)

Energy Relative To The Central Energy (MeV)

Energy Relative To The Central Energy (MeV)

In order to achieve the large variation of gain, two sets of electrodes are used and their output mixed. Finally, when the frequency spread in the stack is small enough, one goes to a higher frequency system to pull together the core. The superconducting filters protect this core from thermal noise of the high gain tail system.

The box shown as a TWT (travelling wave tube) before each kicker system is actually many (50) TWT's, each driving a small number of kickers. It is very important to have a linear system so that unwanted intermodulation products are not generated. Such products will act the same as noise. Therefore the TWT's are only operated at a small fraction of their rated power in order to assure adequate linearity.

It is interesting to see that the higher frequency core systems can produce much steeper gradients in the density than does the lower frequency tail system. (Note $E_d \sim 1/W^2$, Eq. (10.5.6)).

Such a complicated system is not achieved without extensive computer simulation. However, the theory we have outlined forms the basis for extensive codes that were generated originally at CERN and used later at FNAL. We have left out two effects that must be included in a complete system. One is the intra-beam scattering. This is the coulomb interaction of particles of slightly different energies in the core. This effect limits the ultimate density that can be usefully achieved. The core cooling ultimately comes into equilibrium with this random process and ψ grows in width rather than increasing. In designing machines this scattering process is approximated as an additional term in D_1. The sum $D_0 + D_1$ is shown in Figure 10.7.3.

We have not said much about interaction with the lattice. However, this interaction dominates the design. Some requirements can be listed:

1. As much as 10 meters of free space along the beam may be required for the pickup arrays. Several arrays for both transverse and longitudinal cooling are required.

2. A small β_v at the momentum pickup is necessary so that the vertical beam size will be small. This means h (Eq. (10.5.7)) is smaller and the pickup sensitivity falls faster with x.

3. A small β_H at the momentum pickup is necessary so that particles of one momentum will be well localized in x. Since the sensitivity is decreasing exponentially in x, a large spread transverse to the beam would lead to strong non-linearities.

4. A large momentum dispersion is necessary to convert the exponential x dependence into a suitable energy dependence.

5. A suitable η.

6. A magnet with a small aperture to keep the cost of the system under control.

7. 5-10 meters of zero dispersion space for the momentum kickers.

In regard to this last point, it should be noted that if an attempt is made to tailor the gain by letting the beam go through the kickers off axis in a dispersive region (similar to the momentum pickups) there will be excitation of transverse oscillations. Under certain circumstances this effect may be useful for simultaneous cooling of momentum and horizontal betatron oscillation.[23,24]

The second effect we have not included is the so-called beam feedback. We will now cover this subject briefly.

11. BEAM FEEDBACK

Consider the block diagram of the system we have been considering.
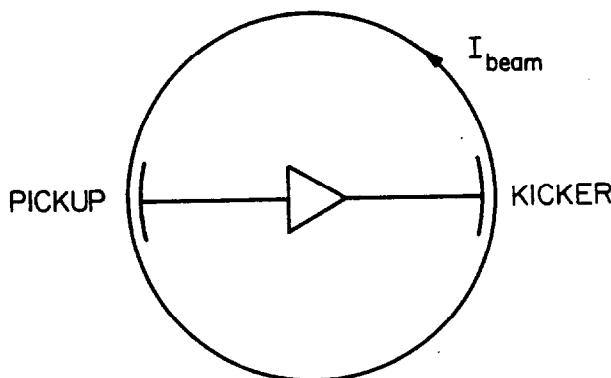
We have calculated the effect of the kickers in modifying a perturbation in the beam sensed by the pickups a half turn earlier. It has been implied that the mixing is small enough so that the perturbation will not smear out too badly in half a turn. However, if this is true, then it must also be true that a signal from the kicker will be transmitted back to the input of the amplifier via the beam on the top half of its turn. This action may be most easily visualized as an electrical element connecting the output to the input. This element has complicated electrical properties but nevertheless amounts to a simple feedback loop. The phase shift and feedback factor will modify the gain of the amplifier and the system may be stable or unstable, just as in the case of any feedback system. Indeed we will show that the system gain may be written in the form

$$G = \frac{A}{1-A\beta}$$

11.1. Time dependent equation for particle density

We wish now to consider a system of particles circulating in a machine and described by a density function $\psi(\phi,E,t)$, i.e., this density varies around the machine with azimuth ϕ and changes with E and time. The density $\psi = d^2N/dEd\psi$. There will be a kicker at one point in the system, $\phi = 0$, that can change the energy of the particles when they cross $\phi = 0$ by $V(t)$.

$$\dot{E}(t) = e \; f_o \; V(t) \; \delta(\phi)$$

$$= \frac{e}{2\pi T_o} \; V(t) \; \sum_n e^{in\phi}$$

(11.1.1)

We must have conservation of charge. Changing variables in $\rho = e\psi(r,\phi,t)$ to E, ϕ, and t we can get the equation for ψ. Or, conversely, we can use Liouville since E and ϕ are conjugate variables and write

$$\frac{d\psi}{dt} = 0$$

(11.1.2)

$$\frac{\partial\psi}{\partial t} + \dot{\phi} \; \frac{\partial\psi}{\partial\phi} + \dot{E} \; \frac{\partial\psi}{\partial E} = 0$$

Now we wish to expand around small perturbations to the equilibrium situation.

$$\psi = \psi_o(E) + \psi_1(E,\phi,t), \text{ where } \psi_1 \text{ is small} \qquad (11.1.3)$$

Let E be the deviation from E_o, the central value. Then we can write

$$\dot{\phi}(t) = \omega_o + \frac{\partial\omega}{\partial E} \; E \qquad\qquad (11.1.4)$$

Using the definition of η, we have

$$\dot{\phi} = \omega_o - \frac{\omega_o\eta}{\beta^2 E_o} \; E = \omega_o + KE$$

(11.1.5)

$$K = - \frac{\omega_o \eta}{\beta^2 E_o} \ .$$

Substitute in Eq. (11.1.2):

$$\frac{\partial \psi_1}{\partial t} + (\omega_o + KE) \frac{\partial \psi_1}{\partial \phi} + e f_o \frac{V(t)}{2\pi} \frac{d\psi_o}{dE} \sum_n e^{in\phi} = 0 \qquad (11.1.6)$$

where we have dropped second order terms. Note that $\psi_o(E)$ represents the stable unperturbed part of the beam.

Now we expand

$$\psi_1 = \sum_n \psi_n (E,t) e^{in\phi} \qquad (11.1.7)$$

and substitute into Eq. (11.1.6):

$$\frac{\partial \psi_n}{\partial t} + in(\omega_o + KE)\phi_n = - \frac{e}{2\pi T_o} V(t) \frac{d\psi_o}{dE} \qquad (11.1.8)$$

Now if $V(t)$ is a sine wave voltage, we have

$$V(t) = V(\Omega) e^{-i\Omega t}$$

and we can similarly set

$$\psi_n(E,t) = \psi_n(E,\Omega) e^{-i\Omega t}$$

(Note slightly confusing nomenclature).

Substituting into Eq. (11.1.8), we get

$$\psi_n (E,\Omega) = - \frac{ie}{2\pi T_o} \frac{V(\Omega)(d\psi_o/dE)}{\Omega - n(\omega_o + KE)} \qquad (11.1.9)$$

Finally, we can get $\psi(E,\phi,t)$ for a sinusoidal drive voltage:

$$\psi(E,\phi,t) = \psi_o(E) + \sum_n \frac{-i(e/2\pi T_o)V(\Omega)(d\psi_o/dE)}{\Omega - n(\omega_o + KE)} e^{i(n\phi - \Omega t)} \qquad (11.1.10)$$

Expressing this as a current

$$dI = dQ/dt = \frac{edN}{dt} = \frac{e\psi dE d\phi}{dt} = e\omega_o \ \psi(E,\phi,t) \ dE$$
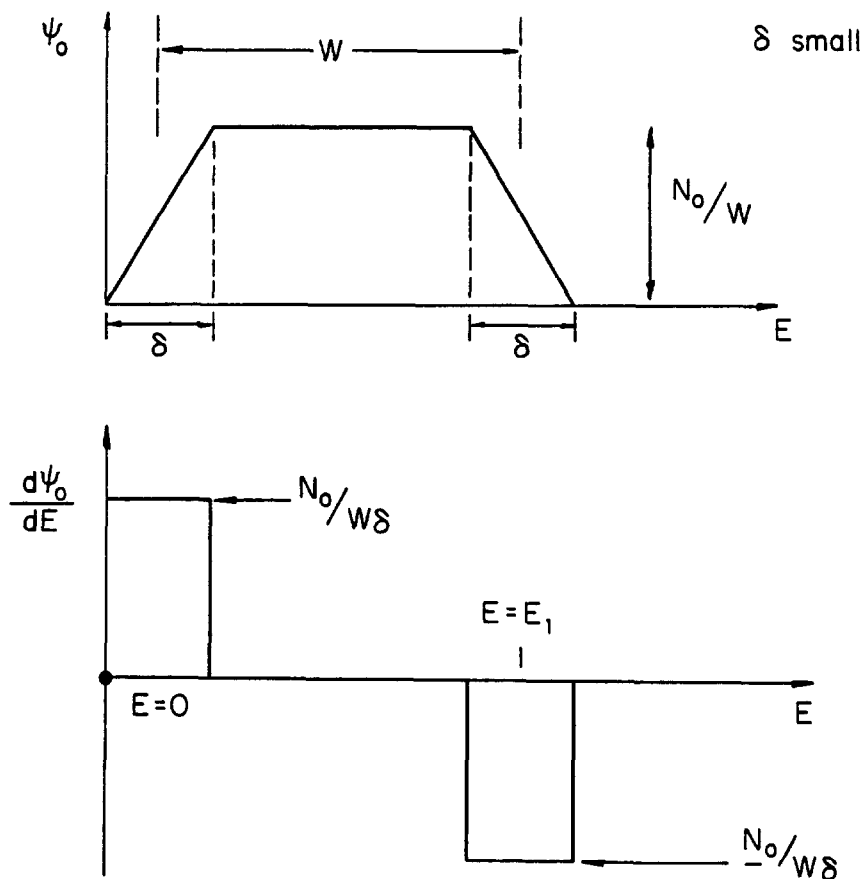
98

$$I(\Omega) = \sum_n e\omega_o \int_E \frac{(-ie/2\pi T_o)V(\Omega)(d\psi/dE)e^{i(n\phi-\Omega t)}dE}{[\Omega-n(\omega_o+KE)]} \qquad (11.1.11)$$

Where we have dropped the DC term containing ψ_o and integrated over all energies in the beam.

This equation tells us how the circulating beam responds to a sinusoidal perturbation. The pole that exists in the denominator leads to a principal value integral plus a constant term evaluated at the pole.

11.2. Simple Example

Equation (11.1.11) tells us that if $d\psi/dE$ does not exist, then $I(\Omega) = 0$. A simple example will help understand this. Consider
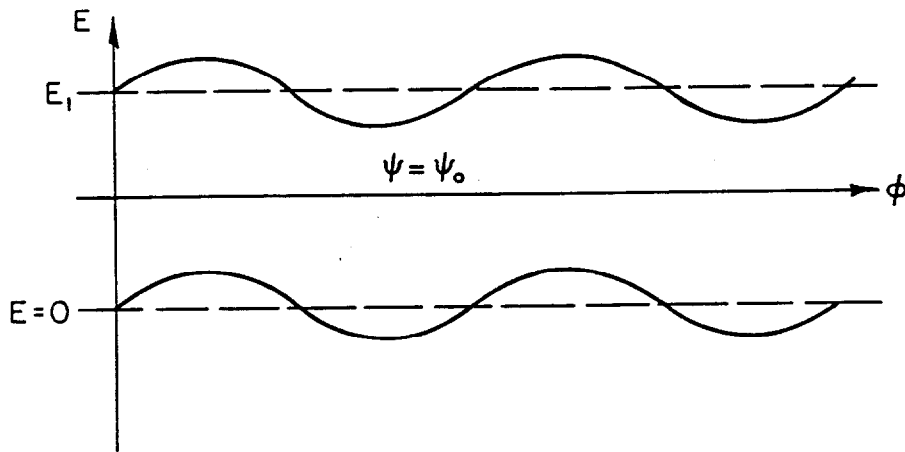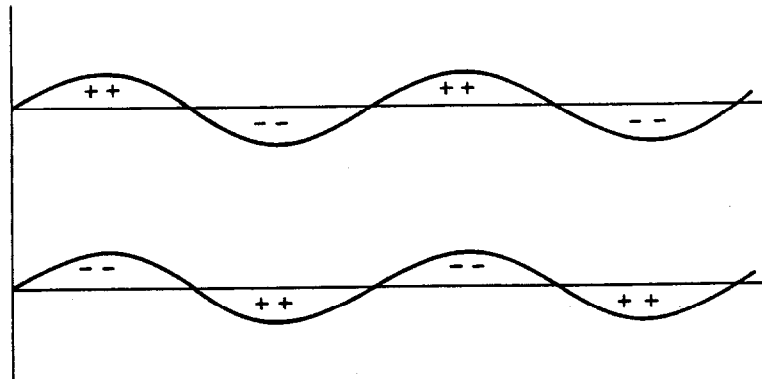

Then

$$I(\Omega) = \frac{-ie^2}{T_o^2} V(\Omega)e^{-i\Omega t} \left(\frac{N_o}{W}\right) \sum_n e^{in\phi} \left[\frac{1}{\Omega-n\omega_o} - \frac{1}{\Omega-n(\omega_o+KE_1)}\right]$$

<div align="right">(11.2.1)</div>

We have assumed $\delta \ll W$ and we chose Ω so as to avoid the singularities in the denominators.

Now consider the situation at $\phi = 0^+$. The (E,ϕ) phase space of the beam looks like (for $n = 1$)

The particles are modulated in energy sinusoidally, but we could equally well subtract out ψ_o and leave two bands of alternating charge density.

These two bands represent two alternating currents located at the two edges of the ribbon of charge around the machine. If it were not for the term KE_1 in the second denominator, the total current at frequency Ω would equal zero.

Consider the various ways that we could detect this current. First suppose we use a current transformer as described in Section 8.1. Such a detector has no position sensitivity. Nevertheless, it will produce a signal provided $K \neq 0$, i.e., there is dispersion in the machine.

However, there is a second possibility of detecting a modulation with a pickup electrode, even if $K = 0$. This arises for electrodes that do not couple uniformly to all energies in the beam. The exponential behavior of the electrodes considered in Section 8.2.1 represent such a case. The electrodes couple more strongly to one edge of the beam than the other and the two induced signals do not cancel even though the currents may be equal.

These simple examples indicate the role played by dispersion, $\partial\psi/\partial E$ and variation of pickup sensitivity across the gap. Equation 11.1.11 does not include this latter variable, but it is easily incorporated into the development if needed.
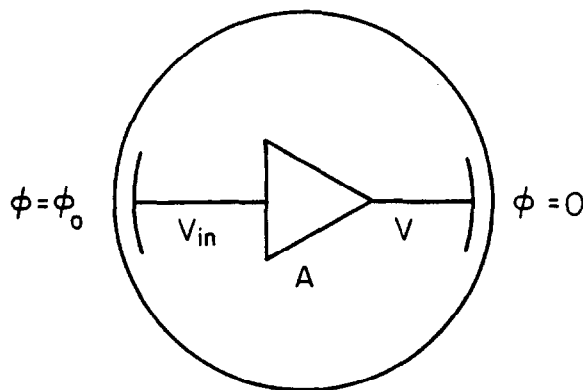
11.3. Modified Amplifier Gain

We now consider the complete system. If we apply $V(\Omega)e^{-i\Omega t}$ to the kickers, Eq. (11.1.11) gives us the amplitude of the current at any point in the ring.

$$I_B(\phi,\Omega) = V(\Omega)\, G_m(\phi,\Omega) \tag{11.3.1}$$

$$G_m(\phi,\Omega) = -ie^2 f_o^2 \sum_n \int_E \frac{(d\psi/dE)e^{in\phi}dE}{\Omega - n(\omega_o + KE)} \tag{11.3.2}$$

where we have dropped the time factor $e^{-i\Omega t}$. Consider the complete cooling system:

We have at the kicker:

$$I_B(0,\Omega) = V(\Omega) \, G_m(0,\Omega) \qquad\qquad (11.3.3)$$

which becomes at the pickup

$$I_B(\phi_o,\Omega) = V(\Omega) \, G_m(\phi_o,\Omega) \qquad\qquad (11.3.4)$$

At the pickup we consider what will happen if the beam at some energy E has a small perturbation that the cooling system is designed to remove. This perturbation will have a complete Schottky spectrum of harmonics at frequencies $\Omega = n\,\omega(E)$. Let one of these, $I_s(\Omega)$, generate signal input to the amplifier. Then we can write

$$V_{in}(\Omega) = Z_{PU}(\Omega) \, [I_s(\Omega) + I_B(\phi_o,\Omega)] \qquad\qquad (11.3.5)$$

Here we emphasize that $I_s(\Omega)$ is one Schottky harmonic of a small perturbation in the beam at an energy E. I_B on the other hand is the response of the whole beam to a signal from the kicker, i.e., the expression for I_B has been integrated over all the energies present. We are treating the beam as a continuous smooth medium whereas its fluctuations are represented by the very small perturbation, I_s.

One more equation completes the system

$$V(\Omega) = A(\Omega) \, V_{in}(\Omega) \qquad\qquad (11.3.6)$$

Substitute in this expression (11.3.5) and (11.3.4) and we find

$$V(\Omega) = I_s(\Omega) \, \frac{A(\Omega)Z_{PU}(\Omega)}{1 - A(\Omega)G_m(\phi_o,\Omega)Z_{PU}(\Omega)} \qquad\qquad (11.3.7)$$

Thus the amplifier can be treated as one whose gain has been modified:

$$A'(\Omega) = \frac{A(\Omega)}{1 - A(\Omega)\beta(\Omega)} \qquad\qquad (11.3.8)$$

$$\beta(\Omega) = Z_{PU}(\Omega) \, G_m(\phi_o,\Omega) \qquad\qquad (11.3.9)$$

This gain must now be used for the amplifier in the cooling equations of Section 10. Note that the gain will now be a function of time as the stack builds up since G_m depends on integration over the stack density $\psi(E)$. The general effect of this effect is to lower the gain of the system (negative feedback). However, it also requires very careful design so that Nyquist criterion is satisfied and the system does not oscillate. The real and imaginary parts of $A(\Omega) \times \beta(\Omega)$ for the FNAL accumulator are shown for one Schottky band (at 1.5. GHz) in Fig. 11.3.1. The parameter that varies along the curve is the energy within the stack. Stability is insured by avoiding the point (1,0).

Again, to handle this complex problem in a satisfactory way, computer calculations are necessary, and these effects are included in the codes that are in use.

1.5 GHz

FG Imaginary Part

FG Real Part
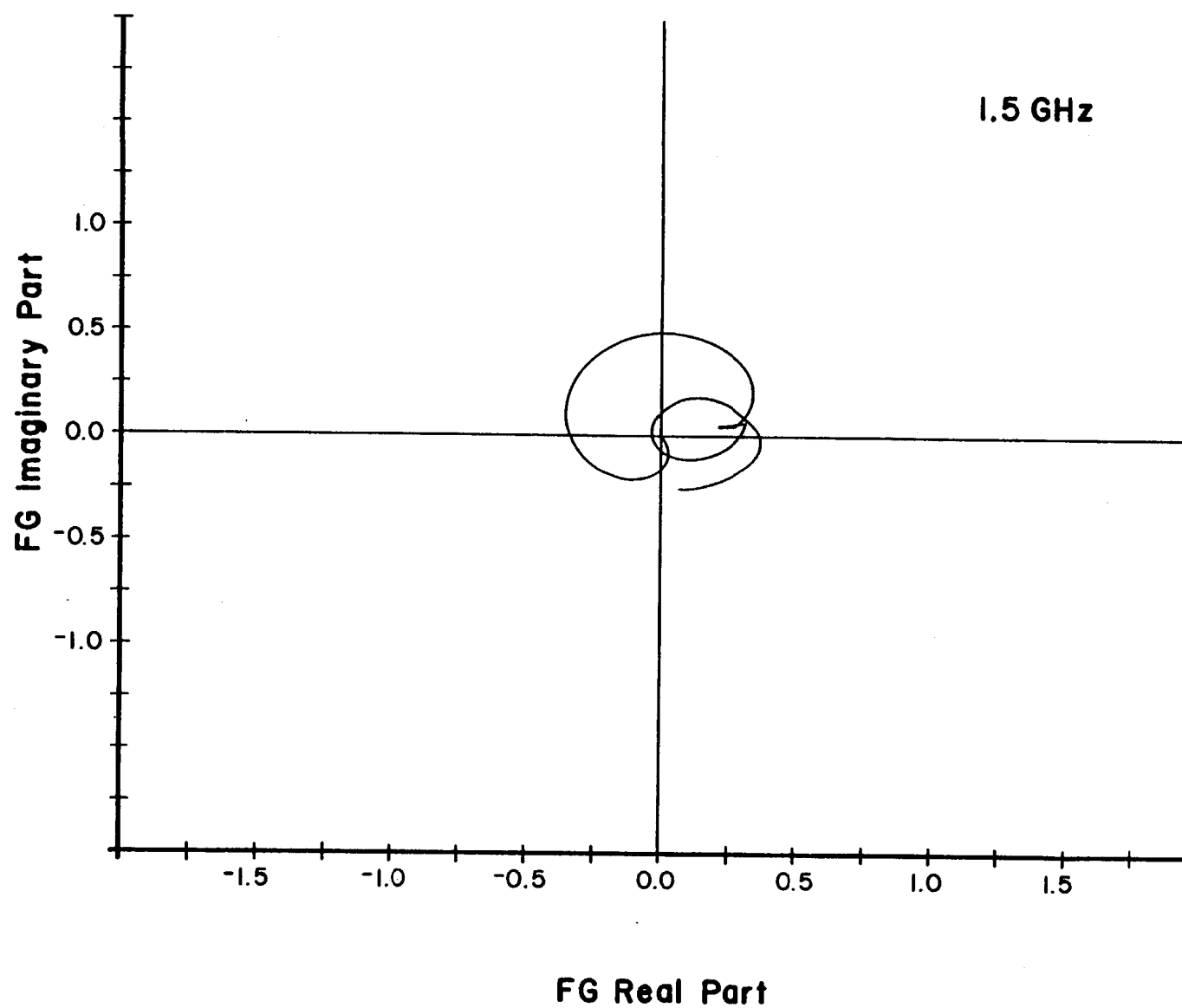
12. CONCLUSION

We conclude this simple discussion of stochastic cooling with the following observations. The science is new and rapidly developing. At present, there are technical problems in generating, and cooling large fluxes of $\bar{p}$'s. However, ways have been suggested of targeting the large numbers of protons that are readily available from present day accelerators. The cooling systems are at the lower edge of present day RF technology. For instance, traveling wave tubes covering the band of 2 to 18 GHz are available. The challenge is to use this available hardware in the most effective means. We can look forward to fluxes perhaps an order of magnitude higher in the near future, and maybe very wide bandwidth systems will even allow us to actually cool bunched beams at high energies in colliders. The challenge is there and the problems fascinating!

104

REFERENCES

1. Design Study of a Proton-Antiproton Colliding-Beam Facility, CERN/PS/AA/78-3(1978).

2. Design Report, Tevatron I Project, Fermilab (1982).

3. Fermilab Dedicated Collider Proposal (April, 1983).

4. Design Study of a Facility for Experiments with Low-Energy Antiprotons (Ed. G. Plass), CERN/PS/DL/80-7 (1980).

5. W. Hardt, D. LeFevre, D. Mohl, G. Plass, The LEAR Project, Proc. 5th European Symposium on Nucleon-Antinucleon Interactions, Bressanone, 1980 (CLEUP, Podua, 1980), p. 663.

6. P. LeFevre, D. Mohl, G. Plass, The Low-Energy Antiproton Ring (LEAR) Project, Proc. 11th Int. Conf. on High-Energy Accelerators, Geneva, 1980 (Birkhauser, Baule, 1980), p. 819.

7. U. Gastaldi, R. Klapisch, The LEAR Project and Physics with Low-Energy Antiprotons, CERN-EP/81-06 (1981).

8. Budker, G, I., in Proc. Int. Symp. on Electron and Positron Storage Rings, Saclay, Atomnaya Energiya 22:246.

9. Budker, G. I., et al., Part. Accel 7: 197-211 (1976).

10. Krienen, F., in Proc. 11th. Int. Conf. on High Energy Accelerators, Geneva, p. 78 (1980).

11. R. Forster et al., in Proc. 1981 Particle Accelerator Conf., IEEE Trans (NS-28), Pt. 1, p. 2386 (1981).

12. For introductory reviews of this subject, see: F. T. Cole and F. E. Mills, Ann. Rev. Nucl. Sci. 31, 295 (1981) and W. Kells, "Electron Cooling", in Physics of High Energy Particle Accelerators, p. 686 (1982).

13. C. Rubbia, "Workshop on the Cooling of High Energy Beams," Wisconsin (1978), p. 13.

14. INP Electron Cooling Group, CERN Report 77-08 (1977).

15. C. Hojvat, A. Van Ginneken, NIM 206, 67 (1983).

16. High Intensity Targeting Workshop, Univ. of Wisconsin Report, Fermilab (April 1980).

17. B.F. Bayanov et al., Fermilab Report TM-1000; B.F. Bayanov et al., NIM 190, 9 (1981) and references therein.

18. H.G. Hereward, Statistical Phenomena Theory, Erice Lectures, CERN 77-13 (1977).

19. G. Lambertson, private communication.

20. R. Shafer, private communication; see also, J. Simpson, et al., "Measured Response of TeV-I Beam Cooling Electrodes," 12th Int. Conf. on High-Energy Acccelerators, Fermilab (1983).

21. D. Mohl, G. Petrucci, L. Thorndahl, S. Van der Meer, CERN/PS /AA/79-23, p. 22.

22. R. Pasquinelli, et al., "Superconducting Notch Filters for the Fermilab Antiproton Source," 12th Int. Conf. on High-Energy Accelerators, Fermilab (1983).

23. CERN/PS/AA/79-23, p. 50.

24. R. Johnson, J. Marriner, Fermilab Pub-82/92 (1982).